Part I

The basic formalism of TDDFT

3
Fundamental existence theorems

3.1 Time-dependent many-body systems

In this section, we will summarize for reference some basic relations governing the time evolution of electronic many-body systems. Some properties, such as the continuity equation and local conservation laws, will be essential for the proofs that follow below in Sections 3.2 and 3.3.

3.1.1 Time-dependent Schrödinger equation

Let us consider a system of N interacting nonrelativistic fermions moving in an explicitly time-dependent external scalar potential[1] $v(\mathbf{r},t)$. We will give some restrictions below as to what kind of potentials will be allowed, but for now, $v(\mathbf{r},t)$ is an arbitrary real function of space and time.

The total Hamiltonian of the N-particle system is given by

$$\hat{H}(t) = \hat{T} + \hat{V}(t) + \hat{W} \,. \tag{3.1}$$

As in the static case (Section 2.1.1), the kinetic-energy operator is

$$\hat{T} = \sum_{j=1}^{N} -\frac{\nabla_j^2}{2} \,. \tag{3.2}$$

The potential operator is now time-dependent,

$$\hat{V}(t) = \sum_{j=1}^{N} v(\mathbf{r}_j, t) \,, \tag{3.3}$$

and the particle–particle interaction is given by

$$\hat{W} = \frac{1}{2} \sum_{\substack{j,k \\ j \neq k}}^{N} w(|\mathbf{r}_j - \mathbf{r}_k|) \,. \tag{3.4}$$

Again, the usual choice is the Coulomb interaction $w(|\mathbf{r}_j - \mathbf{r}_k|) = 1/|\mathbf{r}_j - \mathbf{r}_k|$, but we will also consider different forms of the interaction, and the noninteracting case $w = 0$. For simplicity, we shall often refer to the fermionic particles as "electrons," even if their interaction $w(|\mathbf{r}_j - \mathbf{r}_k|)$ is not Coulombic.

[1] We will consider vector potentials in Chapter 10 when we discuss time-dependent current-DFT.

The time evolution of the system is governed by the time-dependent many-body Schrödinger equation,[2]

$$i\frac{\partial}{\partial t}\Psi(\mathbf{x}_1,\ldots,\mathbf{x}_N,t) = \hat{H}(t)\Psi(\mathbf{x}_1,\ldots,\mathbf{x}_N,t)\,, \tag{3.5}$$

which propagates a given initial state $\Psi(t_0) \equiv \Psi_0$ over some time interval $[t_0, t_1]$, starting from the initial time t_0 up until some final time t_1. In many practical applications, the system is initially in its ground state, and a time-dependent external potential is switched on at t_0. In that case, we can write

$$v(\mathbf{r},t) = v_0(\mathbf{r}) + v_1(\mathbf{r},t)\theta(t-t_0). \tag{3.6}$$

3.1.2 Time evolution operators

Formally, the solution of the time-dependent Schrödinger equation (3.5) can be written in terms of a time evolution operator:

$$\Psi(t) = \hat{U}(t,t_0)\Psi_0. \tag{3.7}$$

The time evolution operator $\hat{U}(t,t_0)$ acting on the initial state Ψ_0 yields the state $\Psi(t)$ at some time $t \geq t_0$. The two most important properties of the time evolution operator are the composition property, and unitarity. The composition property states that

$$\hat{U}(t_2,t_0) = \hat{U}(t_2,t_1)\hat{U}(t_1,t_0), \quad t_2 \geq t_1 \geq t_0, \tag{3.8}$$

which means that we can either directly propagate from t_0 to t_2, or first propagate to some intermediate time t_1 and then proceed from there to t_2. The second important property of the time evolution operator is unitarity:

$$\hat{U}^\dagger(t,t_0)\hat{U}(t,t_0) = 1 \quad \text{or} \quad \hat{U}^\dagger(t,t_0) = \hat{U}^{-1}(t,t_0)\,, \tag{3.9}$$

where $\hat{U}^\dagger$ stands for the Hermitian conjugate of $\hat{U}$. Unitary time propagation ensures that the norm of the wave function is conserved. To convince ourselves that this is true, let us explicitly consider the norm of $\Psi(t)$:

$$\begin{aligned}\langle\Psi(t)|\Psi(t)\rangle &= \langle\hat{U}(t,t_0)\Psi_0|\hat{U}(t,t_0)\Psi_0\rangle \\ &= \langle\Psi_0|\hat{U}^\dagger(t,t_0)\hat{U}(t,t_0)|\Psi_0\rangle = \langle\Psi_0|\Psi_0\rangle = N\,.\end{aligned} \tag{3.10}$$

We can give a simple explicit expression for the time evolution operator in the case where the Hamiltonian is independent of time, $\hat{H}(t) = \hat{H}_0$:

$$\hat{U}(t,t_0) = e^{-i\hat{H}_0(t-t_0)}\,, \tag{3.11}$$

where the exponential of an operator is defined in the usual way as an expansion in powers of the operator in the exponent.

[2] As in the static case (Chapter 2), $\mathbf{x}_j \equiv (\mathbf{r}_j,\sigma_j)$ is a shorthand notation for the space and spin coordinates of the jth electron. In the following, we shall not explicitly indicate the arguments $\mathbf{x}_1,\ldots,\mathbf{x}_N$ of an N-electron wave function, unless needed.

In the case of a general time-dependent Hamiltonian $\hat{H}(t)$, we can write the time evolution operator as

$$\hat{U}(t,t_0) = \hat{\mathcal{T}} \exp\left\{-i \int_{t_0}^{t} dt'\, \hat{H}(t')\right\} , \tag{3.12}$$

where $\hat{\mathcal{T}}$ is a time-ordering operator. This expression is important from a formal point of view, but rather difficult for practical evaluation.

We will see later, in Chapter 4, that time evolution operators are a convenient starting point to derive numerical methods for solving time-dependent single-particle Schrödinger equations.

Another area where time evolution operators are important is time-dependent perturbation theory. Let us consider the case where the time-dependent Hamiltonian can be written as follows:

$$\hat{H}(t) = \hat{H}_0 + \hat{H}_1(t) , \tag{3.13}$$

where $\hat{H}_1(t)$ describes a time-dependent perturbation which is finite only for $t \geq t_0$. To determine the associated time evolution operator, it is convenient to define

$$\hat{U}(t,t_0) = e^{-i\hat{H}_0(t-t_0)} \hat{U}_1(t,t_0) . \tag{3.14}$$

From the time-dependent Schrödinger equation, one can easily derive that

$$i\frac{\partial}{\partial t}\hat{U}_1(t,t_0) = e^{i\hat{H}_0(t-t_0)} \hat{H}_1(t) e^{-i\hat{H}_0(t-t_0)} \hat{U}_1(t,t_0) , \tag{3.15}$$

with the initial condition $\hat{U}_1(t_0,t_0) = 1$. Equation (3.15) can be solved iteratively. Of particular interest is the first-order approximation, which is obtained by substituting the zero-order solution $\hat{U}_1(t,t_0) = 1$ in the right-hand side and then integrating over time. One finds

$$\hat{U}_1(t,t_0) \approx 1 - i \int_{t_0}^{t} dt'\, e^{i\hat{H}_0(t'-t_0)} \hat{H}_1(t') e^{-i\hat{H}_0(t'-t_0)} . \tag{3.16}$$

At this point we assume that the perturbation has the form

$$\hat{H}_1(t) = F(t)\hat{\beta} , \tag{3.17}$$

where $F(t)$ is an external field that couples to an observable $\hat{\beta}$. In the interaction picture representation, the observable is written as

$$\hat{\beta}(\widetilde{t}) = e^{i\hat{H}_0\widetilde{t}} \hat{\beta} e^{-i\hat{H}_0\widetilde{t}} . \tag{3.18}$$

We thus obtain the following first-order approximation to the time evolution operator:

$$\hat{U}(t,t_0) \approx e^{-i\hat{H}_0(t-t_0)} \left\{1 - i \int_{t_0}^{t} dt'\, F(t')\hat{\beta}(t'-t_0)\right\} . \tag{3.19}$$

This expression will be essential for the derivation of the basic formulas of linear-response theory, which will be the subject of Section 7.1.

3.1.3 Continuity equation and local conservation laws

The density operator of an N-electron system is defined as

$$\hat{n}(\mathbf{r}) = \sum_{l=1}^{N} \delta(\mathbf{r} - \mathbf{r}_l) \,, \tag{3.20}$$

and the (paramagnetic) current-density operator is

$$\hat{\mathbf{j}}(\mathbf{r}) = \frac{1}{2i} \sum_{l=1}^{N} \left[\nabla_l \delta(\mathbf{r} - \mathbf{r}_l) + \delta(\mathbf{r} - \mathbf{r}_l) \nabla_l \right] \,. \tag{3.21}$$

The expectation values of the density and the current-density operators give the time-dependent density and current density (see also Appendix C),

$$n(\mathbf{r},t) = \langle \Psi(t) | \hat{n}(\mathbf{r}) | \Psi(t) \rangle \qquad \text{and} \qquad \mathbf{j}(\mathbf{r},t) = \langle \Psi(t) | \hat{\mathbf{j}}(\mathbf{r}) | \Psi(t) \rangle \,. \tag{3.22}$$

We now consider the equation of motion of the expectation value of an operator $\hat{O}(t)$:

$$i\frac{d}{dt} \langle \Psi(t) | \hat{O}(t) | \Psi(t) \rangle = \left\langle \Psi(t) \left| i\frac{\partial}{\partial t} \hat{O}(t) + [\hat{O}(t), \hat{H}(t)] \right| \Psi(t) \right\rangle \,. \tag{3.23}$$

For the density operator (3.20), this gives

$$i\frac{\partial}{\partial t} n(\mathbf{r},t) = \langle \Psi(t) | [\hat{n}(\mathbf{r}), \hat{H}(t)] | \Psi(t) \rangle \,. \tag{3.24}$$

The commutator between $\hat{n}(\mathbf{r})$ and $\hat{H}(t)$ is easily worked out, and one obtains the well-known continuity equation

$$\frac{\partial}{\partial t} n(\mathbf{r},t) = -\nabla \cdot \mathbf{j}(\mathbf{r},t) \,. \tag{3.25}$$

The continuity equation expresses the elementary law of conservation of particle number: the rate of change of the number of particles in a given volume is determined by the flux of particle current across the boundary of the volume.

One can derive an analogous equation for the current density, starting from the equation of motion for $\hat{\mathbf{j}}(\mathbf{r})$:

$$i\frac{\partial}{\partial t} \mathbf{j}(\mathbf{r},t) = \langle \Psi(t) | [\hat{\mathbf{j}}(\mathbf{r}), \hat{H}(t)] | \Psi(t) \rangle \,. \tag{3.26}$$

Working out the commutator on the right-hand side is a bit more involved but still quite straightforward, and gives the following result:

$$\frac{\partial}{\partial t} j_\mu(\mathbf{r},t) = -n(\mathbf{r},t) \frac{\partial}{\partial r_\mu} v(\mathbf{r},t) - F_\mu^{\rm kin}(\mathbf{r},t) - F_\mu^{\rm int}(\mathbf{r},t) \,, \tag{3.27}$$

where $\mu, \nu = 1, 2, 3$ are indices which label Cartesian coordinates. Equation (3.27) can be interpreted as a local force balance equation in the fixed laboratory reference frame.

The vectors $F_\mu^{\rm kin}$ and $F_\mu^{\rm int}$ correspond to the internal force densities of the many-body system due to kinetic and interaction effects. Both can be formally expressed as the divergence of stress tensors. For the kinetic force, we have $F_\mu^{\rm kin} = \sum_\nu \partial\tau_{\mu\nu}(\mathbf{r},t)/\partial r_\nu$, where the kinetic stress tensor is given by

$$\tau_{\mu\nu}(\mathbf{r},t) = \frac{1}{2}\left[\lim_{\mathbf{r}'\to\mathbf{r}}\left(\frac{\partial}{\partial r_\mu}\frac{\partial}{\partial r'_\nu} + \frac{\partial}{\partial r_\nu}\frac{\partial}{\partial r'_\mu}\right)\rho(\mathbf{r},\mathbf{r}',t) - \frac{\delta_{\mu\nu}}{2}\nabla^2 n(\mathbf{r},t)\right] , \tag{3.28}$$

and $\rho(\mathbf{r},\mathbf{r}',t)$ is the one-particle density matrix (see Appendix C).

The interaction force density is obtained from the commutator in eqn (3.26) as

$$F_\mu^{\rm int}(\mathbf{r},t) = 2\int d^3r'\,\rho_2(\mathbf{r},\mathbf{r}',t)\frac{\partial}{\partial r_\mu}w(|\mathbf{r}-\mathbf{r}'|) , \tag{3.29}$$

where ρ_2 is the diagonal two-particle density matrix. The interaction force can be recast as $F_\mu^{\rm int} = \sum_\nu \partial w_{\mu\nu}(\mathbf{r},t)/\partial r_\nu$, where the interaction stress tensor is given by[3]

$$w_{\mu\nu}(\mathbf{r},t) = -\int d^3r'\,\frac{r'_\mu r'_\nu}{r'}\frac{\partial w(r')}{\partial r'}\int_0^1 d\lambda\,\rho_2(\mathbf{r}+\lambda\mathbf{r}',\mathbf{r}-(1-\lambda)\mathbf{r}',t) . \tag{3.30}$$

The physical meaning of eqn (3.27) becomes clearer if we integrate it over all space. Defining the momentum of the system as

$$\mathbf{P}(t) = \int d^3r\,\mathbf{j}(\mathbf{r},t) , \tag{3.31}$$

we obtain

$$\frac{\partial}{\partial t}\mathbf{P}(t) = -\int d^3r\,n(\mathbf{r},t)\nabla v(\mathbf{r},t) . \tag{3.32}$$

The internal kinetic and interaction forces do not contribute, since the integral over the divergence of a stress tensor is zero (assuming the stress tensor vanishes sufficiently rapidly at infinity); this is a consequence of Newton's third law. The rate of change of the total momentum of a many-body system therefore equals the total external force on it. A similar statement can be proved for the total angular momentum of the system,

$$\mathbf{L}(t) = \int d^3r\,\mathbf{r}\times\mathbf{j}(\mathbf{r},t) ; \tag{3.33}$$

we obtain

$$\frac{\partial}{\partial t}\mathbf{L}(t) = -\int d^3r\,n(\mathbf{r},t)\mathbf{r}\times\nabla v(\mathbf{r},t) . \tag{3.34}$$

In other words, the rate of change of the total angular momentum of the system is determined exclusively by the torque coming from external forces, and the net torque coming from electron interaction forces vanishes.

This concludes our brief summary of the basic properties of time-dependent many-body systems, and will be all we need for the moment to prove the basic existence theorems of TDDFT.

[3]This relation was first given by Puff and Gillis (1968) and proved in detail by Tokatly (2005*a*). The λ-integration is understood to be along the line that connects two interacting particles.

3.2 The Runge–Gross theorem

The time-dependent Schrödinger equation (3.5) formally defines a map by which each external potential $v(\mathbf{r},t)$ produces a time-dependent wave function $\Psi(t)$, for a given initial state Ψ_0. A second map generates a density $n(\mathbf{r},t)$ from $\Psi(t)$. This can be illustrated as follows:

$$v(\mathbf{r},t) \xrightarrow[\text{fixed } \Psi_0]{i\partial\Psi/\partial t = \hat{H}(t)\Psi} \Psi(t) \xrightarrow{\langle\Psi(t)|\hat{n}|\Psi(t)\rangle} n(\mathbf{r},t)\,. \tag{3.35}$$

Physically, this means that the dynamics of the system is determined by the time-dependent potential, via the Schrödinger equation.

To construct a time-dependent density-functional theory, the map (3.35) needs to be turned around: we need to show that the time-dependent density $n(\mathbf{r},t)$ is equally valid as a variable which completely determines the dynamics of the system. To do this, it must be proved that there is a unique, one-to-one correspondence between time-dependent densities and potentials. Such a correspondence was first established by Runge and Gross (1984),[4] and we shall now discuss their proof.

What needs to be shown is that two different time-dependent potentials, $v(\mathbf{r},t)$ and $v'(\mathbf{r},t)$, acting on a system with a given fixed initial state, will always cause different time-dependent densities $n(\mathbf{r},t)$ and $n'(\mathbf{r},t)$. In other words, a potential $v(\mathbf{r},t)$ is uniquely associated with a density $n(\mathbf{r},t)$, and vice versa.

Let us first of all clarify what we mean by "different potentials." If two potentials differ only by an additive time-dependent scalar function $c(t)$, then the corresponding wave functions differ only by a simple time-dependent phase factor:

$$\widetilde{v}(\mathbf{r},t) = v(\mathbf{r},t) + c(t) \qquad \Longrightarrow \qquad \widetilde{\Psi}(t) = e^{-i\alpha(t)}\Psi(t)\,, \tag{3.36}$$

where $d\alpha(t)/dt = c(t)$. This follows easily from the time-dependent Schrödinger equation. The resulting densities will be identical, since the phase factors cancel out:[5]

$$\widetilde{n}(\mathbf{r},t) = \langle\widetilde{\Psi}(t)|\hat{n}(\mathbf{r})|\widetilde{\Psi}(t)\rangle = \langle\Psi(t)|e^{i\alpha(t)}\hat{n}(\mathbf{r})e^{-i\alpha(t)}|\Psi(t)\rangle = \langle\Psi(t)|\hat{n}(\mathbf{r})|\Psi(t)\rangle = n(\mathbf{r},t)\,. \tag{3.37}$$

Therefore, in the following we shall consider two potentials that differ by more than just a time-dependent function: $v(\mathbf{r},t) - v'(\mathbf{r},t) \neq c(t)$.

The next question concerns the analytical structure of admissible time-dependent potentials. We first consider the time dependence, and will discuss the spatial dependence later. We use the condition that the potentials can be expanded in a Taylor series about the initial time:

$$v(\mathbf{r},t) = \sum_{k=0}^{\infty} \frac{1}{k!} v_k(\mathbf{r})(t-t_0)^k\,, \tag{3.38}$$

[4]Earlier work towards a rigorous formulation of TDDFT, carried out by Bartolotti (1981, 1982) and Deb and Ghosh (1982), was restricted to special cases such as periodic potentials and adiabatic processes. The Runge–Gross proof was the first for general time-dependent scalar potentials.

[5]This is generally true for the expectation values $\langle\Psi(t)|\hat{O}|\Psi(t)\rangle$ of any operator $\hat{O}$ that does not contain time derivatives.

and similarly for $v'(\mathbf{r},t)$ with expansion coefficients $v'_k(\mathbf{r})$. The statement that the two potentials v and v' differ by more than just a function $c(t)$ can then be expressed through the requirement that there exists a smallest integer $k \geq 0$ such that

$$v_k(\mathbf{r}) - v'_k(\mathbf{r}) \neq \text{const.} \tag{3.39}$$

At this point, we do not make any assumptions about the radius of convergence of the series (3.38), except that it is greater than zero. Notice in particular that the initial state of the system, Ψ_0, is not required to be an eigenstate of the initial potential $v(\mathbf{r},t_0)$. This means that the case of sudden switching is included in the formalism.

The Runge–Gross proof now proceeds in two steps. First, we will establish the uniqueness of the current densities, and proceed from there to the particle densities.

Step 1. We start from the equation of motion for the current density, eqn (3.26). Since both $\Psi(t)$ and $\Psi'(t)$ evolve from the same initial state Ψ_0, we get

$$\begin{aligned}\frac{\partial}{\partial t}\left\{\mathbf{j}(\mathbf{r},t) - \mathbf{j}'(\mathbf{r},t)\right\}\Big|_{t=t_0} &= -i\langle\Psi_0|[\hat{\mathbf{j}}(\mathbf{r}), \hat{H}(t_0) - \hat{H}'(t_0)]|\Psi_0\rangle \\ &= -n(\mathbf{r},t_0)\nabla\left\{v(\mathbf{r},t_0) - v'(\mathbf{r},t_0)\right\}\ . \end{aligned} \tag{3.40}$$

Since we start from the same initial state, the internal kinetic and interaction forces in eqn (3.27) are identical at t_0 in the unprimed and primed systems and cancel out.

From eqn (3.40), it follows immediately that the two current densities $\mathbf{j}$ and $\mathbf{j}'$ will differ infinitesimally later than t_0 if the two potentials v and v' are different. If the condition (3.39) is satisfied for $k = 0$, i.e., the potentials are different at t_0, then the right-hand side of eqn (3.40) is different from zero and the two current densities $\mathbf{j}$ and $\mathbf{j}'$ will become different infinitesimally later than t_0.

If the smallest integer k for which eqn (3.39) holds is greater than zero, then the first time derivatives of the currents are equal, and the difference between $\mathbf{j}$ and $\mathbf{j}'$ shows up in higher time derivatives. Using the equation of motion (3.23) k times, we then get

$$\frac{\partial^{k+1}}{\partial t^{k+1}}\left\{\mathbf{j}(\mathbf{r},t) - \mathbf{j}'(\mathbf{r},t)\right\}\Big|_{t=t_0} = -n(\mathbf{r},t_0)\nabla\left\{v_k(\mathbf{r}) - v'_k(\mathbf{r})\right\}\ , \tag{3.41}$$

where, according to eqn (3.39), k is the smallest integer for which the right-hand side does not vanish. We therefore conclude that $\mathbf{j}(\mathbf{r},t) \neq \mathbf{j}'(\mathbf{r},t)$ for $t > t_0$.

Step 2. Now we need to show that having different current densities means that the densities themselves are different. We start from the continuity equation (3.25) and calculate the $(k+1)$st time derivative of it:

$$\begin{aligned}\frac{\partial^{k+2}}{\partial t^{k+2}}\left\{n(\mathbf{r},t) - n'(\mathbf{r},t)\right\}\Big|_{t=t_0} &= -\nabla\cdot\frac{\partial^{k+1}}{\partial t^{k+1}}\left\{\mathbf{j}(\mathbf{r},t) - \mathbf{j}'(\mathbf{r},t)\right\}\Big|_{t=t_0} \\ &= -\nabla\cdot(n_0(\mathbf{r})\nabla w_k(\mathbf{r})), \end{aligned} \tag{3.42}$$

where we have defined $w_k(\mathbf{r}) = v_k(\mathbf{r}) - v'_k(\mathbf{r})$ and $n_0(\mathbf{r}) = n(\mathbf{r},t_0)$. We now need to show that the right-hand side of eqn (3.42) cannot vanish identically as long as eqn

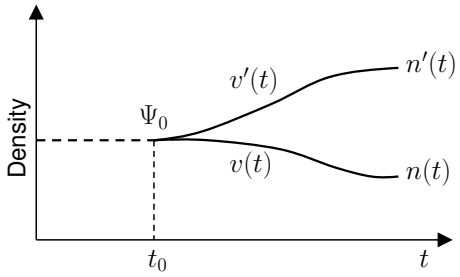

Fig. 3.1 Illustration of the Runge–Gross theorem: if a many-body system evolves under the influence of two different time-dependent potentials $v(\mathbf{r},t)$ and $v'(\mathbf{r},t)$, starting from a fixed initial state Ψ_0, then the resulting time-dependent densities $n(\mathbf{r},t)$ and $n'(\mathbf{r},t)$ will become different infinitesimally later than t_0.

(3.39) holds, i.e., as long as $w_k(\mathbf{r})$ is not zero for some integer k. For this, we consider the following relation, which follows from Green's integral theorem:

$$\int d^3r\, n_0(\mathbf{r})(\nabla w_k(\mathbf{r}))^2 = -\int d^3r\, w_k(\mathbf{r})\nabla\cdot(n_0(\mathbf{r})\nabla w_k(\mathbf{r})) + \oint d\mathbf{S}\cdot(n_0(\mathbf{r})w_k(\mathbf{r})\nabla w_k(\mathbf{r})). \tag{3.43}$$

The crucial object in this equation is the surface integral on the right-hand side: the Runge–Gross proof hinges on the fact that it vanishes for all physically realistic potentials, i.e., potentials which arise from finite normalizable external charge distributions. It can be shown that such potentials go to zero at least as fast as $1/r$, so that the surface integral indeed vanishes (Gross and Kohn, 1990).[6]

Now that we have got rid of the surface integral, let us look at what is left in eqn (3.43). The left-hand side does not vanish, since by assumption $w_k \neq 0$, and the integrand is therefore nonnegative everywhere. As a consequence, the first integral on the right-hand side of eqn (3.43) is also nonvanishing, which, together with $w_k \neq 0$, immediately implies that $\nabla\cdot(n_0(\mathbf{r})\nabla w_k(\mathbf{r})) \neq 0$.

This completes Step 2 of the Runge–Gross proof: we have indeed shown that the right-hand side of eqn (3.42) cannot vanish identically, and therefore the densities themselves are different infinitesimally later than t_0. An illustration is given in Fig. 3.1. Let us now summarize and discuss what we have proved in this section:

> **Runge–Gross theorem.** Two densities $n(\mathbf{r},t)$ and $n'(\mathbf{r},t)$, evolving from a common initial many-body state Ψ_0 under the influence of two different potentials $v(\mathbf{r},t)$ and $v'(\mathbf{r},t) \neq v(\mathbf{r},t)+c(t)$ (both assumed to be Taylor-expandable around t_0), will start to become different infinitesimally later than t_0. Therefore, there is a one-to-one correspondence between densities and potentials, for any fixed initial many-body state.

[6]This covers essentially all situations encountered in practice; some counterexamples have been given in the literature (Xu and Rajagopal, 1985), which, however, have turned out to be unphysical. This was discussed by Gross and Kohn (1990), including more general classes of potentials for which the surface integral in eqn (3.43) vanishes.

This is the fundamental existence theorem of TDDFT: from the one-to-one correspondence, it follows immediately that the time-dependent density is a unique functional of the potential, but also, vice versa, that the external potential in eqn (3.3) is a unique functional of the time-dependent density (for a given fixed initial state). This means that the many-body Hamiltonian $\hat{H}(t)$ and thus the many-body wave function $\Psi(t)$ are functionals of $n(\mathbf{r},t)$ as well:

$$v(\mathbf{r},t) = v[n,\Psi_0](\mathbf{r},t) \implies \hat{H}(t) = \hat{H}[n,\Psi_0](t) \implies \Psi(t) = \Psi[n,\Psi_0](t)\,. \quad (3.44)$$

Here, we have explicitly indicated the dependence on the fixed initial state Ψ_0. As an immediate consequence, we deduce that all physical observables become functionals of the density:

$$O(t) = \langle \Psi[n,\Psi_0]|\hat{O}(t)|\Psi[n,\Psi_0]\rangle = O[n,\Psi_0](t)\,. \quad (3.45)$$

This provides the fundamental underpinnings of TDDFT: it tells us that, at least on a formal level, the time-dependent density is all we need to obtain any desired observable of a time-dependent many-particle system. We shall see later, when it comes to practical applications, that some observables are easily expressed as explicit functionals of the density, whereas others are not.

To conclude this section and provide motivation for further development, let us now make a few general remarks about the conditions of validity and the limitations of the Runge–Gross theorem.

As we have seen, it is crucial for the Runge–Gross theorem to be very precise as to what external potentials are allowed. In eqn (3.38) we imposed the requirement that $v(\mathbf{r},t)$ be expandable in a Taylor series about the initial time t_0. It turns out that this requirement rules out an important class of potentials, namely those that are adiabatically switched on starting from $t_0 = -\infty$ and using a switch-on function $e^{\eta t}$, where η is a real positive infinitesimal. Mathematically, the root of the problem is that the function $e^{\eta t}$ has an essential singularity at $-\infty$ and thus cannot be Taylor-expanded. Such potentials play a role if one wishes to describe a monochromatic wave acting on the system. However, there is no need for despair: all we need to do is to switch on the potential not in the infinite past, but at some large but finite negative time t_0. As long as the parameter η remains larger than $1/|t_0|$ (not a serious limitation if t_0 is sufficiently large), the conditions for the Runge–Gross theorem are safely satisfied.[7]

Now let us come to some real limitations. First of all, the Runge–Gross theorem deals only with scalar potentials. This means that a large class of practically important phenomena, namely those involving electromagnetic waves or time-varying magnetic fields, are not described by it. We shall come back to this point in Chapter 10 when we describe time-dependent current-DFT, which will allow us to treat vector potentials.

Secondly, the Runge–Gross proof as it was presented here is restricted to finite systems, where the surface integral in eqn (3.43) can be shown to vanish. We will need to address the question of what happens in infinitely extended systems such as periodic solids. This will be discussed in Section 12.4.

[7] As we will see later in Section 7.3, this is also not an obstacle to the formulation of the frequency-dependent linear response in TDDFT.

To be useful in practice, we would like a scheme, analogous to the Kohn–Sham formalism of static DFT, that allows us to calculate time-dependent densities in a simpler manner than by solving the full many-body Schrödinger equation (3.5). The formal proof which will eventually allow us to use a time-dependent Kohn–Sham formalism is provided by the van Leeuwen theorem, which will be the subject of the next section.

3.3 The van Leeuwen theorem

In the previous section we proved that the time-dependent density $n(\mathbf{r},t)$ of a many-body system with a given particle–particle interaction $w(|\mathbf{r}-\mathbf{r}'|)$ and a given fixed initial state Ψ_0 is a unique functional of the time-dependent potential $v(\mathbf{r},t)$. This basic and universal property of electronic many-body systems is the reason why we can formally speak of "density functionals" in a rigorous and meaningful way.

When it comes to practical applications of TDDFT, we would very much like to use the same trick that works so beautifully in static DFT, namely, replacing the interacting system with an auxiliary noninteracting system that reproduces the same density. However, the Runge–Gross theorem does not prove that we are actually allowed to do this—we need to go a bit further.

The question is the following: can exactly the same density $n(\mathbf{r},t)$ be reproduced in a many-body system with different two-particle interactions $w'(|\mathbf{r}-\mathbf{r}'|)$ (which could be zero!), starting from a different initial state Ψ_0' and under the influence of a different external potential $v'(\mathbf{r},t)$? And if so, is this potential unique (up to within a purely time-dependent function)? This question was answered in the affirmative by van Leeuwen (1999), under some rather mild restrictions, as we shall now discuss. More than that, it will turn out that van Leeuwen's theorem does a number of remarkable things, as we shall see below after having gone through the proof.

We consider a second many-body system with the Hamiltonian

$$\hat{H}'(t) = \hat{T} + \hat{V}'(t) + \hat{W}' \,, \tag{3.46}$$

with a time-evolved many-body state $\Psi'(t)$ and initial state Ψ_0'. The goal is to construct $v'(\mathbf{r},t)$ explicitly and uniquely, with the only constraint being that $v'(\mathbf{r},t)$ vanishes at infinity, just like $v(\mathbf{r},t)$. Let us write down the Taylor series[8]

$$v'(\mathbf{r},t) = \sum_{k=0}^{\infty} \frac{1}{k!} v_k'(\mathbf{r})(t-t_0)^k, \tag{3.47}$$

where $v_k'(\mathbf{r}) = \partial^k v'(\mathbf{r},t)/\partial t^k\big|_{t=t_0}$. Construction of $v'(\mathbf{r},t)$ thus requires a way to determine the Taylor expansion coefficients $v_k'(\mathbf{r})$ in a unique manner. To do this, let us go back to Section 3.1.3, where we considered conservation laws of time-dependent

[8]From this, the potential $v'(\mathbf{r},t)$ is completely determined within the convergence radius of the Taylor series. We shall assume that this convergence radius is not zero, which rules out nonanalyticities of the density and potentials at t_0. If the convergence radius is nonzero but finite, one can carry out an analytic continuation along the real time axis by first propagating to a finite time t_1 within the convergence radius, and then restarting the procedure taking t_1 as the new initial time.

many-body systems. Let us take the divergence of eqn (3.27) and use the continuity equation (3.25), which gives

$$\frac{\partial^2}{\partial t^2} n(\mathbf{r},t) = \nabla \cdot (n(\mathbf{r},t) \nabla v(\mathbf{r},t)) + q(\mathbf{r},t). \tag{3.48}$$

Here, the quantity $q(\mathbf{r},t)$ is given by

$$q(\mathbf{r},t) = \nabla \cdot \mathbf{F}^{\rm kin}(\mathbf{r},t) + \nabla \cdot \mathbf{F}^{\rm int}(\mathbf{r},t), \tag{3.49}$$

where the kinetic and interaction forces $\mathbf{F}^{\rm kin}$ and $\mathbf{F}^{\rm int}$ are defined in Section 3.1.3. Equation (3.48) is valid for any many-body system. Assuming that the two densities $n(\mathbf{r},t)$ and $n'(\mathbf{r},t)$ are identical at all times, we can subtract eqns (3.48) for the primed and unprimed systems, which gives

$$\nabla \cdot (n(\mathbf{r},t) \nabla \gamma(\mathbf{r},t)) = \zeta(\mathbf{r},t), \tag{3.50}$$

where $\gamma(\mathbf{r},t) = v(\mathbf{r},t) - v'(\mathbf{r},t)$ and $\zeta(\mathbf{r},t) = q'(\mathbf{r},t) - q(\mathbf{r},t)$.

Equation (3.50) will be central to the following argument, since it directly connects densities and potentials. Let us now see how this works. First of all, eqn (3.50) originates from the second-order differential equation in time (3.48), and therefore requires two initial conditions. The first one is pretty obvious, namely, that the initial states Ψ_0 and Ψ_0' yield the same density,

$$n(\mathbf{r},t_0) = n'(\mathbf{r},t_0). \tag{3.51}$$

The second initial condition is

$$\left.\frac{\partial}{\partial t} n(\mathbf{r},t)\right|_{t=t_0} = \left.\frac{\partial}{\partial t} n'(\mathbf{r},t)\right|_{t=t_0}. \tag{3.52}$$

This condition implies another rather obvious physical requirement, which follows directly from the expression for the total momentum

$$\mathbf{P}(t) = \int d^3r\, \mathbf{j}(\mathbf{r},t) = \int d^3r\, \mathbf{r} \frac{\partial}{\partial t} n(\mathbf{r},t), \tag{3.53}$$

namely that the initial state Ψ_0' must be chosen such that the initial momenta of the two systems are the same.[9] Furthermore, we also require the total momentum of Ψ_0 to be finite, and likewise for Ψ_0' via eqn (3.53). We ensure this by limiting ourselves to finite systems for which the densities and currents vanish at infinity.

Equation (3.50) does not contain any time derivatives, which means that the time variable enters as a parameter only. Let us specify the boundary condition $\gamma(\mathbf{r},t) = 0$ at infinity, which also implies that we fix the arbitrary time-dependent function $c(t)$

[9] If the densities $n(\mathbf{r},t)$ and $n'(\mathbf{r},t)$ are the same at all times, then eqn (3.53) implies that the total momenta of the systems are equal at all times. This cannot be satisfied if the initial momenta at t_0 are different, since this would require an infinite force to make them equal for $t > t_0$. This illustrates the physical meaning behind the constraint (3.52).

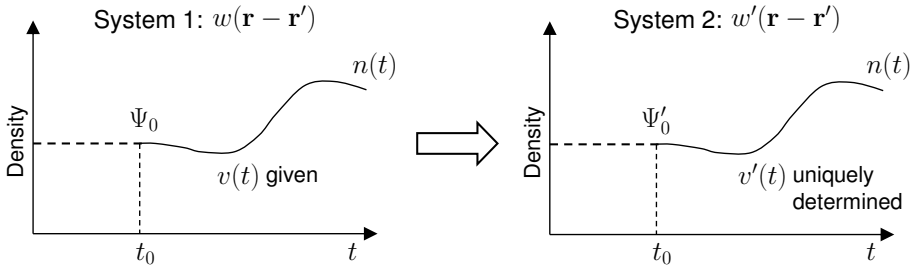

Fig. 3.2 Illustration of the van Leeuwen theorem: a time-dependent density coming from a many-body system with interaction $w(\mathbf{r}-\mathbf{r}')$ and potential $v(\mathbf{r},t)$ (System 1) can be reproduced in a different many-body system with interaction $w'(\mathbf{r}-\mathbf{r}')$ and potential $v'(\mathbf{r},t)$ (System 2). The potential $v'(\mathbf{r},t)$ is uniquely determined by explicit construction.

in $v'(\mathbf{r},t)$. Then, eqn (3.50) has a unique solution for $\gamma(\mathbf{r},t)$ if $n(\mathbf{r},t)$ and $\zeta(\mathbf{r},t)$ are given.[10]

Let us first look at $t=t_0$, where eqn (3.50) becomes

$$\nabla\cdot(n(\mathbf{r},t_0)\nabla v_0'(\mathbf{r})) = \nabla\cdot(n(\mathbf{r},t_0)\nabla v_0(\mathbf{r})) - \zeta(\mathbf{r},t_0). \tag{3.54}$$

This equation yields a unique solution for the zero-order term $v_0'(\mathbf{r})$ in the Taylor expansion (3.47), since $n(\mathbf{r},t)$ and $v(\mathbf{r},t)$ are known at all times and the quantity $\zeta(\mathbf{r},t_0)$ can be calculated from the given initial states Ψ_0 and Ψ_0'.

Next, we take the first time derivative of eqn (3.50) at $t=t_0$:

$$\begin{aligned}\nabla\cdot(n(\mathbf{r},t_0)\nabla v_1'(\mathbf{r})) = \nabla\cdot(n(\mathbf{r},t_0)\nabla v_1(\mathbf{r})) - \left.\frac{\partial\zeta(\mathbf{r},t)}{\partial t}\right|_{t=t_0} \\ - \nabla\cdot\left(\left.\frac{\partial n(\mathbf{r},t)}{\partial t}\right|_{t=t_0}\nabla(v_0(\mathbf{r})-v_0'(\mathbf{r}))\right).\end{aligned} \tag{3.55}$$

Again, all quantities on the right-hand side are known: the quantity $\partial\zeta(\mathbf{r},t)/\partial t|_{t=t_0}$ can again be calculated[11] from the given initial states Ψ_0 and Ψ_0', and $v_0'(\mathbf{r})$ has already been determined from eqn (3.54). Therefore, eqns (3.55) and (3.54) have the same structure, and we can obtain a unique solution for $v_1'(\mathbf{r})$.

The procedure can now be repeated for the second and higher time derivatives of eqn (3.50) at $t=t_0$, and we can see the emerging pattern: the coefficients $v_k'(t)$ in the Taylor expansion (3.47) are calculated in a recursive manner from differential equations of the type (3.54) and (3.55), where the right-hand sides involve only known quantities and coefficients up to $v_{k-1}'(\mathbf{r})$ that have already been calculated.

This constructive procedure determines $v'(\mathbf{r},t)$ completely. Let us now summarize what we have proved (see also the illustration in Fig. 3.2):

[10] This follows since eqn (3.50) is of the Sturm–Liouville type, as discussed in van Leeuwen (2001).

[11] We have $\partial\zeta(\mathbf{r},t)/\partial t|_{t=t_0} = i\langle\Psi_0|[\hat{q}(\mathbf{r}),\hat{H}(t_0)]|\Psi_0\rangle - i\langle\Psi_0'|[\hat{q}'(\mathbf{r}),\hat{H}'(t_0)]|\Psi_0'\rangle$, where the operator $\hat{q}(\mathbf{r})$ is defined via $q(\mathbf{r},t)=\langle\Psi(t)|\hat{q}(\mathbf{r})|\Psi(t)\rangle$. Higher time derivatives of ζ involve multiple commutators of $\hat{q}(\mathbf{r})$ and $\hat{q}'(\mathbf{r})$ with $\hat{H}$ and $\hat{H}'$.

Van Leeuwen theorem. For a time-dependent density $n(\mathbf{r}, t)$ associated with a many-body system with a given particle–particle interaction $w(|\mathbf{r} - \mathbf{r}'|)$, external potential $v(\mathbf{r}, t)$, and initial state Ψ_0, there exists a different many-body system featuring an interaction $w'(|\mathbf{r} - \mathbf{r}'|)$ and a unique external potential $v'(\mathbf{r}, t)$ [up to a purely time-dependent $c(t)$] which reproduces the same time-dependent density. The initial state Ψ_0' in this system must be chosen such that it correctly yields the given density and its time derivative at the initial time.

The true power of this theorem becomes clear if we consider two special cases. Let us first take $w' = w$, i.e., two many-body systems with the same interaction. At first sight this may seem a somewhat strange thing to do, but one immediately discovers that this reduces to something very familiar. If we choose $\Psi_0' = \Psi_0$, which means that the primed system trivially reproduces the initial density and its time derivative for the unprimed system, then it is proved that there exists a unique potential $v'(\mathbf{r}, t)$ that yields $n(\mathbf{r}, t)$. This is precisely the content of the Runge–Gross theorem, which is thus shown to emerge as a special case of the van Leeuwen theorem.

The other case of particular interest is $w' = 0$, i.e., we choose the second system to be a noninteracting one. Assuming there exists a noninteracting initial state $\Psi_0' \equiv \Phi_0$ with the correct initial density and time derivative of the density, the van Leeuwen theorem tells us that there is a unique potential $v_s(\mathbf{r}, t)$ [apart from the usual time-dependent function $c(t)$] in a noninteracting system which produces $n(\mathbf{r}, t)$ at all times $t > t_0$. This provides the formal justification for the time-dependent Kohn–Sham approach, which will be discussed in the next chapter.

The question of whether one can always find a potential which reproduces a given density is known as the *v-representability problem* and has a long history in DFT (see Section 2.1.3). A general overview and a discussion of v-representability in TDDFT on lattice spaces were given by Li and Ullrich (2008) and Verdozzi (2008). Several formal and mathematical aspects of the existence of the effective potentials in TDDFT were recently investigated by Ruggenthaler *et al.* (2009, 2010).

The van Leeuwen theorem relies on a Taylor expansion of the potential around the initial time and, in addition, requires the density to be analytic in time at t_0 [see eqn (3.55)]. Under these restrictions, the noninteracting v-representability problem in TDDFT is solved by the van Leeuwen theorem, provided we can find an initial state with the required properties.[12] Of particular interest are switch-on processes, where the system has been in the ground state at all previous times $t < t_0$, and where the associated initial state Ψ_0 leads to a density with zero time derivative at t_0. In that case, it is always possible to find a noninteracting initial state with the given density by construction (Harriman, 1981). This means that for this kind of switch-on process, a time-dependent Kohn–Sham potential always exists.

However, it was recently discovered (Maitra *et al.*, 2010) that there exist densities that are *nonanalytic* in time, although they come from reasonable (i.e., Taylor-expandable) time-dependent potentials. These cases are related to spatial singularities:

[12]Whether or not this initial state can be chosen as a noninteracting ground state cannot be definitely answered in general—this is again the noninteracting v-representability problem for ground-state systems.

important examples are provided by densities that have cusps. Take, for instance, a hydrogen atom and suddenly remove the nucleus; the cusp immediately becomes smooth, which indicates a locally nonanalytic behavior. Other examples also exist. The proof of the van Leeuwen theorem which was given above becomes questionable for densities with nonanalytic time dependence.

At present, intense efforts are under way to find alternative proofs which do not rely on the Taylor-expandability of the potential or the density. Some progress has recently been made for lattice systems (Tokatly, 2011). Other attempts have focused on eqn (3.48): the goal is to find a direct solution for $v(\mathbf{r},t)$ for a given $n(\mathbf{r},t)$, using mathematical tools in the field of nonlinear differential equations (Maitra *et al.*, 2010). A global fixed-point proof of the uniqueness of the solution of eqn (3.48) has recently been found (Ruggenthaler and van Leeuwen, 2011), but a complete existence proof is still missing.

Fortunately, the foundations of TDDFT remain sound: the Runge–Gross theorem is still valid as long as the *potential* is Taylor-expandable—even for nonanalytic densities (Yang *et al.*, 2012). The remaining unresolved questions regarding the van Leeuwen theorem and time-dependent v-representability are the subject of current research.

Exercise 3.1 Work out the commutator $[\hat{n},\hat{H}]$ to prove the continuity equation (3.25).

Exercise 3.2 Prove eqn (3.34), using the current continuity equation (3.27) [you can find an outline of the proof in van Leeuwen (2001)].

Exercise 3.3 The continuity equation (3.25) and the force balance equation (3.27) can also be formulated in terms of the density and the velocity field $\mathbf{u}(\mathbf{r},t)=\mathbf{j}(\mathbf{r},t)/n(\mathbf{r},t)$. Show that they have the following form:

$$\begin{aligned} D_t n(\mathbf{r},t) &= -n(\mathbf{r},t)\nabla\cdot\mathbf{u}(\mathbf{r},t)\,, \\ n(\mathbf{r},t)D_t u_\mu(\mathbf{r},t) &= -n(\mathbf{r},t)\frac{\partial}{\partial r_\mu}v(\mathbf{r},t)-\sum_\nu\frac{\partial}{\partial r_\nu}\left(\tau'_{\mu\nu}(\mathbf{r},t)+w_{\mu\nu}(\mathbf{r},t)\right), \end{aligned}$$

where $D_t=\partial/\partial t+\mathbf{u}\nabla$ is the convective derivative. How is the kinetic stress tensor $\tau'_{\mu\nu}$ different from $\tau_{\mu\nu}$ defined in eqn (3.28)?

Exercise 3.4 (a) Prove the continuity equation (3.25) for a single particle directly from the Schrödinger equation. (b) Prove the force-balance equation (3.27) for a single particle by directly working out the time derivative of the current density and the kinetic force density.

Exercise 3.5 Express the two-particle density matrix $\rho_2(\mathbf{r},\mathbf{r}',t)$ in eqn (3.29) in terms of the xc hole $\rho_{\rm xc}(\mathbf{r},\mathbf{r}',t)$ (see Appendix C). Show that the interaction force density can then be written as

$$F^{\rm int}_\mu(\mathbf{r},t)=n(\mathbf{r},t)\frac{\partial v_{\rm H}(\mathbf{r},t)}{\partial r_\mu}+\sum_\nu\frac{\partial}{\partial r_\nu}w^{\rm xc}_{\mu\nu}(\mathbf{r},t)\,,$$

where $v_{\rm H}(\mathbf{r},t)=\int d^3r'\,n(\mathbf{r}',t)/|\mathbf{r}-\mathbf{r}'|$ is the Hartree potential, and

$$w^{\rm xc}_{\mu\nu}(\mathbf{r},t)=-\int d^3r'\,\frac{r'_\mu r'_\nu}{r'}\frac{\partial w(r')}{\partial r'}\int_0^1 d\lambda\,n(\mathbf{r}+\lambda\mathbf{r}',t)\rho_{\rm xc}(\mathbf{r}+\lambda\mathbf{r}',\mathbf{r}-(1-\lambda)\mathbf{r}',t)\,.$$

4

The time-dependent Kohn–Sham scheme

4.1 The time-dependent Kohn–Sham equation

The van Leeuwen theorem, discussed in the previous section, guarantees that the time-dependent density $n(\mathbf{r},t)$ of an interacting system, evolving from an initial state Ψ_0 under the influence of a potential $v(\mathbf{r},t)$, can also be reproduced by a noninteracting system. This noninteracting system evolves under the effective potential

$$v_s[n,\Psi_0,\Phi_0](\mathbf{r},t), \tag{4.1}$$

which is in general a functional of the time-dependent density, the initial many-body state, and the initial state Φ_0 of the noninteracting system.

In practice one often encounters situations where the system is in the ground state at the initial time t_0 (and has been for all times $t < t_0$), and then begins to evolve under the influence of an explicitly time-dependent external potential. We can write this as follows:

$$v(\mathbf{r},t) = v_0(\mathbf{r}) + v_1(\mathbf{r},t)\theta(t-t_0)\,, \tag{4.2}$$

where $\theta(t-t_0)$ denotes the step function (1 or 0 for a positive or a negative argument, respectively). In such situations, the Hohenberg–Kohn theorem of static DFT applies to the initial state, and the initial wave functions Ψ_0 and Φ_0 are both functionals of the ground-state density $n_0(\mathbf{r})$. This leads to considerable formal simplifications, since now the effective potential (4.1) becomes a density functional only, $v_s[n](\mathbf{r},t)$.

The initial noninteracting wave function Φ_0 is a single Slater determinant made up of N Kohn–Sham orbitals $\varphi_j^0(\mathbf{r})$, following from a self-consistent solution of the static Kohn–Sham equation

$$\left[-\frac{\nabla^2}{2} + v_s^0[n_0](\mathbf{r})\right]\varphi_j^0(\mathbf{r}) = \varepsilon_j\varphi_j^0(\mathbf{r})\,, \tag{4.3}$$

where the ground-state density is given by

$$n_0(\mathbf{r}) = \sum_{j=1}^{N} |\varphi_j^0(\mathbf{r})|^2 \tag{4.4}$$

and the static Kohn–Sham effective potential is

$$v_s^0[n_0](\mathbf{r}) = v_0(\mathbf{r}) + \int d^3r' \frac{n_0(\mathbf{r}')}{|\mathbf{r}-\mathbf{r}'|} + v_{\rm xc}^0[n_0](\mathbf{r}) \,. \tag{4.5}$$

The general formalism of ground-state DFT and static Kohn–Sham theory was introduced and discussed in Chapter 2.

Immediately after the initial time t_0, the time-dependent potential $v_1(\mathbf{r},t)$ kicks in and the system starts to evolve in time under its influence. The time-dependent density is given by

$$n(\mathbf{r},t) = \sum_{j=1}^{N} |\varphi_j(\mathbf{r},t)|^2 \,, \tag{4.6}$$

where the single-particle orbitals $\varphi_j(\mathbf{r},t)$ follow from the time-dependent Kohn–Sham (TDKS) equation

$$\left[-\frac{\nabla^2}{2} + v_s[n](\mathbf{r},t)\right] \varphi_j(\mathbf{r},t) = i\frac{\partial}{\partial t}\varphi_j(\mathbf{r},t) \,, \tag{4.7}$$

with the initial condition

$$\varphi_j(\mathbf{r},t_0) = \varphi_j^0(\mathbf{r}) \,. \tag{4.8}$$

In other words, we time-propagate, via solution of the TDKS equation (4.7), only those single-particle orbitals that were initially occupied. The time evolution of initially empty Kohn–Sham orbitals is not of interest in TDDFT.

The effective potential in eqn (4.7) is given by

$$v_s[n](\mathbf{r},t) = v(\mathbf{r},t) + \int d^3r' \frac{n(\mathbf{r}',t)}{|\mathbf{r}-\mathbf{r}'|} + v_{\rm xc}[n](\mathbf{r},t) \,. \tag{4.9}$$

This *defines* the time-dependent xc potential $v_{\rm xc}[n](\mathbf{r},t)$. The second term on the right-hand side is the time-dependent Hartree potential $v_{\rm H}(\mathbf{r},t)$, which depends only on the density at the same time t.

The TDKS formalism summarized here produces, in principle, the *exact* time-dependent density of the N-electron system evolving in the external potential (4.2), starting from the ground state associated with $v_0(\mathbf{r})$. To make this a workable scheme in practice, several steps are involved, each requiring its own approximations:

- Preparation of the initial state of the system by solving the static Kohn–Sham equation self-consistently. This requires an approximation to the static xc potential $v_{\rm xc}^0[n_0](\mathbf{r})$.
- Time propagation of the N initially occupied single-particle orbitals $\varphi_j(\mathbf{r},t)$ from the initial time t_0 to some chosen final time t_1. This requires an approximation to the time-dependent xc potential $v_{\rm xc}[n](\mathbf{r},t)$. The most basic one, the adiabatic approximation, will be discussed in Section 4.3. Various rigorous properties of $v_{\rm xc}[n](\mathbf{r},t)$ will be addressed in Chapter 6.
- We will need an understanding of the concept of self-consistency in TDDFT, which has a somewhat different meaning from static DFT. In practice, we will of course need numerical algorithms for time propagation, which allow us to solve the TDKS equation on a computer. We will discuss these issues in Sections 4.4 and 4.5.

- Once we have obtained the time-dependent density $n(\mathbf{r}, t)$, we need to use it as input for the physical observables of interest to get the answers we seek. In other words, we need to be able to express physical observables as density functionals, which may be easy in some cases and more difficult in others. This will be the subject of Chapter 5.

Another important point needs to be mentioned here, namely, that the static xc potential that is used to calculate the initial ground state and the time-dependent xc potential which is used for the time propagation have to match at the initial time. This means that the approximate functionals we choose in our calculation have to satisfy the condition $v_{\rm xc}[n_0](\mathbf{r}, t_0) = v^0_{\rm xc}[n_0](\mathbf{r})$. Only then is it guaranteed that the density remains static if the system is not subject to any time-dependent potential at $t > t_0$ or to any sudden change at $t = t_0$.

We point out, finally, that the assumption that the system starts initially from the ground state is convenient but not fundamentally essential. The same TDKS equations hold when the system does not start from a ground state (as long as Φ_0 is a single Slater determinant); the only difference is that then the xc potential becomes a functional of the initial states, as indicated in eqn (4.1).[1]

4.2 Spin-dependent systems

So far, we have not said anything about spin. Just as in ground-state DFT, the TDKS equations are often written in a form which explicitly carries a spin index $\sigma = \uparrow, \downarrow$:

$$\left[-\frac{\nabla^2}{2} + v_\sigma(\mathbf{r}, t) + \int d^3r' \frac{n(\mathbf{r}', t)}{|\mathbf{r} - \mathbf{r}'|} + v_{{\rm xc},\sigma}[n_\uparrow, n_\downarrow](\mathbf{r}, t)\right] \varphi_{j\sigma}(\mathbf{r}, t) = i\frac{\partial}{\partial t}\varphi_{j\sigma}(\mathbf{r}, t)\,, \tag{4.10}$$

where the total density is given by the sum of the spin-up and spin-down densities:

$$n(\mathbf{r}, t) = \sum_{\sigma=\uparrow,\downarrow} n_\sigma(\mathbf{r}, t) = \sum_{\sigma=\uparrow,\downarrow} \sum_{j=1}^{N_\sigma} |\varphi_{j\sigma}(\mathbf{r}, t)|^2\,. \tag{4.11}$$

This form of the TDKS equation implies that spin is a good quantum number, which means that it is assumed that there is a fixed quantization axis for the spin—for convenience, we take it to be the z-axis. The spin-dependent external potential can then be written as the sum of the usual (not spin-dependent) external potential, and a Zeeman term involving an external, possibly time-dependent magnetic field:

$$v_\sigma(\mathbf{r}, t) = v(\mathbf{r}, t) \pm \mu_0 B_z(\mathbf{r}, t)\,, \tag{4.12}$$

where μ_0 is the Bohr magneton, and the plus and minus signs are for spin-up and spin-down, respectively.

We will not repeat any of the existence proofs for time-dependent spin-DFT (TDS-DFT) here, since they go through pretty much exactly as in the non-spin-dependent case. Detailed discussions of the formal aspects of static SDFT can be found in the literature (von Barth and Hedin, 1972; Gunnarsson and Lundqvist, 1976; Parr and Yang, 1989; Dreizler and Gross, 1990); see also Section 2.1.4.

[1] See also Section 6.5.2 for the connection between history and initial-state dependence.

4.3 The adiabatic approximation

The key quantity in TDDFT is the time-dependent xc potential $v_{\rm xc}[n](\mathbf{r},t)$. Just as in static DFT, any application of TDDFT requires a suitable approximation to the xc potential, and a considerable portion of this book is dedicated to this issue.

A reasonable starting point in the quest for approximations to the time-dependent xc potential is to utilize the vast body of knowledge from static DFT. The easiest and most obvious thing to do is to simply take the xc potential from static DFT and, without any scruples or hesitation, use it in the TDKS equation (4.7), plugging in the time-dependent density $n(\mathbf{r},t)$ rather than the ground-state density $n_0(\mathbf{r})$. This defines the adiabatic approximation,

$$v_{\rm xc}^{\rm A}(\mathbf{r},t) = v_{\rm xc}^{0}[n_0](\mathbf{r})\big|_{n_0(\mathbf{r})\to n(\mathbf{r},t)} \;, \tag{4.13}$$

where $v_{\rm xc}^{0}[n_0](\mathbf{r})$ is the static xc potential functional, whose exact form, of course, is unknown. The term "adiabatic" means here that $v_{\rm xc}^{\rm A}(\mathbf{r},t)$ becomes exact in the limit where the adiabatic theorem of quantum mechanics applies, i.e., a physical system remains in its instantaneous eigenstate if a perturbation that is acting on it is slow enough.[2] In such a situation, the functional dependence of the xc potential at time t is only on the density at the very same time t, i.e., there is no memory.

It will not come as a surprise that truly adiabatic time evolution of quantum systems occurs only in exceptional cases.[3] Most situations of practical interest are nonadiabatic at least to some degree. In spite of this, it turns out that the adiabatic approximation often works surprisingly well in practice, as the example below will show. The general applicability of the adiabatic approximation is thus one of the central questions of TDDFT, and we will come back to it several times in this book.

In any practical application, one utilizes one of the many available approximate static xc potentials $v_{\rm xc}^{0,{\rm approx}}[n_0](\mathbf{r})$ such as one of the various forms of GGA, and the corresponding adiabatic approximation is given by

$$v_{\rm xc}^{\rm A,approx}(\mathbf{r},t) = v_{\rm xc}^{0,{\rm approx}}[n_0](\mathbf{r})\big|_{n_0(\mathbf{r})\to n(\mathbf{r},t)} \,. \tag{4.14}$$

The most widely used example of this class of time-dependent xc potentials is the adiabatic local-density approximation (ALDA),

$$v_{\rm xc}^{\rm ALDA}(\mathbf{r},t) = \left.\frac{de_{\rm xc}^{h}(\bar{n})}{d\bar{n}}\right|_{\bar{n}=n(\mathbf{r},t)} , \tag{4.15}$$

where $e_{\rm xc}^{h}(\bar{n})$ is the xc energy density of a homogeneous electron liquid of particle density $\bar{n}$ (see Chapter 2). Notice that there are two levels of approximation involved

[2]This requires the system to have an intrinsic timescale which determines the meaning of "slow" and "fast." A typical case is where the eigenstate under consideration is separated by a gap from the rest of the spectrum of the Hamiltonian. The situation is more complicated for gapless systems such as electron liquids. We will return to this problem in quite some detail in Chapter 10. For a recent review of the adiabatic theorem of quantum mechanics, see Comparat (2009).

[3]A class of highly counterintuitive examples where the adiabatic approximation of TDDFT becomes exact is that of situations where a strong external potential varies so rapidly that the electronic wave function can't follow anymore, but settles into particular quasi-stationary states (Baer, 2009). However, this does not constitute an adiabatic time evolution in the true sense, since these states are not eigenstates in the instantaneous external potential.

in eqns (4.14) and (4.15): we use a functional from static DFT and evaluate it with a time-dependent density, thus ignoring any memory effects; the static xc functional itself is of course an approximation, too.

Important insight can be gained by testing the adiabatic approximation for exactly solvable benchmark systems. Assume that a time-dependent density $n(\mathbf{r},t)$ has been obtained in a time interval $t_0 \leq t \leq t_1$ by exact solution of the time-dependent Schrödinger equation for an interacting system under the influence of an external potential $v(\mathbf{r},t)$. In Appendix E, we show how the exact time-dependent xc potential $v_{\rm xc}(\mathbf{r},t)$ can be constructed that reproduces a given time-dependent density in a TDKS calculation.

The adiabatically exact TDKS potential $v_s^{\rm A}(\mathbf{r},\widetilde{t})$ is defined at a given time $\widetilde{t}$ as that local potential which yields the density $n(\mathbf{r},\widetilde{t})$ at that very instant in time as its ground-state density (Thiele *et al.*, 2008):

$$\left[-\frac{\nabla^2}{2}+v_s^{\rm A}(\mathbf{r},\widetilde{t})\right]\varphi_j^{\rm A}(\mathbf{r},\widetilde{t})=\varepsilon_j^{\rm A}(\widetilde{t})\varphi_j^{\rm A}(\mathbf{r},\widetilde{t})\,,\qquad n(\mathbf{r},\widetilde{t})=\sum_{j=1}^{N}|\varphi_j^{\rm A}(\mathbf{r},\widetilde{t})|^2\,, \tag{4.16}$$

where the time $\widetilde{t}$ is treated as a parameter. According to the Hohenberg–Kohn theorem, there is a unique correspondence between $n(\mathbf{r},\widetilde{t})$ and $v_s^{\rm A}(\mathbf{r},\widetilde{t})$. The adiabatically exact xc potential is then defined as

$$v_{\rm xc}^{\rm A}(\mathbf{r},\widetilde{t})=v_s^{\rm A}(\mathbf{r},\widetilde{t})-v_0^{\rm A}(\mathbf{r},\widetilde{t})-\int d^3r'\,\frac{n(\mathbf{r}',\widetilde{t})}{|\mathbf{r}-\mathbf{r}'|}\,. \tag{4.17}$$

Here, $v_0^{\rm A}(\mathbf{r},\widetilde{t})$ is the local external potential which produces $n(\mathbf{r},\widetilde{t})$ as the ground-state density in an interacting, static N-particle system. To obtain it explicitly requires inversion of the N-particle interacting Schrödinger equation, which can be a computationally formidable task.

Let us now discuss the example of two interacting electrons in a one-dimensional model helium atom (Thiele *et al.*, 2008). Such one-dimensional "atoms" are, obviously, computationally much simpler than real atoms, and have been widely used to simulate the strong-field dynamics of interacting systems (Liu *et al.*, 1999; Lein *et al.*, 2000). All Coulomb interactions in this model are described by soft-core interaction potentials of the form $W(z)=C/\sqrt{z^2+1}$, where $C=-2$ for the electron–nuclear interaction in helium and $C=1$ for the electron–electron repulsion. This is not only computationally convenient, since it avoids dealing with the Coulomb singularity, but also mimics how the real, three-dimensional electrons can pass by each other. The resulting "helium atom" has a ground-state energy of -2.238 a.u. and an ionization threshold of 0.754 a.u. The system may then be subjected to an external time-dependent potential of the form $-z\mathcal{E}(t)$ (see the discussion of the dipole approximation in Appendix H), where $\mathcal{E}(t)$ is a time-dependent electric field. The two-particle time-dependent Schrödinger equation defined in this way can be solved numerically on a real-space grid.

Figures 4.1 and 4.2 show snapshots of the time-dependent density, the TDKS potential $v_s(z,t)$, and the correlation potential $v_{\rm c}$. The latter is defined via $v_{\rm xc}(z,t)=v_{\rm x}(z,t)+v_{\rm c}(z,t)$, where for two-electron singlet systems the exchange potential is simply given by $v_{\rm x}(z,t)=-v_{\rm H}(z,t)/2$. This relation holds in the nonadiabatic case as

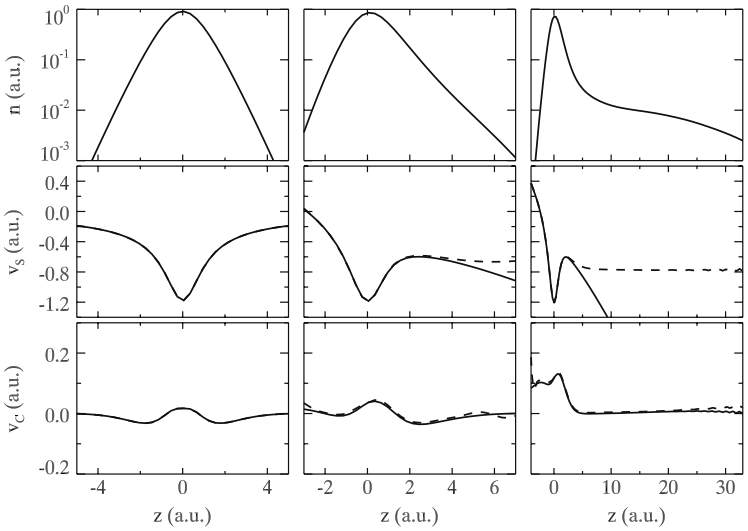

Fig. 4.1 Density, TDKS potential, and correlation potential at $t = 0$, 21.5, and 43.0 a.u. for a one-dimensional model helium atom subject to a DC electric field that is ramped up over a time of 27 a.u. and then held constant. Solid lines in the middle and bottom panels: exact potentials; dashed lines: adiabatically exact potentials. [Reproduced with permission from APS from Thiele *et al.* (2008), ©2008.]

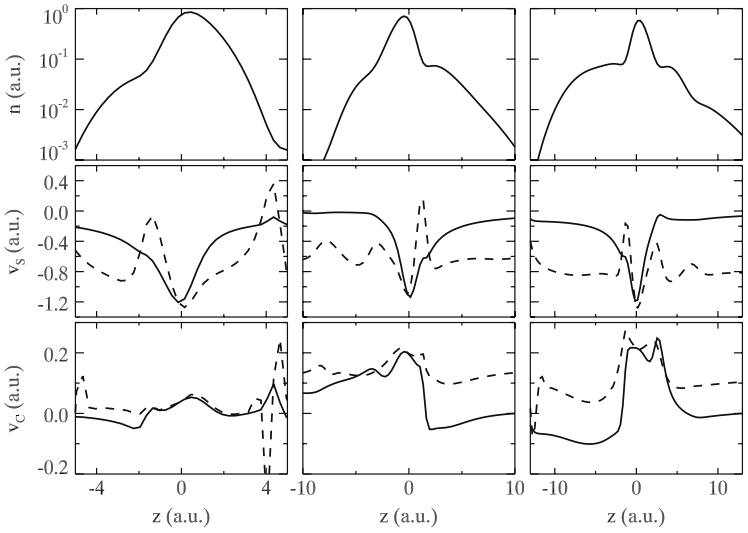

Fig. 4.2 As Fig. 4.1, but for the periodic, high-frequency driving potential of eqn (4.18) at times $t = T/2$, T, and $3T/2$, where $T = 7.0$ a.u. [Reproduced with permission from APS from Thiele *et al.* (2008), ©2008.]

well as in the adiabatically exact case. In other words, the exchange potential in a two-electron singlet system does not contain any nonadiabatic effects; the memory resides entirely in the correlation part. This will be discussed in more detail in Chapter 11.

Figure 4.1 shows results corresponding to the case where $\mathcal{E}(t)$ is a DC electric field that is gradually ramped up over a time period of 27 a.u. (corresponding to 0.65 fs) to a maximum field strength of $\mathcal{E}_{\max} = 0.141$ a.u. (see Appendix A for a discussion of atomic units). The system starts in the two-electron ground state at $t = 0$ and becomes increasingly deformed, leading eventually to field-induced ionization as the electrons escape to $z \to \infty$. One finds that v_s and v_s^{A} differ qualitatively, since the former is associated with an excited-state density in the presence of a time-dependent potential, whereas the latter describes a bound ground state in a global potential minimum. However, it is interesting to see that the exact and the adiabatic correlation potentials agree very closely at all times. This indicates that memory effects in the correlation potential are negligible in this process.

The second case, shown in Fig. 4.2, considers an external potential in which the density is deformed much more rapidly:

$$v(z,t) = -\frac{2}{\sqrt{(z - 0.5\sin\omega t)^2 + 1}}\,, \tag{4.18}$$

which mimics an oscillatory motion of the nucleus with frequency $\omega = 0.9$ a.u. The density gets drastically shaken up and deformed, and does not return to its initial shape after a full cycle of the external potential. To produce such a density as a ground state, $v_s^{\mathrm{A}}(z,t)$ has additional minima which are not present in $v_s(z,t)$. The correlation potentials are also drastically different, which shows that nonadiabatic effects become important in this scenario.

4.4 The meaning of self-consistency in DFT and TDDFT

Formally, the TDKS equation (4.7) is a partial differential equation of second order in space and first order in time, and, just like the time-dependent Schrödinger equation (3.5), poses an initial-value problem in which an initial wave function (or set of wave functions) is propagated forward in time. However, in contrast to the time-dependent Schrödinger equation, the effective potential of the TDKS equation is density-dependent, which introduces a nonlinearity. We will now discuss some of the consequences of this nonlinearity and how to deal with them.

Let us first look at the static Kohn–Sham equation (4.3) of ground-state DFT. As we discussed above, its solution requires self-consistency, which means the following. The static Kohn–Sham equation (4.3) gives rise to a set of orbitals, from which one obtains the density $n_0(\mathbf{r})$ via equation (4.4). The density then enters into the effective potential $v_s^0[n_0](\mathbf{r})$, and thus into the Hamiltonian. But the Hamiltonian, in turn, determines the orbitals, which closes the circle. In other words, the orbitals are self-consistent if they give rise to that very Kohn–Sham Hamiltonian which is needed to produce them. This is illustrated schematically in the upper part of Fig. 4.3. There, it is also indicated that the potential $v_s^0[n_0]$ at a point $\mathbf{r}$ is determined by the density over all space.

In practice, static self-consistency is obtained by iteration, using the following steps:

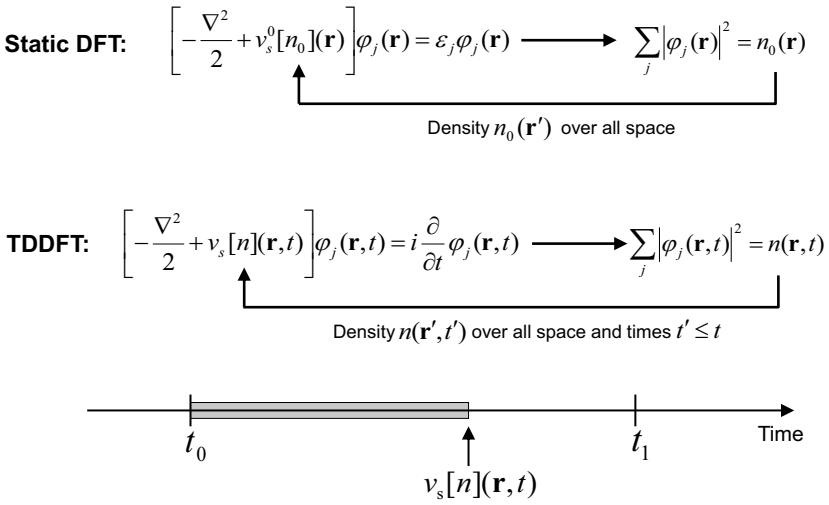

Fig. 4.3 Illustration of self-consistency in static DFT and TDDFT. In the time-dependent case, the xc potential at time t depends on densities at times $t' \le t$.

1. Start with an initial guess for the ground-state density $n^1(\mathbf{r})$.
2. Determine a new set of orbitals $\varphi_j^{i+1}(\mathbf{r})$ by solving the static Kohn–Sham equation with $v_s^0[n^i](\mathbf{r})$ evaluated using the density of the previous step, $n^i(\mathbf{r})$.
3. Obtain the new density $n^{i+1}(\mathbf{r})$, and compare it with the previous density $n^i(\mathbf{r})$. If the difference is greater than some given threshold criterion, repeat steps 2 and 3 until the criterion is satisfied.

Self-consistent solution of the ground-state Kohn–Sham equation produces the correct spatial dependence of all occupied (and unoccupied) single-particle orbitals $\varphi_j^0(\mathbf{r})$.

In the TDKS scheme, one needs to determine the correct time evolution of the orbitals, from the start at t_0 (assumed to be the ground state) up until the desired final time t_1. The extra level of difficulty is now that the effective potential $v_s[n]$ at point $\mathbf{r}$ and time t depends on the densities over all space and at all times $t' < t$.

More formally, in static DFT we need to solve a self-consistent eigenvalue problem, whereas in TDDFT the self-consistency must be built into the time propagation scheme. Such a procedure can be defined as follows (see the lower part of Fig. 4.3):

1. Obtain the self-consistent Kohn–Sham ground state of the system, with initial density $n(\mathbf{r}, t_0) = n_0(\mathbf{r})$.
2. Make an initial guess of the time-dependent density function $n(\mathbf{r}, t)$ for all times $t_0 \le t \le t_1$.
3. Determine a new set of orbitals $\varphi_j^{i+1}(\mathbf{r}, t)$ by propagating the TDKS equation with $v_s[n^i](\mathbf{r}, t)$ evaluated using the density of the previous step, $n^i(\mathbf{r}, t)$.
4. Obtain the new density $n^{i+1}(\mathbf{r}, t)$, $t_0 \le t \le t_1$, and compare it with the previous density $n^i(\mathbf{r}, t)$. If the difference over the entire time interval is greater than some given threshold criterion, repeat steps 2 and 3 until the criterion is satisfied.

This "global" time propagation scheme seems a bit awkward, for two reasons. First of all, it requires a starting guess of a time-dependent density (or of the time-dependent xc potential) for all times between t_0 and t_1. If that initial guess is too far off the mark, especially if propagation over a long time span is desired, convergence might happen slowly or not at all. Second, the scheme implies that we need to store the density for all $t_0 \leq t \leq t_1$ in memory, even if we work with an adiabatic approximation for the xc potential, ignoring its dependence on the density at previous times.

In practice, self-consistent propagation of the TDKS equation is carried out in a different way, namely step by step, rather than globally over the entire time interval.[4] This will be explained in the following section.

4.5 Numerical time propagation

The numerical solution of the time-dependent Schrödinger equation is a well-known problem that has been around for a while (Goldberg *et al.*, 1967), and there exist a large variety of numerical propagation techniques. A complete survey of the various time propagation schemes is beyond the scope of this book [see, e.g., Castro *et al.* (2004*b*)]. We will focus here on just one specific, widely used algorithm for the self-consistent propagation of the TDKS equation.

4.5.1 The Crank–Nicolson algorithm

Let us begin by considering the single-particle Schrödinger equation in a given, time-dependent external potential,

$$i\frac{\partial}{\partial t}\psi(\mathbf{r},t) = \hat{H}(t)\psi(\mathbf{r},t) = \left[-\frac{\nabla^2}{2} + v_{\rm ext}(\mathbf{r},t)\right]\psi(\mathbf{r},t)\,, \tag{4.19}$$

where the initial wave function $\psi(\mathbf{r},t_0)$ is the ground state associated with $v_{\rm ext}(\mathbf{r},t_0)$. The external potential is assumed to be static for $t < t_0$, and becomes explicitly time-dependent after t_0.

We now discretize the time variable, $t \to \tau_j$, and consider discrete time steps $\Delta\tau$. The basic task is to propagate the wave function ψ from time τ_j to the next time step $\tau_{j+1} = \tau_j + \Delta\tau$, assuming that $\psi(\tau_j)$ is known. In Section 3.1.2 we saw that the solution of the time-dependent Schrödinger equation can be formally expressed in terms of a time evolution operator; therefore we can write, formally exactly,

$$\psi(\tau_j + \Delta\tau) = \hat{U}(\tau_j + \Delta\tau, \tau_j)\psi(\tau_j)\,. \tag{4.20}$$

Let us now find an explicit expression for the time evolution operator $\hat{U}(\tau_j + \Delta\tau, \tau_j)$ which takes us forward by just one time step $\Delta\tau$. The exact form of $\hat{U}$ for a time-dependent external potential is given by eqn (3.12); however, if the time step $\Delta\tau$ is sufficiently small, we can approximate this by

$$\hat{U}(\tau_j + \Delta\tau, \tau_j) \approx e^{-i\hat{H}(\tau_j + \Delta\tau/2)\Delta\tau} \equiv e^{-i\hat{H}(\tau_{j+1/2})\Delta\tau}\,, \tag{4.21}$$

i.e., we evaluate the time-dependent external potential halfway between τ_j and τ_{j+1}. The midpoint evaluation of the potential is dictated by the obvious requirement that

[4] However, examples of successful TDKS calculations using a global iteration scheme do exist (Wijewardane and Ullrich, 2008).

the propagation $\tau_j \to \tau_{j+1}$ followed by the backward propagation $\tau_{j+1} \to \tau_j$ must lead back to where we started: $\psi(\tau_j) = \hat{U}(\tau_j, \tau_{j+1})\psi(\tau_{j+1}) = \hat{U}(\tau_j, \tau_{j+1})\hat{U}(\tau_{j+1}, \tau_j)\psi(\tau_j)$, which implies $\hat{U}(\tau_j, \tau_{j+1})\hat{U}(\tau_{j+1}, \tau_j) = 1$. The approximation (4.21) for the time evolution operator is easily seen to satisfy this.[5]

The next task is to deal with the exponential in eqn (4.21). The so-called Crank–Nicolson algorithm (Press *et al.*, 2007) uses the following approximation:

$$e^{-i\hat{H}\,\Delta\tau} \approx \frac{1 - i\hat{H}\,\Delta\tau/2}{1 + i\hat{H}\,\Delta\tau/2}\,, \tag{4.22}$$

which is correct to second order in $\Delta\tau$ and unitary. Substituting this into eqn (4.20) gives

$$\left(1 + \frac{i}{2}\hat{H}(\tau_{j+1/2})\,\Delta\tau\right)\psi(\tau_{j+1}) = \left(1 - \frac{i}{2}\hat{H}(\tau_{j+1/2})\,\Delta\tau\right)\psi(\tau_j)\,. \tag{4.23}$$

This is an example of a so-called implicit propagation scheme (Press *et al.*, 2007), which means that the solution $\psi(\tau_{j+1})$ is obtained from the known right-hand side of eqn (4.23) by inversion of the operator $1 + i\hat{H}(\tau_{j+1/2})\,\Delta\tau/2$. In practice, one usually expresses the wave function on a spatial grid or a discrete basis. Equation (4.23) then becomes a system of linear equations which can be solved for each time step $\tau_j \to \tau_{j+1}$ using standard numerical algorithms.

4.5.2 The predictor–corrector scheme

As we have seen, the time-dependent single-particle Schrödinger equation can be solved numerically through step-by-step propagation with the Crank–Nicolson algorithm. The same approach works for the TDKS equation too, but there is an additional difficulty that is related to the self-consistency requirement we discussed above in Section 4.3.

To carry out the propagation of the TDKS orbitals from time τ_j to τ_{j+1} using eqn (4.23), we need the TDKS Hamiltonian at the midpoint, that is, we need $v_s[n](\mathbf{r}, \tau_{j+1/2})$. However, at this stage we only know the time-dependent densities for times $\leq \tau_j$; this is as far as we have got with the propagation. So, to perform the next time step, it appears as if we have to look a little bit into the future! However, this does not imply a violation of causality. What it means is that the propagation step from τ_j to τ_{j+1} has to be done with a potential $v_s[n](\mathbf{r}, \tau_{j+1/2})$ that is consistent with the TDKS orbitals at τ_j as well as τ_{j+1}; in other words, it is the self-consistency requirement of Section 4.3, but not in a "global" sense as was presented there, but "locally" for an individual time propagation step.

In practice, self-consistency can be reached through an iterative procedure, called the predictor–corrector scheme, which we now discuss.

[5] From a practical point of view, a more tempting choice would have been to evaluate the potential at the beginning of the time propagation step, $\hat{U}(\tau_j + \Delta\tau, \tau_j) = e^{-i\hat{H}(\tau_j)}$. However, this would imply $\hat{U}(\tau_j, \tau_{j+1})\hat{U}(\tau_{j+1}, \tau_j) = e^{i\hat{H}(\tau_{j+1})}e^{-i\hat{H}(\tau_j)} \neq 1$.

Predictor Step. As a guess for $\varphi(\tau_{j+1})$, we propagate $\varphi(\tau_j)$ using the Crank–Nicolson formula with the Hamiltonian evaluated at time τ_j (where the density is known) instead of at $\tau_{j+1/2}$:

$$\left(1 + \frac{i}{2}\hat{H}(\tau_j)\,\Delta\tau\right)\varphi^{(1)}(\tau_{j+1}) = \left(1 - \frac{i}{2}\hat{H}(\tau_j)\,\Delta\tau\right)\varphi(\tau_j)\,. \tag{4.24}$$

If the time interval is short, this is probably not bad as a first shot (anyway, it's the easiest thing to do). But now, we need to refine our guess, which we'll do in several iterations.

nth Corrector Step. We take the TDKS orbitals $\varphi^{(n)}(\tau_{j+1})$ resulting from the predictor step (if $n = 1$) or from the previous corrector step (if $n > 1$) to get an approximation for the density at time τ_{j+1}. This gives an approximation to the TDKS Hamiltonian at time τ_{j+1}, and the Hamiltonian at the midpoint can be interpolated as

$$\hat{H}^{(n)}(\tau_{j+1/2}) = \frac{1}{2}\left[\hat{H}(\tau_j) + \hat{H}^{(n)}(\tau_{j+1})\right]\,. \tag{4.25}$$

With this, we find a new, refined guess for the TDKS orbitals:

$$\left(1 + \frac{i}{2}\hat{H}^{(n)}(\tau_{j+1/2})\,\Delta\tau\right)\varphi^{(n+1)}(\tau_{j+1}) = \left(1 - \frac{i}{2}\hat{H}^{(n)}(\tau_{j+1/2})\,\Delta\tau\right)\varphi(\tau_j)\,. \tag{4.26}$$

One can repeat as many corrector steps as desired during each propagation step $\tau_j \to \tau_{j+1}$. Once the corrector steps are completed, one moves on to the next propagation step $\tau_{j+1} \to \tau_{j+2}$, and so on, until the final time t_1.

Self-consistency is reached if the density $n(\mathbf{r}, t)$ remains unchanged over the entire time interval $[t_0, t_1]$, within a given tolerance, upon addition of another corrector step in the time propagation scheme. In practice, two corrector steps are often sufficient. This, however, depends on the choice of the time step: a large $\Delta\tau$ obviously requires more corrector steps, which may increase the overall computational cost. As always in numerical analysis, this requires some form of compromise between accuracy and computational cost.

4.5.3 Absorbing boundary conditions

A key characteristic of unitary time propagation is the conservation of the norm of each time-dependent wave function. In other words, $\int d^3r\, n(\mathbf{r}, t) = N$ at all times, which of course implies the very reasonable concept of particle conservation, i.e., probability density is neither created nor destroyed. On the other hand, there are many situations of great practical interest where finite systems are subject to driving fields, which causes charges to be moved around within the system (charge transfer) or to escape altogether (ionization). In this case, the electronic probability density is initially well confined to the atom or molecule of interest, but starts to spread out upon excitation, resulting in electronic charge density flowing away.

Let us now assume that we are carrying out a numerical solution of the TDKS equation on a real-space grid. If the exciting field is strong, and if we want to follow the dynamics for a long time, then the numerical grid required has to have a very large

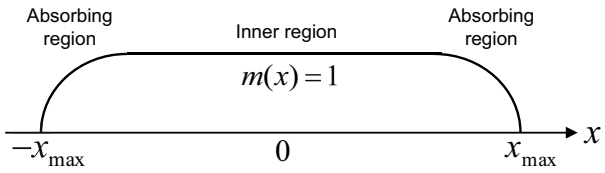

Fig. 4.4 Mask function $m(x)$ for a one-dimensional spatial grid with absorbing boundary conditions. During time propagation, the TDKS orbitals are multiplied by $m(x)$ after each time step, which prevents reflection from the edges of the grid.

size, which can be computationally expensive. It is therefore desirable to limit the size of the numerical grid, thus making the calculation more efficient. However, this may have the unwanted side effect that electronic flux corresponding to ionized electrons hits the grid boundary, gets artificially reflected there, and reenters the central region of the calculation. To avoid such unphysical effects in finite spatial grids, it is common practice to introduce absorbing boundary conditions. This is a well-studied subject in numerical simulations of partial differential equations (Kosloff and Kosloff, 1986; Fevens and Jiang, 1999). Here, we shall just briefly mention two common approaches to implementing absorbing boundary conditions.

The first approach is to add a short-ranged negative imaginary potential to the total potential in the asymptotic region far away from the system that is being ionized (Neuhauser and Baer, 1989; Vibók and Balint-Kurti, 1992). These complex potentials can be optimized to minimize reflection of electron flux for a wide range of energies.

The second approach is even easier to implement and uses a so-called mask function (Krause *et al.*, 1992). A mask function is a very simple object: to define it, we partition our finite spatial grid into an inner region, which is large enough to completely contain the finite system of interest, and a border region, where outgoing flux is to be absorbed. The mask function $m(\mathbf{r})$ has a value of 1 in the inner region and drops smoothly to zero in the absorbing border region, for instance using a $\cos^{1/4}$ behavior. Such a function is illustrated in Fig. 4.4 for a one-dimensional grid. During time propagation, the TDKS orbitals are multiplied by $m(\mathbf{r})$ after each time propagation step, which forces them to be zero at the edges of the grid, thus preventing unwanted reflection.

Exercise 4.1 Prove that the Crank–Nicolson form of the time evolution operator, eqn (4.22), is correct to second order in Δt and unitary. In particular, convince yourself that the simple, obvious choice $e^{-i\hat{H}\,\Delta t} \approx 1 - i\hat{H}\,\Delta t$, apart from being correct only to first order in Δt, is not unitary and is thus not suited for time propagation.

Exercise 4.2 The best way to understand how numerical time propagation algorithms work is to write your own computer code. This is, in fact, not such a difficult thing to do! In this exercise, we go through the steps leading to a simple code for N noninteracting electrons on a finite 1D lattice. This code will be used for several numerical exercises in this and later chapters.

Define a 1D lattice as a collection of M equidistant points, $x_1, x_2, \ldots, x_M$, with grid spacing $\Delta = x_{j+1} - x_j$. You could, for instance, choose $M = 50$ and $\Delta = 0.1$, but this depends on the problem you want to study and the accuracy you want to achieve. Even tiny lattices with only two or three points can occasionally be interesting!

Next, the single-particle wave functions are discretized. The M values of a single-particle wave function on the lattice points are arranged to form a vector:

$$\varphi(x) \longrightarrow \vec{\varphi} = \begin{pmatrix} \varphi(x_1) \\ \varphi(x_2) \\ \vdots \\ \varphi(x_M) \end{pmatrix} = \begin{pmatrix} \varphi_1 \\ \varphi_2 \\ \vdots \\ \varphi_M \end{pmatrix} . \tag{4.27}$$

Now consider the single-particle Hamiltonian $\hat{h} = -(1/2)(d^2/dx^2) + v(x)$. The kinetic-energy operator involves the second spatial derivative, which has the two-point finite-difference representation

$$\frac{d^2}{dx^2} f(x) \longrightarrow \frac{f(x_{j+1}) - 2f(x_j) + f(x_{j-1})}{\Delta^2} . \tag{4.28}$$

The local one-body potential is discretized on the lattice, $v(x) \longrightarrow (v_1, v_2, \ldots, v_M)$. The single-particle Hamiltonian thus transforms into a tridiagonal $M \times M$ matrix,

$$\mathbb{h} = \begin{pmatrix} v_1 + \frac{1}{\Delta^2} & \frac{-1}{2\Delta^2} & & & & \\ \frac{-1}{2\Delta^2} & v_2 + \frac{1}{\Delta^2} & \frac{-1}{2\Delta^2} & & & \\ & \ddots & \ddots & \ddots & & \\ & & \frac{-1}{2\Delta^2} & v_{M-1} + \frac{1}{\Delta^2} & \frac{-1}{2\Delta^2} & \\ & & & \frac{-1}{2\Delta^2} & v_M + \frac{1}{\Delta^2} & \end{pmatrix} , \tag{4.29}$$

and the static Schrödinger equation becomes a standard matrix–vector eigenvalue problem,

$$\mathbb{h}\vec{\varphi}_j = \varepsilon_j \vec{\varphi}_j , \qquad j = 1, \ldots, N. \tag{4.30}$$

Now write a computer program in your favorite programming language which solves this eigenvalue problem. There exist a wealth of program libraries for linear-algebra tasks, so you don't have to code your own eigenvalue solver. See, for example, `http://gams.nist.gov` or Press *et al.* (2007). Make sure that the wave functions are properly normalized! You will have to write a suitable integration subroutine for your lattice system.

Solve the noninteracting Schrödinger equation (4.30) for a given potential, which defines the N-electron ground state. You could, for instance, take a harmonic-oscillator potential or a constant potential (i.e., N noninteracting particles in a box).

The next task is to solve the time-dependent Schrödinger equation on the lattice,

$$i\frac{\partial}{\partial t}\vec{\varphi}_j(t) = \mathbb{h}(t)\vec{\varphi}_j(t) , \qquad j = 1, \ldots, N, \tag{4.31}$$

under the influence of a time-dependent potential. The first thing you need to do is read in the initial wave functions that come from the static Schrödinger equation (4.30), and convert them into complex arrays. Then you need to write a subroutine for the Crank–Nicolson algorithm (4.23). As you will see, this requires solving a linear equation for $\vec{\varphi}_j(\tau_{l+1})$ at each time step $\tau_l \to \tau_{l+1}$. Again, you can use subroutines from a linear-algebra program library.

Here are two safety checks to convince yourself that your program works properly:
1. Calculate the norm of the wave functions at each time step and make sure it is conserved.
2. If the external potential is time-independent, the single-particle wave functions should have the form $\vec{\varphi}_j(t) = \vec{\varphi}_j(0)e^{-i\varepsilon_j t}$. Convince yourself that this is indeed the case.

Now you are ready to explore your code! First, find out how sensitively your numerical solution depends on the time step $\Delta\tau$. Your goal should be the best compromise between accuracy and computational efficiency.

Try out various types of external driving potentials, and see how the density responds. A standard choice is the potential corresponding to a pulsed dipole field (see Appendix H),

$$v(x_j, t) = \mathcal{E} f(t) x_j \sin(\omega t) \,, \tag{4.32}$$

where $\mathcal{E}$ is the electric-field amplitude, ω is the frequency of the laser generating the field, and $f(t)$ is the pulse envelope. Plot snapshots of the density at various times, or discover your talent for making movies!

Exercise 4.3 This is a follow-up to the previous exercise, based on your homemade numerical code for 1D lattice systems. Consider the case where you have only one electron which is initially bound in a shallow potential well at the center of your lattice. Now hit the system with a pulsed dipole field (4.32) that is strong enough to cause the density to spill out.

Write a subroutine that implements absorbing boundary conditions, using the mask function of Fig. 4.4. Plot the norm of the wave function at each time step and see how it decreases. This allows you to simulate ionization using a finite-size lattice.

Try different forms of absorbing boundaries, including mask functions of different shapes, or complex potentials. Your goal is to make them as smooth as possible to minimize reflection off the edges of the grid.

Exercise 4.4 In Appendix E, it is shown how to construct the external potential that produces a given density in a noninteracting system. Try this out on a 1D lattice system.

Consider two examples of a given time-dependent density distribution, the sloshing and breathing modes that are defined in Appendix L. Assume that $N = 2$. What is the potential that gives rise to these density distributions? Plot snapshots of the densities and the corresponding potentials.

Exercise 4.5 In this exercise, you will again use your homemade code for propagating single-particle wave functions on a 1D lattice. Your task is now to include the Hartree potential in the static and time-dependent single-particle Schrödinger equations (4.30) and (4.31). This means that you will have to solve these equations self-consistently.

Consider a 1D system of two electrons subject to a soft-core Coulomb interaction

$$w(x) = C/\sqrt{x^2 + 1} \,, \tag{4.33}$$

where $C = -2$ for the attractive binding potential (this mimics a 1D helium atom) and $C = 1$ for the electron–electron repulsion.

First, write a subroutine that calculates the Hartree potential corresponding to this form of electron–electron interaction. Now modify your code for solving eqn (4.30) so that it finds the self-consistent solution in an iterative manner.

Next, modify your time-propagation code for eqn (4.31) and implement the predictor–corrector scheme. Make sure that the safety checks of Exercise 4.2 (norm conservation and electronic phase factors) are still satisfied.

Test the performance of your predictor–corrector algorithm by varying the number of corrector steps, as well as the time step $\Delta\tau$. Usually, two corrector steps should be enough, but see what happens if you include more than two corrector steps, or none at all!

5
Time-dependent observables

When we discussed the Runge–Gross theorem in Section 3.2 we found that all physical observables $O[n](t)$ can be expressed, at least formally, as functionals of the time-dependent density. This means that, in principle, the time-dependent density $n(\mathbf{r}, t)$ tells us all we want to know about the structure and dynamics of any electronic system. The key issue is how to extract the desired physical information from the density, which is often not a straightforward task.

In this chapter, we give an overview of the observable quantities that are of interest in TDDFT and how to calculate them. We will see that some of these observables carry over directly from static DFT; other static observables, such as the energy, acquire an altogether different meaning in the time domain.

In the following, we shall distinguish between "easy" and "difficult" observables,[1] depending on whether they can be obtained directly from the time-dependent density with relatively little numerical effort, or whether they are only implicit density functionals and therefore require more elaborate procedures or can only be obtained in some approximate manner. A distinction will also be made between local quantities, where the spatial dependence is of interest, and global quantities, which involve some form of integration over all space or over certain finite regions of space.

5.1 Explicit density functionals

5.1.1 The density and other visualization tools

The most straightforward observable from the point of view of TDDFT is the time-dependent probability density $n(\mathbf{r}, t)$ itself. It tells us how the electrons are distributed in the system at a given time.

The electron density of molecules can be experimentally observed using X-ray scattering techniques. In this way, one obtains what are known as electron density maps, which are of great interest in structural chemistry and biology. During the past decade, it has become possible to carry out time-resolved X-ray scattering measurements (Chergui and Zewail, 2009). The achievable time resolution is limited by the pulse length of the X-ray source; current synchrotron sources thus yield a time resolution of about 100 ps, which is not sufficient to observe atomic motion, let alone charge-density dynamics; yet, the technique yields valuable information about ultrafast structural changes in materials. Figure 5.1 illustrates the function of the protein

[1] Needless to say, these attributes are based mainly on a theorist's point of view. Experimentalists may have entirely different opinions as to which observables are easy or difficult to measure.

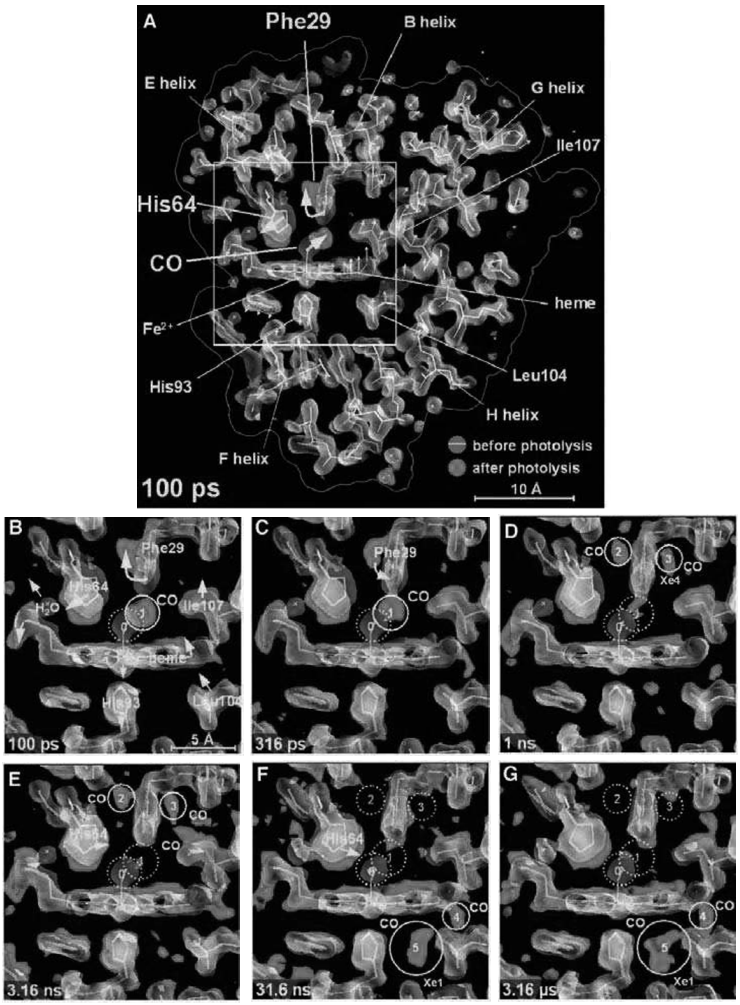

Fig. 5.1 Experimentally determined electron density map of the myoglobin molecule obtained using time-resolved X-ray scattering. Snapshots of the photolysis process (panels B–G) reveal a short-lived CO intermediate. [Reproduced with permission from AAAS from Schotte *et al.* (2003), ©2003).]

myoglobin on a subnanosecond timescale (Schotte *et al.*, 2003), showing how a CO ligand moves between docking sites in less than 100 ps upon photoexcitation.

Direct imaging of the dynamics of the charge-density flow in an excited molecule would require diffraction techniques with fs or even sub-fs time resolution. At present, this is still a distant goal, but there has been recent progress in which X-ray absorption techniques in the 100 fs domain were demonstrated (Bressler *et al.*, 2009).

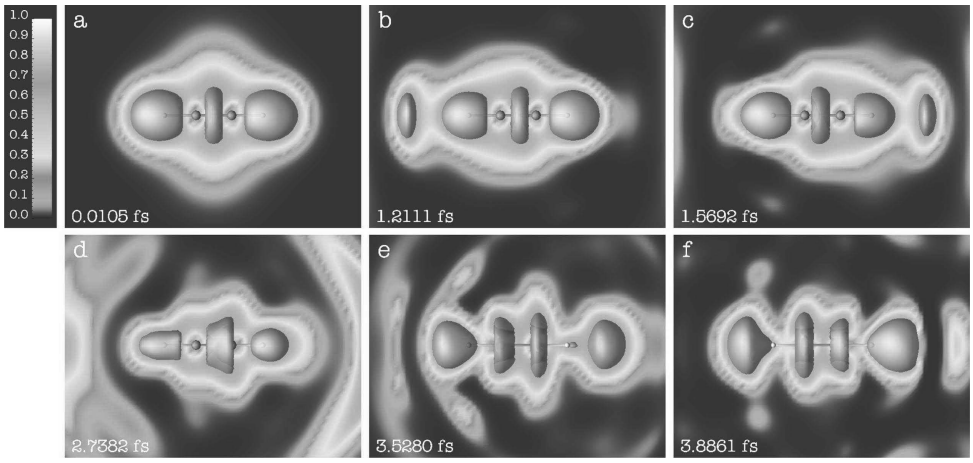

Fig. 5.2 Snapshots of the TDELF for a laser-excited acetylene molecule. [Reproduced with permission from APS from Burnus *et al.* (2005), ©2005.]

While the electronic probability density distribution is certainly a quantity of interest for visualizing molecular geometries or structural changes during chemical reactions or photoinduced processes, it does not reveal important quantum mechanical features such as atomic shell structure, covalent molecular bonds, or lone pairs. These concepts are vital for an understanding of the chemical properties of molecules and materials.

The Laplacian of the density, $\nabla^2 n$, is better suited for visualizing such features, and indeed does reveal atomic shell structure (except for heavy atomic systems) and electron pairs (Bader and Essén, 1984; Bader, 1990). However, its physical significance is not entirely clear, and it is also somewhat inconvenient for graphic representation since the Laplacian can vary widely, from negative infinity around the atomic nucleus to unbounded large positive values elsewhere.

The time-dependent electron localization function (TDELF) (Burnus *et al.*, 2005), which is a generalization of the static electron localization function developed by Becke and Edgecombe (1990), represents a convenient tool for visualizing molecular bonds and electron localization. It is defined as a positive quantity with a magnitude between zero and one:

$$f_{\mathrm{ELF}}(\mathbf{r},t) = \frac{1}{1+[D_\sigma(\mathbf{r},t)/D^0_\sigma(\mathbf{r},t)]^2}\,, \tag{5.1}$$

where

$$D_\sigma(\mathbf{r},t) = \tau_\sigma(\mathbf{r},t) - \frac{|\nabla n_\sigma(\mathbf{r},t)|^2}{8n_\sigma(\mathbf{r},t)} - \frac{|\mathbf{j}_\sigma(\mathbf{r},t)|^2}{2n_\sigma(\mathbf{r},t)} \tag{5.2}$$

and

$$\tau_\sigma(\mathbf{r},t) = \frac{1}{2}\sum_{j=1}^{N_\sigma} |\nabla\varphi_{j\sigma}(\mathbf{r},t)|^2\,. \tag{5.3}$$

Clearly, $D_\sigma(\mathbf{r},t)$ is not an explicit density functional, but it is expressed in terms of the density, the current,[2] and the TDKS orbitals via the kinetic-energy density $\tau_\sigma(\mathbf{r},t)$. The reference quantity D_σ^0 in eqn (5.1) is given by the kinetic-energy density of the homogeneous electron liquid:

$$D_\sigma^0(\mathbf{r},t) = \frac{3}{10}(6\pi^2)^{3/2} n_\sigma^{5/3}(\mathbf{r},t) = \tau_\sigma^h(\mathbf{r},t)\,. \tag{5.4}$$

The quantity $D_\sigma(\mathbf{r},t)$ is a measure of the probability of finding an electron in the vicinity of another electron of the same spin σ at $(\mathbf{r},t)$. It is proportional to the noninteracting Fermi hole curvature $C_\sigma(\mathbf{r},t)$ (Dobson, 1993; Räsänen *et al.*, 2008*a*):

$$D_\sigma(\mathbf{r},t) = \frac{C_\sigma(\mathbf{r},t)}{4n_\sigma(\mathbf{r},t)}\,, \qquad C_\sigma(\mathbf{r},t) = 2\lim_{\mathbf{r}'\to\mathbf{r}} \nabla'^2 \rho_2(\mathbf{r},\sigma,\mathbf{r}',\sigma,t)\,, \tag{5.5}$$

where $\rho_2(\mathbf{r},\sigma,\mathbf{r}',\sigma,t)$ is the diagonal of the noninteracting two-particle reduced density matrix (see Appendix C). Another interpretation of $D_\sigma(\mathbf{r},t)$ is as the spherical average of the Pauli pressure, which is related to the exclusion principle (Tao *et al.*, 2008*c*).

A typical TDELF plot is shown in Fig. 5.2 (Burnus *et al.*, 2005). This example is of an acetylene molecule, C_2H_2, excited by a laser pulse with photon energy 17.15 eV, a duration of 7 fs, and an intensity of $1.2\times10^{14}\,\mathrm{W/cm^2}$, polarized along the molecular axis. In the figure, a slice of the TDELF is plotted which passes through the plane of the molecule, on which isosurfaces with $f_{\mathrm{ELF}} = 0.8$ are superimposed.

At the initial time, the localization function clearly illustrates the triple bond between the two carbon atoms as a compact torus in the middle, and two "blobs" surrounding the hydrogen atoms at each end. The laser then induces charge-density oscillations in the molecule, causing ionization in the form of density packets leaking out. As time progresses, the torus in the middle becomes broader and eventually separates into two tori around each C atom. This indicates a transition from the bonding π state to the antibonding π^* excited state.

5.1.2 The particle number

The most straightforward global observable that can be calculated from the density is the number of particles. As we discussed at the beginning of Section 4.5.3, the norm of the TDKS orbitals is conserved under unitary propagation. This means that

$$\int_{\substack{\text{all}\\\text{space}}} d^3r\, n(\mathbf{r},t) = N\,, \tag{5.6}$$

independent of time. As a time-dependent observable, this is of course a rather boring quantity, since we always know what N is. On the other hand, in dynamical situations, in particular when strong excitations occur, it may be of great interest to know the number of particles in a given finite spatial region at a given moment. For instance, we may wish to know how much charge is moving from one region of a molecule to another

[2]Strictly speaking, the Kohn–Sham current density $\mathbf{j}_s(\mathbf{r},t) = (2i)^{-1}\sum_k^N \left[\varphi_k^*\nabla\varphi_k - \varphi_k\nabla\varphi_k^*\right]$ is not guaranteed to be equal to the exact current density of the interacting system. As we will discuss in Chapter 10, the exact current density $\mathbf{j}(\mathbf{r},t)$ cannot be obtained from TDDFT but requires TDCDFT.

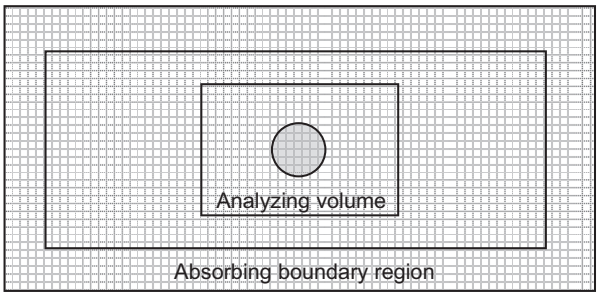

Fig. 5.3 Schematic illustration of the various regions in a spatial grid. The finite system (represented by the circle) is surrounded by an analyzing region $\mathcal{V}_\mathrm{A}$, which is used to calculate global observables.

during a charge-transfer process, or how charge is distributed among fragments during a molecular breakup. An even simpler question can be asked in relation to ionization processes: how much charge density escapes to the continuum following an excitation with a laser pulse or a colliding projectile, and how fast does this happen? Let us focus on such ionization processes first.

To study numerically the ionization of a finite system such as an atom under strong excitation, one often works with a large but finite spatial grid. It is convenient to define an analyzing volume $\mathcal{V}_\mathrm{A}$ of finite size (typically much smaller than the spatial extent of the numerical grid), as illustrated in Fig. 5.3. Here, the atom is placed at the center of the grid, with the analyzing box surrounding it. The grid is terminated by an absorbing boundary (see Section 4.5.3). There is no universal prescription for the actual size and shape of the analyzing box; it is chosen mainly for convenience. A reasonable requirement is that at the initial time the ground-state wave function of the system should be essentially completely contained within $\mathcal{V}_\mathrm{A}$, i.e., $\int_{\mathcal{V}_\mathrm{A}} d^3r\, n_0(\mathbf{r}) = N - \Delta_N$, where Δ_N is a very small fraction of the total particle number.[3] The assumption is then made that during time evolution subject to excitations, this analyzing box contains essentially all of the bound-state parts of the time-dependent wave function. All the density that lies outside of $\mathcal{V}_\mathrm{A}$ is assumed to correspond to continuum electrons. We therefore define

$$N_\mathrm{bound}(t) = \int_{\mathcal{V}_\mathrm{A}} d^3r\, n(\mathbf{r}, t) \tag{5.7}$$

as the number of bound electrons at a given time. Consequently,

$$N_\mathrm{esc}(t) = N - N_\mathrm{bound}(t) \tag{5.8}$$

indicates the number of escaped (or ionized) electrons.

The bottom panels of Fig. 5.4 give an illustration of $N_\mathrm{esc}(t)$, calculated for an Na_9^+ cluster in the spherical jellium model, subject to 25 fs Gaussian laser pulses of photon

[3] "Small" is to be understood with respect to the numerical accuracy of integration on the grid. For example, $\Delta_N < 10^{-6}N$ is a reasonable compromise. For a small atom, this can be achieved using an analyzing box with a size of around 20–30a_0.

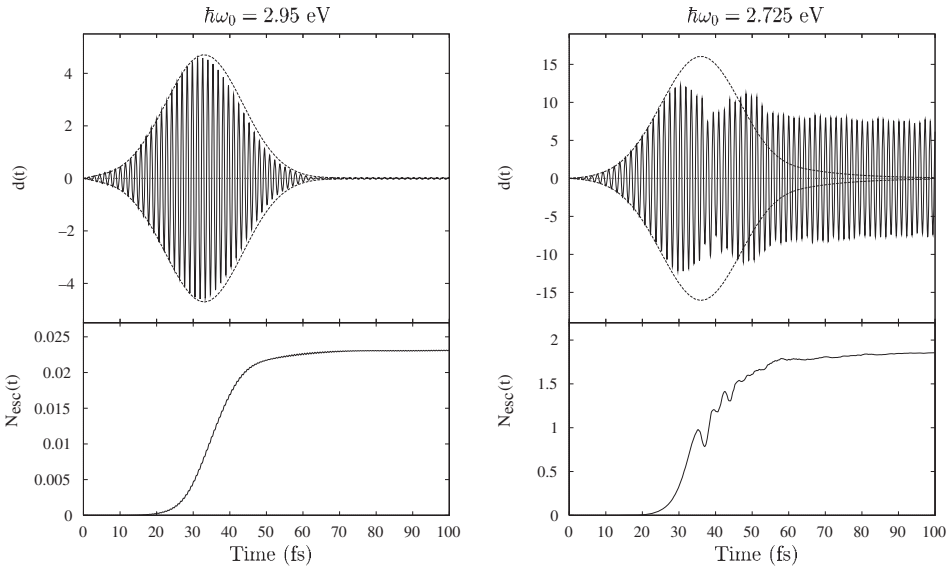

Fig. 5.4 Number of escaped electrons $N_{\rm esc}(t)$ and time-dependent dipole moment $d(t)$ of an Na_9^+ cluster in the spherical jellium model, subject to 25 fs Gaussian laser pulses of photon energy 2.95 eV (left) and 2.725 eV (right) and peak intensity 10^{11} W/cm^2. The dashed lines indicate the pulse envelope. [Reproduced with permission from IOP from Ullrich *et al.* (1997), ©1997.]

energy 2.95 eV (left) and 2.725 eV (right) and with a peak intensity of 10^{11} W/cm^2 (Ullrich *et al.*, 1997; Calvayrac *et al.*, 2000). The calculations were done using time propagation of eight outer-shell electrons using the TDKS equations in the ALDA. In the first case, ionization is very weak: the number of escaped electrons at the end of the pulse is only about 0.02. The second case shows much stronger ionization, almost two electrons after the end of the pulse, since the laser photon energy is very close to the Mie plasmon resonance of the cluster. In both situations, ionization happens quite fast during about 20 fs, with the steepest rate of electron escape occurring at the maximum of the laser pulse.

In the case of stronger ionization at 2.725 eV, $N_{\rm esc}(t)$ is not a monotonic function, but shows some wiggles during its rise. This happens because the continuum electrons are driven back and forth by the oscillating laser field; some of the charge density can therefore temporarily reenter the analyzing box, before finally escaping after the laser pulse is over.

Looking at the results for $N_{\rm esc}(t)$ in Fig. 5.4, a rather obvious question arises: what is the meaning of a fractional number of escaped electrons? We will give an answer when we discuss ion probabilities below.

To study the redistribution of charge within a molecule or during molecular dissociation, the concept of the analyzing volume can be generalized, using a partitioning of space that is suitable for the problem at hand. One can define

$$N_{\mathcal{V}_i}(t) = \int_{\mathcal{V}_i} d^3r\, n(\mathbf{r}, t) \tag{5.9}$$

as the number of electrons contained in the ith analyzing volume, which could for example be centered around the ith atom in a molecule, or about the ith fragment in an exploding cluster. A simple example of a dissociating double quantum well has been studied by Vieira *et al.* (2009), where $N_{\mathcal{V}_i}(t)$ refers to the numbers of electrons found in the left and the right well at a given time. This example is discussed in more detail in Section 11.2.5.

5.1.3 Moments of the density

The next class of explicit density functionals is that of moments of the density. The most commonly used one is the time-dependent dipole moment $\mathbf{d}(t)$, which can be a useful and simple quantity for visualizing the dynamics of an excited system over a certain time span. The individual components of the dipole moment are calculated along the Cartesian directions r_μ, $\mu = 1, 2, 3$:

$$d_\mu(t) = \int_{\mathcal{V}_\mathrm{A}} d^3r\, r_\mu n(\mathbf{r}, t)\,, \tag{5.10}$$

where the integration is again over a finite analyzing volume $\mathcal{V}_\mathrm{A}$ surrounding the system. The top panels of Fig. 5.4 show the oscillating dipole moment $d(t)$ of the laser-excited Na_9^+ cluster. In the near-resonant case, the dipole moment continues to oscillate with a large amplitude after the laser pulse is over, which indicates the presence of a plasmon mode triggered by the laser.

We will discuss in Section 9.6 in much more detail how time-propagation methods can be used to obtain electronic excitation spectra from the time-dependent dipole moment.[4] For a spectral analysis of the dipole moment, one calculates the Fourier transform of $d(t)$ over a finite time window $t_i < t < t_f$:

$$d_\mu(\omega) = \frac{1}{t_f - t_i} \int_{t_i}^{t_f} d_\mu(t) e^{-i\omega t} dt\,. \tag{5.11}$$

This quantity is closely related to the photoabsorption cross section $\sigma(\omega)$ which will be discussed in the linear-response regime in Section 7.2. Instead of $d_\mu(\omega)$, it is preferred in practice to work with the power spectrum $D(\omega)$, which is a positive definite quantity defined as

$$D(\omega) = \sum_{\mu=1}^{3} |d_\mu(\omega)|^2\,. \tag{5.12}$$

As it stands, the numerical evaluation of $d_\mu(\omega)$ via eqn (5.11) is somewhat problematic, since it cuts out a finite time slice of a signal that is assumed to be periodic. This tends to introduce spurious noise into the spectrum. In practice, it is recommended to use

[4] It is often preferable to work with the time-dependent dipole polarization $p_\mu(t) = -d_\mu(t)$, where the minus sign arises from the negative charge of the electron.

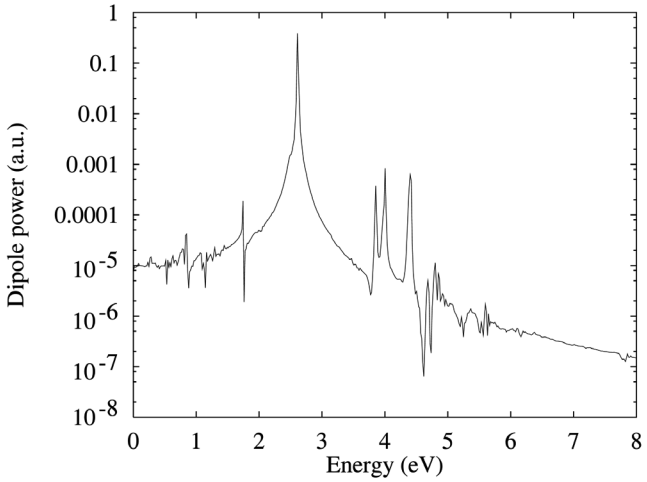

Fig. 5.5 Dipole power spectrum of an Na_9^+ cluster, calculated with the ALDA.

some form of window function when carrying out a Fourier transform over a finite sampling interval (Press *et al.*, 2007).

It is also important to mention that the dipole moment, given in eqn (5.10) in the so-called length form, can also be calculated in alternative ways using the velocity or acceleration form. This is discussed in Appendix H.

Figure 5.5 shows an example of a dipole power spectrum of an Na_9^+ cluster, calculated by time propagation of the TDKS equations (in ALDA and length form) following a weak initial excitation (see Section 9.6.1 for details of the excitation mechanism). The nice dipole oscillations of the cluster that we saw in Fig. 5.4 now translate into a pronounced peak in the spectrum, known as the Mie (surface) plasmon. A few other spectral features can also be observed, which correspond to single-particle excitations and bulk-like higher excitations (Calvayrac *et al.*, 2000).

Higher multipole moments can be considered in a similar fashion (Mundt and Kümmel, 2007; Thiele and Kümmel, 2009). For instance, the time-dependent quadrupole moment is a second-rank tensor defined as

$$q_{\mu\nu}(t) = \int_{\mathcal{V}_\mathrm{A}} d^3r\,(3r_\mu r_\nu - r^2\delta_{\mu\nu})n(\mathbf{r},t)\,, \tag{5.13}$$

with an associated quadrupole power spectrum

$$Q(\omega) = \sum_{\substack{\mu,\nu=1\\ \nu\geq\mu}}^{3} |q_{\mu\nu}(\omega)|^2\,. \tag{5.14}$$

Higher multipole moments can be used to gain access to certain dipole-forbidden transitions.

5.2 Implicit density functionals

5.2.1 Ion probabilities

In experiments studying the ionization of atoms or molecules following laser excitation or collision with a projectile, the most straightforward observable quantity is the number of ions of various charge states that are produced at a given time during or after the excitation. In other words, we are looking for the probability of finding the system in one of the $N+1$ possible charge states to which it can ionize, $P^{+n}(t)$. Here, $P^0(t)$ is the probability that the system stays neutral (i.e., no ionization at all), $P^{+1}(t)$ is the probability that it becomes singly ionized, and so on. $P^{+N}(t)$ is the probability that the system is completely stripped of all its electrons, which is a possible outcome if the excitation is sufficiently intense.

In the context of TDDFT, calculating the ion probabilities $P^{+n}(t)$ is a difficult problem and has been extensively discussed in the literature (Lappas and van Leeuwen, 1998; Petersilka and Gross, 1999; Ullrich, 2000; Dahlen and van Leeuwen, 2001; Dahlen, 2002). To set the stage, let us begin by giving a rigorous definition.

Let us consider a finite N-electron system, initially neutral and in its ground state, which is acted upon by a strong time-dependent external field switched on at t_0 and turned off at some later time t_1. The time-dependent many-body wave function can be expanded in terms of the complete set $\{\Psi_{0j}\}$ of stationary many-body wave functions of the system in the absence of the external field:

$$\Psi[n](t) = \sum_{j=1}^{\infty} a_j[n](t)\, \Psi_{0j}[n_0]\,. \tag{5.15}$$

Since the Ψ_{0j} are functionals of the ground-state density $n_0(\mathbf{r})$ only, the functional dependence of $\Psi(t)$ on the time-dependent density $n(\mathbf{r},t)$ enters exclusively through the complex expansion coefficients $a_j[n](t)$.

The set $\{\Psi_{0j}\}$ can be divided into $N+1$ subsets $\{\Psi^k_{0j}\}$ comprising all stationary many-body wave functions with k particles in the continuum and $(N-k)$ bound particles. Equation (5.15) then becomes

$$\Psi(t) = \sum_{k=0}^{N} \sum_{l=1}^{\infty} a^k_l(t) \Psi^k_{0l}\,. \tag{5.16}$$

At a given time t, the system is in one of the $N+1$ possible charge states from zero to $+N$ with a probability $P^k(t)$, $k = 0, \ldots, N$. The probability for the charge state k is obtained by projecting $\Psi(t)$ onto the subset $\{\Psi^k_{0j}\}$:

$$P^k(t) = \langle \Psi(t)| \left\{ \sum_l |\Psi^k_{0l}\rangle\langle\Psi^k_{0l}| \right\} |\Psi(t)\rangle\,, \tag{5.17}$$

or, making use of eqn (5.16),

$$P^k(t) = \sum_l |a^k_l(t)|^2\,. \tag{5.18}$$

Since the ion probabilities $P^k(t)$ are expressed via a subset of the expansion coefficients $a_j[n](t)$ they are implicit functionals of the time-dependent density $n(\mathbf{r},t)$. For the total numbers of bound and emitted electrons, $N_{\rm bound}(t)$ and $N_{\rm esc}(t)$, we find

$$N_{\rm bound}(t) = \sum_{k=0}^{N}(N-k)P^k(t)\,, \tag{5.19}$$

$$N_{\rm esc}(t) = \sum_{k=0}^{N} kP^k(t)\,. \tag{5.20}$$

Using the fact that the ion probabilities must sum to one, one can easily show that

$$N_{\rm bound}(t) + N_{\rm esc}(t) \;=\; \sum_{k=0}^{N}\big[(N-k)+k\big]P^k(t) \;=\; N\sum_{k=0}^{N}P^k(t) \;=\; N\,. \tag{5.21}$$

The bound and escaped electrons thus add up to the total (integral) number of electrons in the system, as they should. As we saw earlier, $N_{\rm bound}$ and $N_{\rm esc}$ themselves can take on nonintegral values. In the light of eqns (5.19) and (5.20), this expresses the fact that at a given time the system can be in a superposition of more than one charge state, where each state contributes with probability $P^k(t)$.

Equation (5.18) for the ion probabilities is not very practical. It is more convenient to utilize spatial integration over an analyzing region $\mathcal{V}_{\rm A}$ as discussed in Section 5.1.2. With this, it is not difficult to obtain the following expressions:

$$P^0(t) = \int_{\mathcal{V}_{\rm A}} dx_1 \ldots \int_{\mathcal{V}_{\rm A}} dx_N |\Psi(\mathbf{x}_1,\ldots,\mathbf{x}_N,t)|^2, \tag{5.22}$$

$$P^{+1}(t) = \binom{N}{1} \int_{\overline{\mathcal{V}}_{\rm A}} dx_1 \int_{\mathcal{V}_{\rm A}} dx_2 \ldots \int_{\mathcal{V}_{\rm A}} dx_N |\Psi(\mathbf{x}_1,\ldots,\mathbf{x}_N,t)|^2, \tag{5.23}$$

$$P^{+2}(t) = \binom{N}{2} \int_{\overline{\mathcal{V}}_{\rm A}} dx_1 \int_{\overline{\mathcal{V}}_{\rm A}} dx_2 \int_{\mathcal{V}_{\rm A}} dx_3 \ldots \int_{\mathcal{V}_{\rm A}} dx_N |\Psi(\mathbf{x}_1,\ldots,\mathbf{x}_N,t)|^2, \tag{5.24}$$

and similarly for all other P^{+n}, where $\overline{\mathcal{V}}_{\rm A}$ refers to all space outside the integration volume $\mathcal{V}_{\rm A}$. These expressions for the ion probabilities are easily interpreted. Equation (5.22) for P^0 describes the probability of finding all the electrons inside the analyzing box, i.e., in a bound state. Equation (5.23) for P^{+1} is, in turn, the probability of finding one ionized electron outside the box, while all other electrons are bound inside. The prefactor $\binom{N}{1}$ accounts for the fact that the electrons are indistinguishable.

All definitions of the ion probabilities given so far are based on the many-body wave function and require solution of the full time-dependent Schrödinger equation. To arrive at a simpler, approximate way of calculating the $P^k(t)$, we replace the exact N-particle wave function $\Psi(t)$ by the single-determinant TDKS wave function $\Phi(t)$. In analogy with eqns (5.7) and (5.8), we can define the probability for each TDKS orbital to be bound or continuum as

$$N_{\mathrm{bound},j}(t) \equiv N_j(t) = \int_{\mathcal{V}_\mathrm{A}} d^3r\, |\varphi_j(\mathbf{r},t)|^2 \,, \tag{5.25}$$

$$N_{\mathrm{esc},j}(t) \equiv \overline{N}_j(t) = \int_{\overline{\mathcal{V}}_\mathrm{A}} d^3r\, |\varphi_j(\mathbf{r},t)|^2 \,. \tag{5.26}$$

This gives the following approximate ion probabilities $P_s^k(t)$:

$$P_s^0(t) = N_1(t)N_2(t)\ldots N_N(t) \,, \tag{5.27}$$

$$P_s^{+1}(t) = \sum_{n=1}^{N} N_1(t)\ldots\overline{N}_n(t)\ldots N_N(t) \,, \tag{5.28}$$

$$P_s^{+2}(t) = \sum_{n=1}^{N-1}\sum_{\substack{m=2\\m>n}}^{N} N_1(t)\ldots\overline{N}_n(t)\ldots\overline{N}_m(t)\ldots N_N(t) \,, \tag{5.29}$$

and similarly for all other P_s^{+n}. The total numbers of bound and escaped electrons are obtained by inserting the ion probabilities $P_s^k(t)$ into eqns (5.19) and (5.20):

$$N_\mathrm{bound}(t) = \sum_{k=0}^{N}(N-k)P_s^k(t) = \sum_{j=1}^{N} N_j(t) \,, \tag{5.30}$$

$$N_\mathrm{esc}(t) = \sum_{k=0}^{N} kP_s^k(t) = \sum_{j=1}^{N} \overline{N}_j(t) \,. \tag{5.31}$$

Since $n(\mathbf{r},t) = \sum_{j=1}^{N} |\varphi_j(\mathbf{r},t)|^2$, eqns (5.30) and (5.31) reduce to eqns (5.7) and (5.8). In other words, the second approximation step (replacing the exact by the TDKS wave function) affects only the ion probabilities $P^k(t)$, and leaves $N_\mathrm{bound}(t)$ and $N_\mathrm{esc}(t)$ unchanged.

The approximate TDKS ion probabilities $P_s^{+n}(t)$ reduce to the exact $P^{+n}(t)$ in certain limits, such as in the (trivial) case of a one-electron system, and in the limits of almost vanishing and almost complete ionization [within the assumptions leading to eqns (5.7) and (5.8)]. The proof of this is left to Exercise 5.3. The probabilities $P_s^{+n}(t)$ can thus be interpreted as interpolations between these limiting cases, under the constraint that they add up to unity.

For general multiple ionization of N-electron systems, the TDKS ion probabilities become exact in the idealized case when the ionization proceeds in a perfectly sequential manner. This means that no direct double or multiple ionization processes occur, and the system goes through its various charge states one after the other: first, the process $0 \to +1$ takes place until the neutral state is completely depleted; then, the process $+1 \to +2$ takes over until no singly charged species is left, and so on. In other words, at any given time only two ion species, $+n$ and $+n+1$, are present. Strictly speaking, this is almost never exactly the case; on the other hand, nearly sequential ionization of many-electron systems is quite common in practice (see Section 16.1.1).

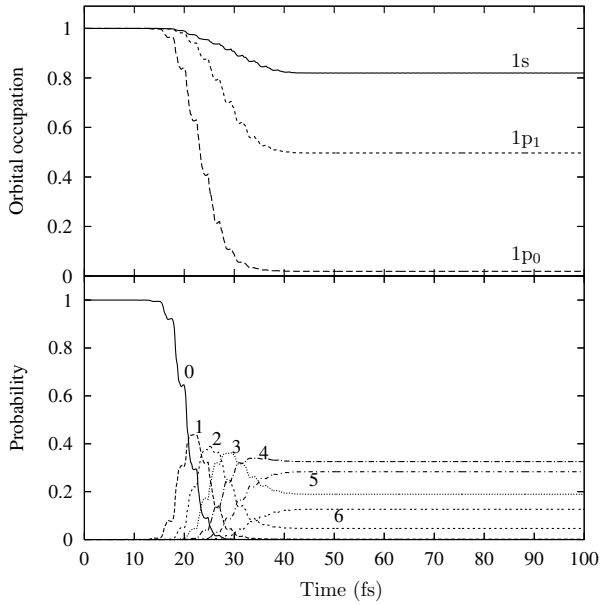

Fig. 5.6 Top: occupation probabilities for the $1s$, $1p_0$, and $1p_1$ orbitals of an Na_9^+ cluster in the spherical jellium model, irradiated with a 25 fs Gaussian laser pulse (peak at 32.2 fs) with photon energy 0.87 eV and intensity 4×10^{13} W/cm^2. Bottom: TDKS ion probabilities.

Detailed calculations of ion probabilities, comparing exact benchmark calculations with TDKS calculations, have been performed for two-electron systems with reduced dimensionality. We will discuss this work in detail later, in Section 16.1.2. For now, let us just illustrate how the ion probabilities work for the case of an Na_9^+ cluster in an intense femtosecond laser pulse (Calvayrac *et al.*, 2000).

In its ground state, the valence electrons of Na_9^+ form a closed shell with a doubly occupied s orbital and three doubly occupied p orbitals, labeled 1s, $1p_0$, $1p_{+1}$, and $1p_{-1}$ (this shell structure is the same as for the 3D harmonic oscillator). We assume the laser to be polarized along the z-axis, so that the initial rotational symmetry (and thus the m quantum number of each TDKS orbital) is conserved. Thus, the $1p_{+1}$ and $1p_{-1}$ orbitals are equivalent for all times, and we label them simply as $1p_1$.

Figure 5.6 shows that ionization happens mostly around the peak of the pulse at 20 fs. The upper panel shows how the orbital norms decrease rapidly. The TDKS ion probabilities illustrate how the cluster temporarily passes through various charge states, and ends up in a state where it is most likely to be found in a fourfold ionized state, with somewhat less probability of fivefold, threefold, and sixfold ionization.

5.2.2 Kinetic-energy spectra

Another spectroscopic observable of experimental interest is the kinetic-energy distribution of photoelectrons. In strong fields, where multiphoton processes play a dominant role, the photoelectron spectra may exhibit characteristic features related to above-threshold ionization (ATI) (see Section 16.1.3).

Formally, the photoelectron energy distribution spectrum can be defined as the probability of finding the system in a state with an energy in the interval $[E, E+dE]$,

$$P(E)\,dE = \lim_{t\to\infty} \sum_{k=1}^{N} |\langle \Psi_E^k | \Psi(t)\rangle|^2 dE\,, \tag{5.32}$$

where $|\Psi_E^k\rangle$ is an eigenstate of the many-body system with k electrons in the continuum, and E is the total kinetic energy of all continuum electrons for that state.[5] The $t \to \infty$ limit ensures that the laser pulse (or any other form of perturbation which has caused the ionization) is over, and the ionized electrons have moved far enough away from the core and are able to propagate freely towards the detector.

The definition (5.32), in principle, includes multiple ionization processes (sequential as well as nonsequential ones). Clearly, for many-electron systems, it is very difficult to calculate photoelectron spectra rigorously using this projection method; applications based on numerically exact wave functions have been mostly restricted to hydrogenic systems or, in the case of larger atoms, to approximate solutions with only a single active electron (Javanainen *et al.*, 1988). But even for hydrogen, using eqn (5.32) is not easy, because it requires generating and storing a very large number of eigenfunctions. There exist alternative spectral analysis methods that are numerically more convenient (Schafer and Kulander, 1990; Grobe and Eberly, 1992).

Obtaining photoelectron spectra with TDDFT again presents the problem of how to express $P[n](E)$ as a functional of the time-dependent density, since the exact definition (5.32) involves the many-body wave functions. Just like the ion probabilities, $P[n](E)$ is an implicit density functional, and in practice one has to rely on approximations to extract photoelectron spectra from a TDKS calculation.

Véniard *et al.* (2003) proposed a simple and intuitive semiclassical way to calculate $P(E)$ directly from the density. A free classical particle, starting from position $x = 0$ at time $t = 0$ and possessing kinetic energy E, will be found at the position $x = t_f\sqrt{2E}$ at a later time t_f. The quantum analog of this time-of-flight analysis can be formulated for a wave packet, initially localized at $x = 0$ and $t = 0$. Thus, assuming a one-dimensional system (generalization to two or three dimensions is straightforward), one defines

$$P(E, \Delta E, t_f) = \int_{x_<}^{x_>} dx\, n(x, t_f) + \int_{-x_>}^{-x_<} dx\, n(x, t_f)\,, \tag{5.33}$$

where

$$x_< = t_f\sqrt{2(E-\Delta E)}\,, \qquad x_> = t_f\sqrt{2(E+\Delta E)}\,. \tag{5.34}$$

In other words, one counts how much probability density reaches a spatial region corresponding to the energy bin $E-\Delta E < E < E+\Delta E$. For large but finite propagation times, $P(E, \Delta E, t_f)$ depends only weakly on t_f. The underlying assumption is that all continuum-state density is "born" instantaneously at the same place and time, and that the electronic wave packets move in an uncorrelated manner and do not feel any residual interaction with the ionic core or with each other.

[5] In the case of a partially ionized many-body state, defining the kinetic energy associated with the continuum electrons may be a bit subtle; see Exercise 5.4.

The resolution which can be achieved with this method depends on the length of the laser pulse, $T_{\rm pulse}$, because photoelectrons can be emitted at essentially any time during the pulse. One finds

$$\frac{\Delta E_{\rm min}}{E} \approx \frac{T_{\rm pulse}}{t_f} \,. \tag{5.35}$$

An alternative method for calculating kinetic-energy spectra is via the TDKS single-particle orbitals (Pohl *et al.*, 2000; Nguyen *et al.*, 2004). This is similar in spirit to the TDKS ion probabilities we considered in Section 5.2.1, in the sense that the observable is expressed as an explicit orbital functional rather than an implicit density functional. One obtains the kinetic-energy distribution $P_s(E)$ by recording the TDKS orbitals $\varphi_j(\mathbf{r},t)$ over time at a point $\mathbf{r}_b$ near the grid boundary and performing subsequent Fourier transformation, so that

$$P_s(E) = \sum_{j=1}^{N} |\varphi_j(\mathbf{r}_b, E)|^2 \,. \tag{5.36}$$

Needless to say, this method ignores correlations contained in the many-body wave function and can only be expected to be reasonably accurate if the ionization processes are sequential and the resulting photoelectrons are not strongly correlated. On the other hand, eqn (5.36) has several practical advantages: it is relatively easy to implement, does not require a very large numerical grid, and is robust under unitary transformations among the occupied single-particle states. Later, in Section 16.1.3, we will discuss some applications.

5.2.3 Other implicit density functionals

There exist many other observables of experimental and theoretical interest whose definition directly involves the many-body wave functions and which therefore cannot be easily formulated as functionals of the time-dependent density. Replacing the exact wave function with the TDKS wave function sometimes works just fine, but, more often than not, this is an uncontrolled approximation and can lead to qualitatively wrong results. Nevertheless, the computational simplicity of (TD)DFT is such an enormous advantage over wave-function-based methods that the search for approximate density functionals for such implicit observables remains a very attractive goal: even such properties as the entanglement of many-body wave functions and quantum computation are nowadays being studied using density-functional methods (Wu *et al.*, 2006; Coe *et al.*, 2008; Gaitan and Nori, 2009).

Let us now briefly discuss two more implicit observables of practical interest, namely transition amplitudes and momentum distributions.

State-to-state transition probabilities. The response of a many-body system to a perturbation can be discussed in terms of state-to-state transition amplitudes,

$$S_{i,f} = \lim_{t\to\infty} \langle \Psi_f | \Psi(t) \rangle \,, \tag{5.37}$$

where the system is assumed to start from an initial eigenstate, $\Psi(t \to -\infty) = \Psi_i$. The transition amplitude (5.37) is the overlap of the time-dependent wave function

with some final state Ψ_f, assumed to be an eigenstate of the unperturbed system. The perturbation is assumed to have finite duration. The state-to-state transition probability is then given as $P_{i,f} = |S_{i,f}|^2$. The transition amplitudes $S_{i,f}$ for all possible initial and final eigenstates form the so-called S-matrix. This plays an important role in scattering processes, but can be defined for arbitrary time-dependent perturbations in which state-to-state transitions occur.

The exact S-matrix is an implicit density functional. A simple approximation is obtained by replacing the many-body wave functions with (TD)KS Slater determinants:

$$S^s_{i,f} = \lim_{t\to\infty} \langle \Phi_f | \Phi(t) \rangle \, . \tag{5.38}$$

Like the TDKS ion probabilities and photoelectron spectra discussed above, this is essentially an uncontrolled approximation. A density functional for the transition amplitudes has recently been developed (Rohringer *et al.*, 2004). This functional is defined in an operational way as a "read-out functional"; in addition to $n(\mathbf{r}, t)$, the density of each excited state Ψ_f is required as input. The procedure was shown to work for two-electron systems, but turns out to be very sensitive to small errors in the density.

Momentum distributions. Let us consider, for simplicity, the case of a one-dimensional two-electron system (generalization to N electrons is straightforward), and define the wave function in momentum space as (Wilken and Bauer, 2007; Rajam *et al.*, 2009)

$$\Psi(k_1, k_2, t) = \frac{1}{2\pi} \int dz_1 \int dz_2 \, \Psi(z_1, z_2, t) e^{-i(k_1 x_1 + k_2 x_2)} \, . \tag{5.39}$$

The spatial integration in eqn (5.39) can be partitioned in a similar way to what was done in the definition of the ion probabilities in eqns (5.22)–(5.24). This allows us to define, for instance, the correlated wave function in momentum space of those electrons set free in a double ionization process:

$$\Psi^{2+}(k_1, k_2, t) = \frac{1}{2\pi} \int_{\overline{\mathcal{V}}_\mathrm{A}} dz_1 \int_{\overline{\mathcal{V}}_\mathrm{A}} dz_2 \, \Psi(z_1, z_2, t) e^{-i(k_1 x_1 + k_2 x_2)} \, . \tag{5.40}$$

In practice, the sharp spatial cutoff associated with the definition of the integration volume $\overline{\mathcal{V}}_\mathrm{A}$ should be replaced with a smoothing or window function in order to avoid numerical artifacts in the Fourier transform (Wilken and Bauer, 2007).

The ion recoil momenta are quantities of much experimental interest. The momentum of the photons is negligibly small; therefore, for a double ionization process, the momentum density of the ion can be simply calculated as

$$n^{2+}_\mathrm{ion}(k_\mathrm{ion}, t) = \int dk \, |\Psi^{2+}(-k_\mathrm{ion} - k, k, t)|^2 \, , \tag{5.41}$$

where momentum conservation implies $-k_\mathrm{ion} = k_1 + k_2$. The TDKS ion momentum density, on the other hand, is obtained by replacing the correlated two-electron wave function with the TDKS wave function. One obtains

$$n^{2+}_{\mathrm{ion},s}(k_\mathrm{ion}, t) = \int dk \, |\varphi^+(-k_\mathrm{ion} - k, t)\varphi^+(k, t)|^2 \, , \tag{5.42}$$

where $\varphi^+(k, t)$ is the Fourier transform of the doubly occupied TDKS orbital $\varphi(z, t)$, calculated over the region $\overline{\mathcal{V}}_\mathrm{A}$. A comparison of the two ion momentum densities is

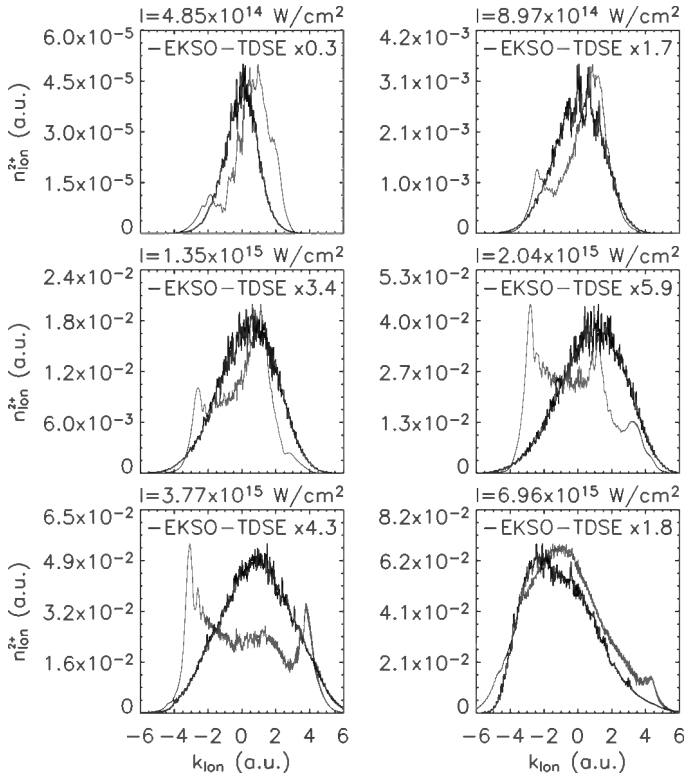

Fig. 5.7 Ion momentum density of a He^{2+} model ion, acted upon by 780 nm laser pulses with varying peak intensities. TDSE: exact $n^{2+}_{\rm ion}$ from eqn (5.41). EKSO: approximate $n^{2+}_{{\rm ion},s}$ from eqn (5.42), using the exact Kohn–Sham orbital. [Reproduced with permission from APS from Wilken and Bauer (2007), ©2007.]

given in Fig. 5.7. Clearly, there are situations where $n^{2+}_{{\rm ion},s}$ is a very poor approximation, even if the exact Kohn–Sham orbitals are used in eqn (5.42). These are cases where the double ionization is highly correlated; on the other hand, the TDKS ion momenta can be acceptable if the ionization proceeds sequentially (see also Section 16.1).

5.3 The time-dependent energy

In static DFT, the ground-state energy E_0 is the central quantity of interest; calculating the excited-state energies E_j is the goal of linear-response TDDFT, as we will discuss in Part II of this book. Let us now ask the question of whether it makes sense, in general, to consider the time-dependent energy as an observable quantity in TDDFT (Hessler *et al.*, 1999).

It is a well-known fact that energy is not a conserved quantity if a system is subject to a time-dependent external potential. Consider for instance an atom in its ground state. If at times $t > t_0$ it becomes subject to a time-varying potential caused by a

laser field or a charged projectile passing by, its electron cloud will be shaken up so that its energy increases.

A quantum mechanical definition of the time-dependent energy can be given using a simple extension of the definition of the energy of a stationary system. To simplify things, we limit ourselves to systems which start from the ground state, with energy E_0. We then simply define the time-dependent energy as the expectation value of the time-dependent Hamiltonian:[6]

$$E(t) = \langle \Psi(t) | \hat{H}(t) | \Psi(t) \rangle \, . \tag{5.43}$$

Expanding the time-dependent wave function $\Psi(t)$ as

$$\Psi(t) = \sum_j c_j(t) e^{-iE_j t} \Psi_j \, , \tag{5.44}$$

we see that the definition (5.43) leads to an expression for $E(t)$ in terms of a weighted sum of the energies of the eigenstates of the system at the initial time,

$$E(t) = \sum_j |c_j(t)|^2 E_j \, . \tag{5.45}$$

Using the form (3.1) of the Hamiltonian, we obtain

$$E(t) = T(t) + \int d^3r \, v(\mathbf{r},t) n(\mathbf{r},t) + W(t) \, , \tag{5.46}$$

where $T(t)$ and $W(t)$ are the instantaneous kinetic energy and electron–electron interaction energy associated with the many-body wave function $\Psi(t)$. Clearly, $E(t)$ is a well-defined quantity, and a functional of the density. In the adiabatic limit $v(\mathbf{r},t) \to v_0(\mathbf{r})$, it reduces to the ground-state density.

Now consider a Kohn–Sham system which produces the same density $n(\mathbf{r},t)$. We define

$$E(t) = T_s(t) + \int d^3r \, v(\mathbf{r},t) n(\mathbf{r},t) + E_{\rm H}(t) + E_{\rm xc}(t) \, , \tag{5.47}$$

where the time-dependent noninteracting kinetic and Hartree energies are given by

$$T_s(t) = -\sum_{j=1}^{N} \varphi_j^*(\mathbf{r},t) \frac{\nabla^2}{2} \varphi_j(\mathbf{r},t) \, , \tag{5.48}$$

$$E_{\rm H}(t) = \frac{1}{2} \int d^3r \int d^3r' \, \frac{n(\mathbf{r},t) n(\mathbf{r}',t)}{|\mathbf{r}-\mathbf{r}'|} \, , \tag{5.49}$$

and the time-dependent xc energy $E_{\rm xc}(t)$ is defined such that the values of $E(t)$ obtained from eqn (5.46) and from eqn (5.47) coincide. Comparing the two expressions, we find

[6] Strictly speaking, $\hat{H}(t)$ should not be called the energy operator of the system; this terminology is reserved for the static Hamiltonian $\hat{H}_0$, which yields the spectrum of energy eigenvalues E_j and associated eigenstates Ψ_j. Given the state $\Psi(t)$ of the system at some time t, we can make a measurement of its energy, which will produce the eigenvalue E_j with probability $|c_j(t)|^2$.

$$E_{\rm xc}(t) = T(t) - T_s(t) + W(t) - E_{\rm H}(t)\,, \tag{5.50}$$

in complete analogy to the static case. Furthermore, we write $T(t) - T_s(t) \equiv T_c(t)$, the correlation part of the time-dependent kinetic energy. Again, $E_{\rm xc}(t)$ is a well-defined functional of the time-dependent density.

In contrast to the static case, the absolute value of the time-dependent energy $E(t)$ is not of practical interest. Furthermore, the variational definition of the static xc potential, $v^0_{\rm xc}(\mathbf{r}) = \delta E^0_{\rm xc}/\delta n(\mathbf{r})$, does not carry over to the time-dependent case; in other words, $v_{\rm xc}(\mathbf{r},t) \neq \delta E_{\rm xc}(t)/\delta n(\mathbf{r},t)$. We will discuss a different time-dependent variational principle for $v_{\rm xc}(\mathbf{r},t)$ in Section 6.6.

Instead, the practical usefulness of time-dependent energies such as $E(t)$ and $E_{\rm xc}(t)$ lies in certain sum rules for $v_{\rm xc}(\mathbf{r},t)$, which we will present in Section 6.2.4.

Exercise 5.1 Derive the ion probability formulas (5.22), (5.23), and (5.24) and the general formula for $P^{+n}(t)$, starting from the normalization condition

$$\int_{\mathcal{V}_{\rm A}+\overline{\mathcal{V}}_{\rm A}} dx_1 \ldots \int_{\mathcal{V}_{\rm A}+\overline{\mathcal{V}}_{\rm A}} dx_N \, |\Psi(x_1,\ldots,x_N,t)|^2 = 1\,. \tag{5.51}$$

Exercise 5.2 The approximate Kohn–Sham probabilities $P^k_s(t)$ can be constructed in an alternative way starting with the following identification:

$$\sum_{k=0}^{N} P^k_s(t) = \prod_{j=1}^{N} \left[N_j(t) + \overline{N}_j(t)\right]\,. \tag{5.52}$$

It is easy to see that both sides of eqn (5.52) are equal to unity, since $N_j(t) + \overline{N}_j(t) = 1$ for all j. We then work out the right-hand side and collect terms containing k factors $\overline{N}_j(t)$ and $(N-k)$ factors $N_j(t)$. These are then associated with the $P^k_s(t)$.

Exercise 5.3 Show that the TDKS ion probabilities become exact in the limit of almost vanishing ionization, $N_{\rm bound}(t) = N - \delta$ and $N_{\rm esc}(t) = \delta$, and in the limit of almost complete ionization, $N_{\rm bound}(t) = \delta$ and $N_{\rm esc}(t) = N - \delta$.

Exercise 5.4 The definition (5.32) of the photoelectron spectrum requires the energy of the continuum part of the many-body wave function. Think about why this is a subtle issue and how, in principle, one could define this energy in the case $t \to \infty$, i.e., long after the end of the external perturbation causing ionization.

Exercise 5.5 Try out the definition (5.36) for the kinetic-energy spectrum of a single electron which suddenly, at time $t = 0$, makes a transition from a bound state to a plane-wave state.

Exercise 5.6 This is a numerical exercise, using the 1D lattice code of Exercise 4.2. Implement a numerical subroutine which calculates the time-dependent energy $E(t)$ for a noninteracting system of N electrons driven by a laser pulse. Convince yourself that the energy increases when the system is driven by the laser field. Make a back-of-the-envelope estimate of the energy transferred to the system by the laser field, and see how it compares with the $E(t)$ which you have calculated numerically.

6
Properties of the time-dependent xc potential

6.1 What is the universal xc functional?

The central idea of the TDKS approach, as we have seen, is to reproduce the time-dependent density $n(\mathbf{r},t)$ of an interacting N-particle system driven by an external potential $v(\mathbf{r},t)$ with a noninteracting system moving in the effective potential (4.1), $v_s[n,\Psi_0,\Phi_0](\mathbf{r},t)$. The fundamental existence theorems of Runge and Gross and van Leeuwen tell us that it is, in principle, possible to do so, and in a unique manner. If we knew the exact time-dependent effective potential, then there would be no need to solve the full many-body Schrödinger equation, and our life would become so much easier!

The catch, of course, is that the xc potential $v_{\rm xc}[n,\Psi_0,\Phi_0](\mathbf{r},t)$, as a universal functional of the density and the initial states, is unknown. All we can do is to use approximations to it, and hope that they are sufficiently accurate. In Section 4.2 we introduced the adiabatic approximation, and later on in this book we will encounter other approximations of various degrees of sophistication.

The goal of this chapter is to get better acquainted with the xc potential, to understand its properties, in particular those that are unique to the time-dependent case, and to list some exact conditions that it must satisfy. This knowledge will help us to construct better approximations to it, or to understand under what circumstances existing approximations will work well or fail.

But before we get into these details, let us think a bit more about the exact, universal xc functional. We know it exists—but how would one go about finding it? To keep things somewhat more transparent, let us say we are interested only in systems that are in the ground state at the initial time t_0, and we want to propagate until a fixed finite time t_1. The xc potential $v_{\rm xc}$ is then a functional of the time-dependent density $n(\mathbf{r},t)$ in the interval $[t_0,t_1]$.[1] Let us try to define a procedure which would produce the exact universal xc functional $v_{\rm xc}[n](\mathbf{r},t)$, assuming we had unlimited time and resources. While such a procedure may not be very realistic (to say the least), it can give us some insight into what the xc functional actually *is*.

The universal xc functional can be viewed as an enormously big library, containing an infinite number of books. Each book contains the time-dependent xc potential $v_{\rm xc}(\mathbf{r},t)$ for a particular time-dependent density. For example, there will be one book

[1] When we discuss memory and causality in Section 6.4, we will show that the xc potential at time t can only depend on densities at times $t' \leq t$.

for each of the following density functions:

$$n_1(\mathbf{r},t) = \frac{N}{\pi^{3/2}s_1(t)^3}e^{-r^2/s_1(t)^2}\,, \qquad s_1(t) = 1 + 0.1\sin[\omega_1(t-t_0)], \tag{6.1}$$

$$n_2(\mathbf{r},t) = \frac{N}{\pi^{3/2}s_2(t)^3}e^{-r^2/s_2(t)^2}\,, \qquad s_2(t) = 1 + 0.1\sin[\omega_2(t-t_0)], \tag{6.2}$$

$$\vdots$$

Each of these spherically symmetric densities integrates to N particles, starts from the same initial density at t_0, and carries out breathing-mode-type oscillations with a slightly different frequency. The book which is entitled "$n_1(\mathbf{r},t)$" then gives us $v_{\rm xc}[n_1](\mathbf{r},t)$ in the interval $[t_0,t_1]$ in the form of a table. For example, we could split up this time interval into a large number of tiny time steps $t_0, t_0+\Delta t, t_0+2\Delta t, \ldots, t_1$, with $\Delta t \ll (t_1 - t_0)$. The jth page of our book then contains $v_{\rm xc}[n_1](\mathbf{r},t_j)$ at a given time t_j, in the form of a table evaluated at discrete spatial grid points.

The neighboring book will be entitled "$n_2(\mathbf{r},t)$" and contains the tabulated values of $v_{\rm xc}[n_2](\mathbf{r},t)$ at each point in space and time between t_0 and t_1. There will be an entire shelf in our library which holds books just for densities similar to (6.1) and (6.2), with different frequencies of the spherical density oscillations. On another shelf, not very far away, one will find books for the same type of spherically symmetric oscillating densities, but with slightly different amplitudes. And so on: one room of our library is dedicated to spherically symmetric time-dependent densities only; other rooms contain the books for nonspherical densities. The library is organized into different wings for total densities integrating to different particle numbers N.

The entire library is a representation of the universal xc functional $v_{\rm xc}[n](\mathbf{r},t)$. To solve the TDKS equation for an N-particle system in a given external potential $v(\mathbf{r},t)$ which yields the exact density $n(\mathbf{r},t)$, we need to look up the book which belongs to this particular density. We can find it by iteration, as outlined in Section 4.4.

But how was this library constructed, and how have the innumerably many books been written? Let us imagine we have an unlimited number of vastly powerful computers at our disposal. We run a calculation on one of them, solving the full time-dependent N-particle Schrödinger equation for an interacting system driven by some external potential $\widetilde{v}(\mathbf{r},t)$, and obtain the time-dependent wave function $\Psi(\mathbf{r}_1,\ldots,\mathbf{r}_N,t)$ and from it the density $\widetilde{n}(\mathbf{r},t)$. Next, we numerically invert[2] the noninteracting Schrödinger equation

$$\left[-\frac{\nabla^2}{2} + \widetilde{v}_s(\mathbf{r},t)\right]\widetilde{\varphi}_j(\mathbf{r},t) = i\frac{\partial}{\partial t}\widetilde{\varphi}_j(\mathbf{r},t)\,, \tag{6.3}$$

which yields the given density as $\widetilde{n}(\mathbf{r},t) = \sum_{j=1}^{N}|\widetilde{\varphi}_j(\mathbf{r},t)|^2$. The xc potential is then given by $v_{\rm xc}[\widetilde{n}](\mathbf{r},t) = \widetilde{v}_s(\mathbf{r},t) - \widetilde{v}(\mathbf{r},t) - v_{\rm H}[\widetilde{n}](\mathbf{r},t)$. The tabulated values of this xc potential are written down in a book entitled "$\widetilde{n}(\mathbf{r},t)$" and put on a shelf in our library. Now we repeat this procedure, starting from a slightly different external potential, getting the exact density from the full many-body Schrödinger equation, inverting the

[2]It is assumed that this numerical inversion can be done in practice. Strategies for the construction of the xc potential from a given density (static or time-dependent) are discussed in Appendix E.

associated TDKS equation, and writing the resulting xc potential down in another book. And so on, ad infinitum, until our library is complete and contains books for all possible densities.

So, each book in the library requires solution of the time-dependent many-body problem. If someone else had done this for us, we could use the library in TDKS calculations and get the exact densities for any desired situation, with very little effort. But, unfortunately, the exact universal xc functional is unknown, although it exists—which is just like standing in front of the library with the doors locked.

6.2 Some exact conditions

While we have to accept the fact that the exact xc functional is unknown (and, in a sense, unknowable), we should at least try to learn as much about this elusive object as we can. In the remainder of this chapter we will give a survey of the exact properties of $v_{\rm xc}(\mathbf{r},t)$ that are known to date, starting in this section with miscellaneous properties that can be viewed as more or less straightforward extensions of exact properties of the static xc potential (Burke, 2006). In later sections, we will consider properties that are unique to the dynamical case.

6.2.1 The adiabatic limit

In Section 4.2 we discussed the adiabatic approximation, $v_{\rm xc}^{\rm A}(\mathbf{r},t)$, which is obtained by evaluating the static xc functional of ground-state DFT with a time-dependent density. As we pointed out there, the adiabatic approximation becomes exact in the limit of slowly varying densities. For the exact xc potential, this implies

$$v_{\rm xc}(\mathbf{r},t) \longrightarrow v_{\rm xc}^{0}[n(t)](\mathbf{r})\,, \tag{6.4}$$

provided that

$$\frac{\partial n(\mathbf{r},t')}{\partial t'} \longrightarrow 0 \tag{6.5}$$

for all $\mathbf{r}$ and all $t' \leq t$. Notice that it is not enough to require the instantaneous density change at time t to be vanishing; instead, because of the memory inherent in the xc potential, one must require that the density becomes static at all previous times. This will become clearer when we discuss memory and causality in Section 6.4.

The condition (6.4) holds for all finite systems and all extended systems with a finite gap; gapless systems can be more tricky and will be addressed later, in Chapters 8 and 10. In particular, it will turn out that there are some subtle issues which come up in the static limit of the linear response of weakly inhomogeneous electron liquids.

6.2.2 The zero-force theorem

In Section 3.1.3 we showed that, owing to Newton's third law, the rate of change of the total momentum of a many-body system equals the external force on it [see eqn (3.32)]. We can write the total momentum (3.31) as follows:

$$\mathbf{P}(t) = \int d^3r\, \mathbf{j}(\mathbf{r},t) = \int d^3r\, \mathbf{r}\, \frac{\partial}{\partial t} n(\mathbf{r},t)\,, \tag{6.6}$$

where we have used the continuity equation (3.25) and integration by parts. Since the densities in the interacting and in the noninteracting system are the same, we have $\mathbf{P}(t) = \mathbf{P}_s(t)$, i.e., the total momentum in the TDKS system is the same as in the interacting many-body system. Thus,

$$0 = \frac{\partial}{\partial t}\mathbf{P}(t) - \frac{\partial}{\partial t}\mathbf{P}_s(t) = -\int d^3r\, n(\mathbf{r},t)\nabla[v(\mathbf{r},t) - v_s(\mathbf{r},t)]$$
$$= \int d^3r\, n(\mathbf{r},t)\nabla[v_{\rm H}(\mathbf{r},t) + v_{\rm xc}(\mathbf{r},t)]\,. \tag{6.7}$$

The right-hand side is the total force on the system exerted by the Hartree and the xc potentials. Since these potentials originate from the Coulomb interaction and are thus internal forces, the total force vanishes, as required by Newton's third law. It turns out that both contributions vanish individually. For the Hartree force, this can be demonstrated directly:

$$\int d^3r\, n(\mathbf{r},t)\nabla v_{\rm H}(\mathbf{r},t) = \int d^3r\, n(\mathbf{r},t)\nabla \int d^3r' \frac{n(\mathbf{r}',t)}{|\mathbf{r}-\mathbf{r}'|}$$
$$= \int d^3r \int d^3r'\, n(\mathbf{r},t)n(\mathbf{r}',t)\frac{\mathbf{r}'-\mathbf{r}}{|\mathbf{r}-\mathbf{r}'|^3}$$
$$= 0\,. \tag{6.8}$$

Via eqn (6.7) this leads to the following exact condition for the xc potential:

$$\int d^3r\, n(\mathbf{r},t)\nabla v_{\rm xc}(\mathbf{r},t) = 0\,, \tag{6.9}$$

which is known as the *zero-force theorem*. It means that a system cannot exert a net force on itself through xc effects.

Another rigorous statement in Section 3.1.3 was that a system cannot exert a net torque on itself, which is again a consequence of Newton's third law. However, the consequences for the xc potential are a bit more involved than for the case of the linear momentum, and we will have to wait until Section 10.3.3 to prove a zero-torque theorem.

The zero-force theorem is one of the few known rigorous constraints that the exact xc potential must satisfy. Some approximations fulfill it automatically, for instance adiabatic approximations such as the ALDA, where the underlying ground-state functional is known to satisfy the static zero-force theorem.[3] In such cases, the zero-force theorem can be a useful check of the accuracy of numerical propagation schemes.

There exist examples of approximate xc functionals which violate the zero-force theorem. One such example is the KLI exchange potential (see Section 11.1.4), where the violation of eqn (6.9) leads to numerical instabilities in the dipole oscillations of the valence electrons of metallic clusters (Mundt *et al.*, 2007). A construction by Kurzweil and Head-Gordon (2009) can be used to enforce the zero-force theorem and other exact conditions for this type of approximate functional.

[3]The (A)LDA is based on a real physical system, the homogeneous electron liquid, and therefore satisfies many exact properties.

6.2.3 Self-interaction

Like the static xc potential, the time-dependent xc potential must be free of self-interaction. This means, for instance, that for one-electron systems the xc potential reduces to

$$v_{\rm xc}(\mathbf{r},t) = -\int d^3r' \frac{n(\mathbf{r}',t)}{|\mathbf{r}-\mathbf{r}'|}\,, \qquad \text{for} \qquad \int d^3r\, n(\mathbf{r},t) = 1\,. \tag{6.10}$$

If this condition is satisfied, the xc potential cancels out the Hartree potential in eqn (4.9), and the TDKS effective potential reduces to the external potential.

6.2.4 Sum rules involving the time-dependent energy

Following Hessler *et al.* (1999), we start with the Heisenberg equation of motion for the expectation value of a general operator,

$$\frac{dO}{dt} = \left\langle \frac{\partial \hat{O}}{\partial t} \right\rangle + i\langle[\hat{H},\hat{O}]\rangle\,. \tag{6.11}$$

This relation can also be applied to the Hamiltonian itself, and, using the definitions in Section 5.3, in particular eqn (5.46), we obtain

$$\frac{dE(t)}{dt} = \int d^3r\, \frac{\partial v(\mathbf{r},t)}{\partial t}\, n(\mathbf{r},t) \tag{6.12}$$

or

$$\frac{dT(t)}{dt} + \frac{dW(t)}{dt} = -\int d^3r\, \frac{\partial n(\mathbf{r},t)}{\partial t}\, v(\mathbf{r},t)\,. \tag{6.13}$$

The same considerations can be repeated for the Kohn–Sham system, and one finds

$$\frac{dT_s(t)}{dt} = -\int d^3r\, \frac{\partial n(\mathbf{r},t)}{\partial t}\, v_s(\mathbf{r},t)\,. \tag{6.14}$$

Subtracting eqn (6.13) from eqn (6.14) and using the definition (5.50) of the time-dependent xc energy, we obtain

$$\frac{dE_{\rm xc}(t)}{dt} = \int d^3r\, \frac{\partial n(\mathbf{r},t)}{\partial t}\, v_{\rm xc}(\mathbf{r},t)\,. \tag{6.15}$$

It is also possible to derive a time-dependent virial theorem (Hessler *et al.*, 1999):

$$E_{\rm xc}(t) + T_c(t) = -\int d^3r\, n(\mathbf{r},t)\mathbf{r}\cdot\nabla v_{\rm xc}(\mathbf{r},t)\,. \tag{6.16}$$

The time-dependent xc energy can be useful in several ways. For instance, the sum rules (6.15) and (6.16) can be used to check the accuracy of a numerical calculation, or even be imposed as constraints to improve the quality of an approximate xc function (Kurzweil and Head-Gordon, 2009). One can also examine the behavior of $E_{\rm xc}(t)$ directly as a quantity to illustrate some of the peculiar features of the electron dynamics in a given situation, such as the deviation from the adiabatic approximation.

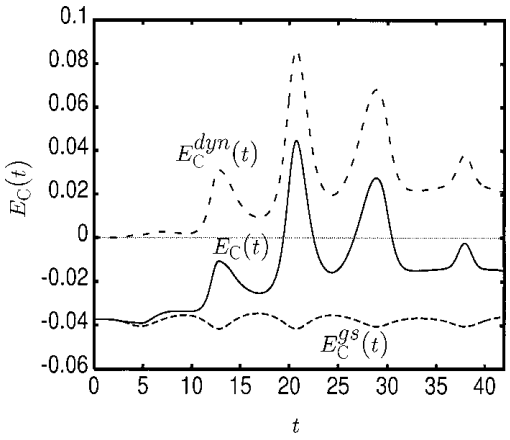

Fig. 6.1 Correlation energy $E_{\rm c}(t)$ of a time-dependent Hooke's atom, together with its adiabatic and dynamic components. [Reproduced with permission from AIP from Hessler *et al.* (2002), ©2002.]

Let us consider an example. Hessler *et al.* (2002) studied the dynamics of a two-electron Hooke's atom[4] with a time-varying spring constant of the form $k(t) = \bar{k} + \epsilon \cos \omega t$. They carried out exact numerical solutions of the two-electron problem, from which they obtained the exact xc potential of the associated Kohn–Sham system. They then evaluated the time-dependent correlation energy $E_{\rm c}(t)$ (the exchange energy in this case is trivially given by minus one-half of the Hartree energy; see Section 2.2.2).

Figure 6.1 shows that $E_{\rm c}(t)$ starts out with a negative value, but then begins to oscillate strongly, and even becomes positive. Notice that the static correlation energy is always a negative quantity. To illustrate this more clearly, one can decompose the correlation energy into

$$E_{\rm c}(t) = E_{\rm c}^{\rm gs}(t) + E_{\rm c}^{\rm dyn}(t)\,, \tag{6.17}$$

where the first term on the right-hand side is the ground-state correlation energy functional evaluated with the instantaneous time-dependent density; this would be the only contribution in the adiabatic approximation. The other term is therefore the truly dynamical contribution to the correlation energy. Figure 6.1 shows that $E_{\rm c}^{\rm gs}$ always remains negative, as expected, and shows only small variations. By contrast, the dynamical contribution $E_{\rm c}^{\rm dyn}$ is positive throughout.

From the behavior of $E_{\rm c}(t)$ and the correlation potential $v_{\rm c}(t)$, one can also conclude that they are very nonlocal functions of time; the system oscillates steadily, as seen from $E_{\rm c}^{\rm gs}$, but the amplitude of $E_{\rm c}^{\rm dyn}$ exhibits much stronger fluctuations. Such a behavior is impossible to capture using an adiabatic approximation.

[4] A Hooke's atom consists of two interacting electrons confined in a three-dimensional harmonic potential. The analytical form of the harmonic potential allows a separation of center-of-mass and relative coordinates, which makes a direct numerical solution much easier than for two interacting electrons in a Coulomb potential (Kestner and Sinanoglu, 1962; Laufer and Krieger, 1986; Kais *et al.*, 1993; Filippi *et al.*, 1994).

6.2.5 Scaling

Let us introduce a parameter λ into the time-dependent many-body Schrödinger equation (3.5), where $0 \leq \lambda \leq 1$. The idea is that this parameter (also known as the coupling constant) can be used to tune the electron–electron interaction from zero to full strength by replacing w with λw in eqn (3.4): the limiting cases $\lambda = 0$ and $\lambda = 1$ correspond to the noninteracting and the physical, fully interacting system, respectively. The key point is that we choose the external potential $v^\lambda(\mathbf{r}, t)$ in such a way that the time-dependent density remains unchanged and equal to its $\lambda = 1$ form (that this can be done in a unique fashion is guaranteed by the van Leeuwen theorem). Thus, the interaction-scaled time-dependent Schrödinger equation reads

$$i\frac{\partial}{\partial t}\Psi^\lambda(t) = (\hat{T} + \hat{V}^\lambda + \lambda\hat{W})\Psi^\lambda(t)\,. \tag{6.18}$$

This scaling will be discussed in more detail later, in Section 13.1, where it will play an important role in deriving a perturbative expansion of the xc potential.

There is also a second kind of scaling, which affects the dependence on the spatial and time coordinates, and one can establish an interesting connection between the interaction-scaled and the coordinate-scaled wave functions and time-dependent xc potentials (Hessler *et al.*, 1999).

We define the coordinate-scaled many-body wave function as follows:[5]

$$\Psi_{\gamma\beta}(\mathbf{r}_1, \ldots, \mathbf{r}_N, t) = \gamma^{3N/2}\Psi(\gamma\mathbf{r}_1, \ldots, \gamma\mathbf{r}_N, \beta t)\,, \tag{6.19}$$

which gives the coordinate-scaled density as

$$n_{\gamma\beta}(\mathbf{r}, t) = \gamma^3 n(\gamma\mathbf{r}, \beta t)\,. \tag{6.20}$$

Substituting the form (6.19) for $\Psi_{\gamma\beta}(t)$ into eqn (6.18) and letting $\gamma = 1/\lambda$ and $\beta = 1/\lambda^2$, we recover the original time-dependent Schrödinger equation (3.5), with scaled coordinates $\mathbf{r}_i/\lambda$ and t/λ^2 but the full interaction strength. This then tells us that the interaction-scaled and the coordinate-scaled wave functions are related as follows:

$$\Psi^\lambda[n, \Psi_0] = \Psi_{\lambda\lambda^2}[n_{1/\lambda, 1/\lambda^2}, \Psi_{0,1/\lambda}]. \tag{6.21}$$

Here, $\Psi_{0\gamma}$ is the initial wave function Ψ_0 with all spatial coordinates scaled by γ. The interaction-scaled time-dependent xc potential therefore satisfies

$$v_{\rm xc}^\lambda[n, \Psi_0, \Phi_0](\mathbf{r}, t) = \lambda^2 v_{\rm xc}[n_{1/\lambda, 1/\lambda^2}, \Psi_{0,1/\lambda}, \Phi_{0,1/\lambda}](\lambda\mathbf{r}, \lambda^2 t)\,. \tag{6.22}$$

Scaling relations have been very important in static DFT, and have provided much guidance for the development of approximate xc functionals. Scaling relations in TDDFT have so far not been very widely explored except for applications to simple model systems (Hessler *et al.*, 2002). However, we will see later, in Section 14.1, that they play an important role in the calculation of correlation energies via the fluctuation–dissipation approach (there, the key quantity is the scaled xc kernel $f_{\rm xc}^\lambda$).

[5]The scaling affects only the spatial coordinates and not the spins, which is why we use the argument $\mathbf{r}$ instead of $\mathbf{x}$ here. See footnote 2 in Section 3.1.1.

6.3 Galilean invariance and the harmonic potential theorem

In this section, we will discuss a class of rigorous properties of the xc potential which are all related to the fundamental behavior of many-body systems under transformations to accelerated reference frames.

6.3.1 Accelerated reference frames and generalized translational invariance

Consider the time-dependent Schrödinger equation (3.5), which describes the time evolution of a many-body system under the influence of a time-dependent external potential $v(\mathbf{r},t)$. Now let us perform a change of reference frame and look at the system from the point of view of a linearly accelerated observer whose position, relative to the original reference frame, is given by the vector $\mathbf{x}(t)$. What is important here is that the two Cartesian coordinate systems have parallel axes at all times, i.e., the moving reference frame does not rotate with respect to the original frame.

The accelerated observer describes the time evolution of the original system by the following transformed time-dependent Schrödinger equation (Vignale, 1995):

$$0 = \left\{ i\frac{\partial}{\partial t} + \sum_{j=1}^{N}\frac{\nabla_j^2}{2} - \frac{1}{2}\sum_{i\neq j}\frac{1}{|\mathbf{r}_i-\mathbf{r}_j|} - \sum_{j=1}^{N} v(\mathbf{r}_j+\mathbf{x},t) \right.$$
$$\left. -\ddot{\mathbf{x}}\cdot\sum_{j=1}^{N}\mathbf{r}_j + \frac{N}{2}\dot{\mathbf{x}}^2 \right\} \Psi_a(\mathbf{r}_1,\mathbf{r}_2,\ldots,\mathbf{r}_N,t)\,. \tag{6.23}$$

Comparing eqn (6.23) with the original time-dependent Schrödinger equation, we note that the potential seen by the accelerated observer is the original potential, evaluated at the position $\mathbf{r}+\mathbf{x}$, plus two extra terms. The first term, $\ddot{\mathbf{x}}\cdot\sum_{j=1}^{N}\mathbf{r}_j$, is associated with a uniform inertial force due to the acceleration $\ddot{\mathbf{x}}$. The second term, $-(N/2)\dot{\mathbf{x}}^2$, is just a time-dependent constant which affects only the phase of the wave function.

The wave function Ψ_a in the accelerated system is obtained from the original wave function Ψ by the following simple transformation:

$$\Psi_a(\mathbf{r}_1,\mathbf{r}_2,\ldots,\mathbf{r}_N,t) = \exp\Big(-i\dot{\mathbf{x}}\cdot\sum_j\mathbf{r}_j\Big)\Psi(\mathbf{r}_1+\mathbf{x},\mathbf{r}_2+\mathbf{x},\ldots,\mathbf{r}_N+\mathbf{x},t)\,. \tag{6.24}$$

All coordinates of Ψ are rigidly translated by $\mathbf{x}$, and the phase factor in front of Ψ describes a boost of the velocity of each electron by $\dot{\mathbf{x}}$. The density in the accelerated system is therefore given by the rigidly translated original density,

$$n_a(\mathbf{r},t) = n(\mathbf{r}+\mathbf{x},t)\,, \tag{6.25}$$

which is what one would have expected. If the velocity of the translated system is constant, i.e., $\mathbf{x}(t)=\mathbf{u}t$, this shows the *Galilean invariance* of the many-body Schrödinger equation. The proof of the transformation (6.23) and (6.24) of the many-body system is quite straightforward (see Exercise 6.2).

Now let us consider the TDKS equation

$$\left(i\frac{\partial}{\partial t}+\frac{\nabla^2}{2}-v(\mathbf{r},t)-v_{\rm H}[n](\mathbf{r},t)-v_{\rm xc}[n](\mathbf{r},t)\right)\varphi_j(\mathbf{r},t)=0\,, \tag{6.26}$$

with $j=1,\ldots,N$, which reproduces the time-dependent density $n(\mathbf{r},t)$ of the original many-body system. In the following, we will assume that the system starts from the ground state at time t_0.

As we did for the interacting system, we now look at the system from the point of view of a linearly accelerated observer whose position, relative to the original reference frame, is given by the vector $\mathbf{x}(t)$. Also assume the initial conditions

$$\mathbf{x}(t_0)=0, \qquad \dot{\mathbf{x}}(t_0)=0\,. \tag{6.27}$$

These initial conditions imply that the original and the accelerated system coincide at t_0, and are both initially in the ground state.

The accelerated observer will describe the time evolution of the system by the following transformed TDKS equation (see Exercise 6.2):

$$\left(i\frac{\partial}{\partial t}+\frac{\nabla^2}{2}-v(\mathbf{r}+\mathbf{x},t)-v_{\rm H}(\mathbf{r}+\mathbf{x},t)-v_{\rm xc}(\mathbf{r}+\mathbf{x},t)-\ddot{\mathbf{x}}\cdot\mathbf{r}+\frac{\dot{\mathbf{x}}^2}{2}\right)\varphi_{a,j}(\mathbf{r},t)=0, \tag{6.28}$$

where the Kohn–Sham orbitals in the accelerated frame are given by

$$\varphi_{a,j}(\mathbf{r},t)=e^{-i\dot{\mathbf{x}}\cdot\mathbf{r}}\varphi_j(\mathbf{r}+\mathbf{x},t)\,. \tag{6.29}$$

The resulting density $n_a(\mathbf{r},t)$ is given by eqn (6.25), just as for the interacting system.

We now direct our attention to the transformation of the Hartree and xc potentials. The transformed xc potential in eqn (6.28) has to be read as follows:

$$v_{\rm xc}(\mathbf{r}+\mathbf{x},t)=v_{\rm xc}[n](\bar{\mathbf{r}},t)|_{\bar{\mathbf{r}}=\mathbf{r}+\mathbf{x}}\,. \tag{6.30}$$

In other words, we assume that we have already solved the original TDKS problem (6.26), which means we know $v_{\rm xc}[n](\mathbf{r},t)$ for all $\mathbf{r}$ and t. Going over to the TDKS equation (6.28) in the accelerated frame, we can simply take the known $v_{\rm xc}[n](\mathbf{r},t)$, treat it the same way as the given external potential $v(\mathbf{r},t)$, and replace $\mathbf{r}$ by $\mathbf{r}+\mathbf{x}$.

Things are defined the same way for the Hartree potential, but there we can immediately go one step further:

$$v_{\rm H}(\mathbf{r}+\mathbf{x},t)=\int d^3r'\,\frac{n(\mathbf{r}',t)}{|\mathbf{r}+\mathbf{x}-\mathbf{r}'|}=\int d^3r'\,\frac{n(\mathbf{r}'+\mathbf{x},t)}{|\mathbf{r}-\mathbf{r}'|}=v_{\rm H}[n_a](\mathbf{r},t)\,. \tag{6.31}$$

This shows that the Hartree potential of the accelerated system is obtained by evaluating the Hartree potential functional of the original system with the density of the system moving relative to it.

We will now prove an analogous relation for the xc potential. To do this, let us look at eqn (6.28) in a different way, not making the assumption that the original

TDKS equation (6.26) has already been solved. Instead, we simply assume that $\mathbf{x}(t)$ and $v(\mathbf{r},t)$ are given, and that we need to solve the following TDKS problem:

$$\left(i\frac{\partial}{\partial t}+\frac{\nabla^2}{2}-v(\mathbf{r}+\mathbf{x},t)-v_{\rm H}[n'](\mathbf{r},t)-v_{\rm xc}[n'](\mathbf{r},t)-\ddot{\mathbf{x}}\cdot\mathbf{r}+\frac{1}{2}\dot{\mathbf{x}}^2\right)\psi_j(\mathbf{r},t)=0\,, \tag{6.32}$$

where

$$n'(\mathbf{r},t)=\sum_j|\psi_j(\mathbf{r},t)|^2\,. \tag{6.33}$$

This TDKS equation has the same external potential as the many-body Schrödinger equation (6.23) in the accelerated reference frame. Therefore,

$$n'(\mathbf{r},t)=n(\mathbf{r}+\mathbf{x},t)=n_a(\mathbf{r},t)\,. \tag{6.34}$$

Now assume an observer moving relative to this system at position $-\mathbf{x}(t)$, which brings us back to the original frame of reference. The transformed TDKS equation is

$$\left(i\frac{\partial}{\partial t}+\frac{\nabla^2}{2}-v(\mathbf{r},t)-v_{\rm H}[n_a](\mathbf{r}-\mathbf{x},t)-v_{\rm xc}[n_a](\mathbf{r}-\mathbf{x},t)\right)e^{i\dot{\mathbf{x}}\cdot\mathbf{r}}\psi_j(\mathbf{r}-\mathbf{x},t)=0\,. \tag{6.35}$$

The density of this system is again $n(\mathbf{r},t)$, and according to the Runge–Gross theorem, there can be only one unique TDKS system which produces it, namely the original TDKS equation (6.26). For this to be true, we must have

$$\psi_j(\mathbf{r},t)=e^{-i\dot{\mathbf{x}}\cdot\mathbf{r}}\varphi_j(\mathbf{r}+\mathbf{x},t)\,. \tag{6.36}$$

In other words, eqns (6.32) and (6.28) are identical, which proves

$$v_{\rm xc}[n_a](\mathbf{r},t)=v_{\rm xc}[n](\mathbf{r}+\mathbf{x},t)\,. \tag{6.37}$$

This shows that the xc potential rigidly follows a rigidly translated density. We call the condition (6.37) the *generalized translational invariance* of the xc potential.

In hindsight, this generalized translational invariance appears to be such a physically obvious requirement that one might wonder why we bother at all. The reason is that it is a crucial test of approximations to $v_{\rm xc}[n](\mathbf{r},t)$ whether they satisfy eqn (6.37). For the adiabatic approximation (4.13), and in particular the ALDA, this can be shown very easily. However, as soon as one wants to go beyond the adiabatic approximation, considerable effort must be spent to ensure translational invariance, as we will see later in Chapter 10.

Generalized translational invariance can also be invoked to derive the zero-force theorem, using the variational principle of TDDFT, which we will discuss below in Section 6.6.2. This will be the subject of Exercise 6.7.

6.3.2 The harmonic potential theorem

In the previous subsection, we considered situations in which the time-dependent density is rigidly translated. Such situations occur, in general, when we change the observer and adopt a moving reference frame. However, there is a special case in which we can

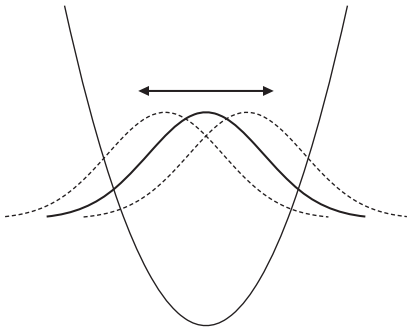

Fig. 6.2 The harmonic potential theorem means that a system of N interacting electrons confined in a parabolic potential can carry out a collective motion in which the ground-state density (shown as a thick line) moves rigidly back and forth.

achieve rigidly translated densities *without* changing the reference frame, namely by a particular choice of external potential. This is the content of the *harmonic potential theorem* (Dobson, 1994), and it will be useful for us since it will give us yet another rigorous constraint which the xc potential must satisfy.

Let us first look at the case of an interacting many-body system. We consider N electrons in a static confining potential

$$v_0(\mathbf{r}) = \frac{1}{2}\mathbf{r}\cdot\mathbb{K}\cdot\mathbf{r}\,. \tag{6.38}$$

Here, $\mathbb{K}$ is a generalized spring-constant matrix, assumed to be symmetric. The most common situation is that $\mathbb{K}$ is diagonal. For instance, $K_{11} = K_{22} = K_{33} = k$ describes a three-dimensional harmonic oscillator potential, known as the Hooke's atom (see footnote 4) or a spherical quantum dot. On the other hand, $K_{11} = K_{22} = 0$, $K_{33} = k$ describes a parabolic quantum well. Examples of such systems are provided by semiconductor nanostructures (see Appendix K), which will appear in several other places in this book.

The many-body ground state (and, of course, all other eigenstates) of the harmonic potential is obtained from the static Schrödinger equation

$$\hat{H}_0\Psi_0(\mathbf{r}_1,\mathbf{r}_2,\ldots,\mathbf{r}_N) = E_0\Psi_0(\mathbf{r}_1,\mathbf{r}_2,\ldots,\mathbf{r}_N)\,, \tag{6.39}$$

where

$$\hat{H}_0 = \sum_{j=1}^{N}\left[-\frac{\nabla^2}{2} + \frac{1}{2}\mathbf{r}_j\cdot\mathbb{K}\cdot\mathbf{r}_j\right] + \frac{1}{2}\sum_{i\neq j}\frac{1}{|\mathbf{r}_i-\mathbf{r}_j|}\,. \tag{6.40}$$

Now consider the dynamics of this system in the presence of a spatially homogeneous electric field of amplitude $\mathbf{E}(t)$. The time-dependent Schrödinger equation of this system is

$$\left[i\frac{\partial}{\partial t} - \hat{H}_0 + \mathbf{E}(t)\cdot\sum_{j=1}^{N}\mathbf{r}_j\right]\Psi(\mathbf{r}_1,\mathbf{r}_2,\ldots,\mathbf{r}_N,t) = 0\,. \tag{6.41}$$

The harmonic potential theorem now states that the solution of this time-dependent Schrödinger equation is simply the static many-body wave function Ψ_0, rigidly translated and multiplied by a phase factor:

$$\Psi(\mathbf{r}_1, \mathbf{r}_2, \ldots, \mathbf{r}_N, t) = e^{Q} \Psi_0(\mathbf{r}_1 - \mathbf{x}, \mathbf{r}_2 - \mathbf{x}, \ldots, \mathbf{r}_N - \mathbf{x}) \,, \tag{6.42}$$

where the shift $\mathbf{x}(t)$ is determined by the equation of motion of a driven harmonic oscillator,

$$\ddot{\mathbf{x}} + \mathbb{K} \cdot \mathbf{x} = \mathbf{E}(t) \,. \tag{6.43}$$

The phase Q is given by

$$Q = -iE_0 t + i\dot{\mathbf{x}} \cdot \sum_{j=1}^{N} \mathbf{r}_j - i \int_{t_0}^{t} dt' \left[\frac{1}{2}\dot{\mathbf{x}}^2 - \frac{1}{2}\mathbf{x}(t') \cdot \mathbb{K} \cdot \mathbf{x}(t') \right] . \tag{6.44}$$

We thus see that in a harmonically confined system, the dynamics of the center of mass is completely decoupled from that of the internal degrees of freedom. There exist quantum states in which a static many-body eigenstate is translated rigidly (up to a phase factor), as in classical motion. The associated time-dependent density $n(\mathbf{r}, t)$ is simply the rigidly translated ground-state density,

$$n(\mathbf{r}, t) = n_0(\mathbf{r} - \mathbf{x}(t)) \,. \tag{6.45}$$

This is illustrated in Fig. 6.2.

Let us now show that TDKS theory is consistent with the harmonic potential theorem. The static Kohn–Sham equation in a harmonic confining potential reads

$$\left[-\frac{\nabla^2}{2} + \frac{1}{2}\mathbf{r} \cdot \mathbb{K} \cdot \mathbf{r} + v_{\rm H}[n_0](\mathbf{r}) + v_{\rm xc}[n_0](\mathbf{r}) \right] \varphi_j(\mathbf{r}) = \varepsilon_j \varphi_j(\mathbf{r}) \,. \tag{6.46}$$

In the presence of a uniform driving field $\mathbf{E}(t)$, we obtain the rigidly shifted time-dependent density (6.45) from the TDKS equation

$$\left[i\frac{\partial}{\partial t} + \frac{\nabla^2}{2} - \frac{1}{2}\mathbf{r} \cdot \mathbb{K} \cdot \mathbf{r} - v_{\rm H}[n](\mathbf{r}, t) - v_{\rm xc}[n](\mathbf{r}, t) + \mathbf{E}(t) \cdot \mathbf{r} \right] \psi_j(\mathbf{r}, t) = 0 \,, \tag{6.47}$$

with the TDKS orbitals

$$\psi_j(\mathbf{r}, t) = \exp\left[-i\varepsilon_j t + i\dot{\mathbf{x}} \cdot \sum_{j=1}^{N} \mathbf{r}_j - \frac{i}{2} \int_{t_0}^{t} dt' \left[\dot{\mathbf{x}}^2 - \mathbf{x}(t') \cdot \mathbb{K} \cdot \mathbf{x}(t') \right] \right] \varphi_j(\mathbf{r} - \mathbf{x}) \,. \tag{6.48}$$

The proof makes use of the generalized translational invariance (6.37) of the xc potential. Thus, any approximate xc potential (such as the ALDA) which satisfies eqn (6.37) automatically satisfies the harmonic potential theorem.

Let us now summarize the results of this and the previous section:

Generalized translational invariance. If a time-dependent density $n_a(\mathbf{r},t)$ is obtained by translating another time-dependent density $n(\mathbf{r},t)$ by a vector $\mathbf{x}(t)$, i.e., $n_a(\mathbf{r},t) = n(\mathbf{r}+\mathbf{x}(t),t)$, then the xc potential associated with the translated density n_a is obtained by rigidly translating the original xc potential:

$$v_{\rm xc}[n_a](\mathbf{r},t) = v_{\rm xc}[n](\mathbf{r}+\mathbf{x},t).$$

In other words, the xc potential "rides along" with a rigidly moving density. In the special case where the density is moving with a constant velocity $\mathbf{u}$, i.e., $\mathbf{x} = \mathbf{u}t$, the translational invariance of $v_{\rm xc}$ is called *Galilean invariance*.

Harmonic potential theorem. In a harmonically confined interacting system with a generalized spring constant $\mathbb{K}$, the center-of-mass motion and the relative motion are decoupled. There exist solutions of the time-dependent Schrödinger equation in the presence of an external field $\mathbf{E}(t)$ in which a static many-body wave function is rigidly translated as in classical motion, with the translation vector $\mathbf{x}$ given by

$$\ddot{\mathbf{x}} + \mathbb{K}\cdot\mathbf{x} = \mathbf{E}(t).$$

Any approximate xc potential that satisfies generalized translational invariance automatically satisfies the harmonic potential theorem.

All of these properties of the xc potential can be viewed as the TDDFT counterparts of corresponding rigorous properties of time-dependent many-body systems. Finally, we should mention that these results can be generalized to the case where a static or a time-dependent magnetic field is included (Vignale, 1995).

6.4 Memory and causality

The complete information about a many-body system at any given time t is contained in its wave function $\Psi(t)$. We do not need to know $\Psi(t')$ at earlier times $t' < t$ to calculate the expectation value of any observable at time t. The time-dependent Schrödinger equation (3.5) is a linear partial differential equation, and the many-body Hamiltonian $\hat{H}(t)$ depends only on the time t: it has no memory of earlier times.

The main appeal of TDDFT is that it uses the time-dependent density $n(\mathbf{r},t)$ as the basic variable instead of $\Psi(t)$, thus replacing a complex variable depending on $3N$ spatial coordinates by a real variable depending on only three spatial coordinates. Just as in static DFT, the price to pay for this enormous simplification is that the TDKS equation is a nonlinear partial differential equation, and that the spatial dependence of the xc potential $v_{\rm xc}[n,\Psi_0,\Phi_0](\mathbf{r},t)$ on the density is highly nonlocal.

But there is an additional consequence which is unique to the dynamical case: the TDKS single-particle Hamiltonian has a memory which, like the spatial nonlocality, comes in through the xc potential $v_{\rm xc}[n,\Psi_0,\Phi_0](\mathbf{r},t)$. The basic physical reason for this memory dependence is that this is how TDDFT encodes the phase information of the many-body wave function $\Psi(t)$ through the real fundamental variable $n(\mathbf{r},t)$.

In the following, we shall explore various issues related to the temporal nonlocality of the xc potential. In this section, we will focus on those memory effects which come from the history dependence of $v_{\rm xc}$, i.e., the fact that it depends on densities at previous times. The dependence on the initial states will be discussed in Section 6.5.

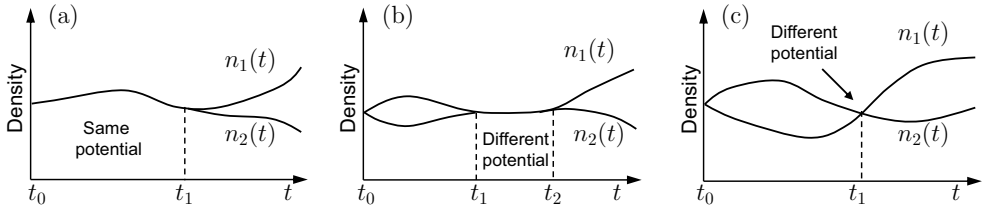

Fig. 6.3 Illustration of two densities $n_1(t)$ and $n_2(t)$ which evolve from the same initial state Ψ_0 and coincide (a) at times $t_0 < t < t_1$, (b) at times $t_1 < t < t_2$, and (c) at time t_1. Owing to causality, identical densities lead to identical potentials $v[n, \Psi_0](t)$ only in situation (a).

6.4.1 Causality of the xc potential, and history dependence

According to the Runge–Gross theorem, there exists a one-to-one mapping between time-dependent densities and potentials. This means that for an interacting system, there exists a unique potential $v[n, \Psi_0](\mathbf{r}, t)$ which produces $n(\mathbf{r}, t)$, for a given initial state Ψ_0. The question now arises of whether and how the potential at time t is determined by densities at different times t'.

Let us first consider the situation illustrated in Fig. 6.3(a). There are two densities, $n_1(t)$ and $n_2(t)$, belonging to a common initial state Ψ_0, which are identical from t_0 up until t_1 and then start to differ. The fact that the two densities are identical in the time interval $[t_0, t_1]$ means that the associated potentials $v_1[n_1]$ and $v_2[n_2]$ must be identical as well over that time interval—it is a consequence of the Runge–Gross theorem that two different potentials cannot produce the same density. The fact that the densities are different for $t > t_1$ is irrelevant: what happens after t_1 does not affect the potential prior to t_1. Vice versa, if only the density for $t \in [t_0, t_1]$ is given, then the potential $v[n, \Psi_0](\mathbf{r}, t)$ for $t > t_1$ cannot be uniquely constructed.

Thus, the potential $v[n, \Psi_0](\mathbf{r}, t)$ is seen to be a *causal* functional of the density: over the time interval $[t_0, t_1]$, it can depend only on densities from that same time interval, and it cannot depend on densities later than t_1. There is no dependence on the future; $v[n, \Psi_0](\mathbf{r}, t)$ can only be a functional of present and past densities.

We now consider part (b) of Fig. 6.3, which shows two densities that start from the same initial state Ψ_0, evolve in a different way until time t_1, and then become identical for $t_1 < t < t_2$. For times greater than t_2, the two densities again become different. Given *only* the density at $t \in [t_1, t_2]$, it is not possible to construct the potential $v(\mathbf{r}, t)$ uniquely, since we do not know the initial many-body state at time t_1. Indeed, in the example shown in Fig. 6.3(b), the two densities become identical at time t_1 but the associated time-dependent many-body states will be different. Therefore, the potentials will be different for $t \in [t_1, t_2]$, in spite of the densities being the same.

Letting the time interval $[t_1, t_2]$ shrink in size, one eventually arrives at the situation shown in Fig. 6.3(c), where the two densities are identical at time t_1 only. Applying a similar argument to that above, it is clear that the potential at time t_1 cannot be constructed using only a knowledge of the density at time t_1. In other words, the potential $v[n, \Psi_0](\mathbf{r}, t)$ at time t is *history-dependent*: it is a functional of the previous densities over the entire time interval $[t_0, t]$.

The causality and memory dependence of the potential as a functional of the density also applies to noninteracting TDKS systems via the van Leeuwen theorem, where the effective potential $v_s[n, \Psi_0, \Phi_0](\mathbf{r}, t)$ depends on both the interacting and the noninteracting initial states. From the definition (4.9) we see immediately that the xc potential

$$v_{\rm xc}[n](\mathbf{r}, t) = v_s[n](\mathbf{r}, t) - v[n](\mathbf{r}, t) - \int d^3r' \frac{n(\mathbf{r}', t)}{|\mathbf{r} - \mathbf{r}'|} \tag{6.49}$$

has the same causality and history dependence as $v_s[n]$ and $v[n]$ (the Hartree potential depends only on the instantaneous density and has no memory).

6.4.2 A simple example and a paradox

It is instructive to look at a simple example where the temporal nonlocality of $v_s[n](\mathbf{r}, t)$ can be explicitly demonstrated. As we will see, this raises an apparent paradox which forces us to think more deeply about causality in the context of an actual time propagation of the TDKS equation.

Let us consider a given functional form for the time-dependent density of a one-dimensional two-electron system:

$$n(x, t) = \frac{2}{a(t)\sqrt{\pi}}\, e^{-x^2/a(t)^2} \,. \tag{6.50}$$

This density distribution is normalized to $N = 2$ and has a simple Gaussian shape with a time-dependent width given by $2\sqrt{\ln 2}\, a(t)$.

In Appendix E, we discuss how the TDKS equation can be inverted to construct that effective potential which produces a given time-dependent density. According to eqn (E.14), we obtain the following for a one-dimensional two-electron system:

$$v_s[n] = \frac{1}{4}(\ln n)'' + \frac{1}{8}(\ln n)'^2 - \frac{\partial \alpha}{\partial t} - \frac{1}{2}(\alpha')^2 \,, \tag{6.51}$$

where a prime denotes a derivative with respect to x, and the phase α follows from solving $\alpha' = j/n$, where the current density is obtained from the one-dimensional continuity equation via $j' = -\partial n/\partial t$.

For our choice (6.50) of the density distribution, the TDKS potential can be constructed analytically, which is left as an exercise. One finds that the density function (6.50) is reproduced in a noninteracting system subject to a harmonic potential with a time-dependent curvature $k(t)$:

$$v_s(x, t) = \frac{1}{2}k(t)x^2 \,, \qquad k(t) = \frac{1}{a(t)^4} - \frac{1}{a(t)}\frac{\partial^2 a(t)}{\partial t^2} \,. \tag{6.52}$$

The first term of eqn (6.52) is the adiabatic potential $v_s^{\rm A}(x, t) = x^2/2a(t)^4$, which produces each $n(x, t)$ as its instantaneous ground-state density. The second term of the TDKS potential, $v_s^{\rm dyn} = -(x^2/a(t))\, \partial^2 a(t)/\partial t^2$, is nonlocal in time: via eqn (6.50), it depends on $\partial^2 n/dt^2$. Notice that we can also express this in terms of the adiabatic and dynamic time-dependent xc potentials as $v_s^{\rm A} = v + v_{\rm H} + v_{\rm xc}^{\rm A}$ and $v_s^{\rm dyn} = v_{\rm xc}^{\rm dyn}$. To obtain $v_{\rm xc}^{\rm A}$ separately, we would have to invert the interacting two-electron Schrödinger

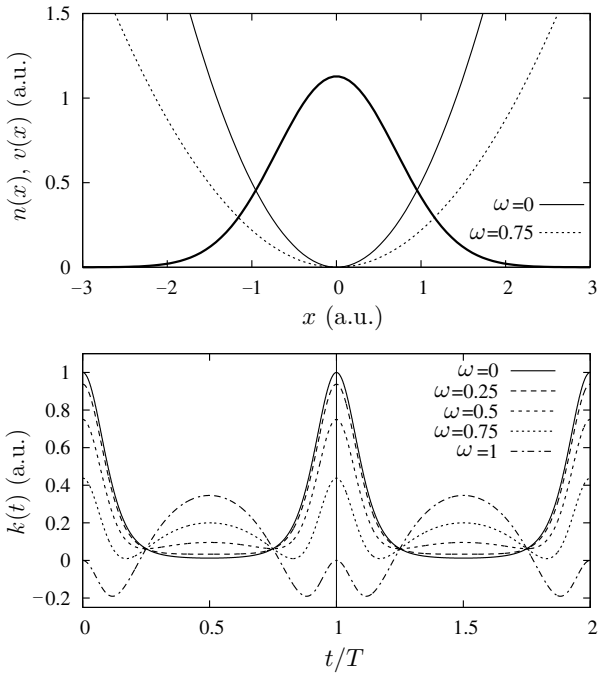

Fig. 6.4 Bottom: curvature $k(t)$ of the harmonic TDKS potential $v_s[n]$ which produces the time-dependent density (6.50) with the oscillating width (6.53), for various frequencies, as labeled. Top: density (thick line) and potentials (thin and dashed lines) after one cycle (time $T = 2\pi/\omega$, see vertical line in bottom panel). Owing to the history dependence, the potentials at time T are different for different frequencies, while the densities are the same.

equation to find that time-dependent external potential $v(x,t)$ which produces the density (6.50), as explained in Section 4.3.

To illustrate this, we choose a width $a(t)$ with an oscillating time dependence,

$$a(t) = \bar{a}(2 - \cos\omega t)\,. \tag{6.53}$$

The associated curvature $k(t)$ of the TDKS potential $v_s[n](x,t)$ is shown in the bottom panel of Fig. 6.4 for $\bar{a} = 1$ and various frequencies. As ω increases, the potential deviates more and more from the adiabatic limit ($\omega = 0$).

Let us now focus specifically on those times where the density returns to its initial shape, which happens after each period $T = 2\pi/\omega$. The curvature of the potential then has the simple form

$$k(T) = \frac{1}{\bar{a}^4} - \omega^2\,. \tag{6.54}$$

The top part of Fig. 6.4 shows how the potential at time T is different for different frequencies, even though the densities at those times are equal. This is an example of the generic situation shown in Fig. 6.3(c), and explicitly illustrates the temporal nonlocality of $v_s[n](t)$.

Further examination of this simple example brings up a rather subtle, yet important point. We have demonstrated that $v_s[n]$ has pronounced nonadiabatic contributions; according to Section 6.4.1, any nonlocality in time can only be attributed to the functional having a memory of previous densities. In our simple example, we have seen that the potential at time t depends on the second time derivative of the density, $\partial^2 n/\partial t^2$. This is a very general outcome of the inversion procedure illustrated in eqns (6.51) and (E.14), and also holds for systems with more than two electrons. At any finite $t > t_0$, the appearance of the second time derivative is compatible with causality since it can be evaluated to the left of t, for instance by using a finite-difference formula of the form $\partial^2 n/\partial t^2|_{\tau_j} = [n(\tau_{j-2}) - 2n(\tau_{j-1}) + n(\tau_j)]/(\Delta\tau)^2$.

However, we seem to be running into some difficulties at the initial time t_0. Since we make no assumptions about earlier times, all we have are the initial density $n(\mathbf{r}, t_0)$ and the initial states Ψ_0 and Φ_0, and this alone is not sufficient to calculate $\partial^2 n/\partial t^2$ at t_0. Without knowing $n(t_0 + \Delta\tau)$ and $n(t_0 + 2\Delta\tau)$, how can we construct the effective potential $v_s[n](\mathbf{r}, t_0)$ which is needed to start off the TDKS time propagation? This seems be a subtle loophole in the causality of the TDKS procedure.[6]

The resolution of this "propagation paradox" was given by Maitra *et al.* (2008). To carry out a TDKS propagation in practice, only $v_{\rm xc}$ is needed in eqn (6.49), since the external potential $v(\mathbf{r}, t)$ is *given* and does not need to be extracted from the density. It follows from this that $v_{\rm xc}[n, \Psi_0, \Phi_0](t_0)$ depends *only* on the initial states; the dependence on $\partial^2 n/\partial t^2$ at t_0 cancels out. Using the van Leeuwen construction described in Section 3.3, Maitra *et al.* (2008) showed explicitly that TDKS time propagation is causal and therefore predictive: at each subsequent time step, $v_{\rm xc}$ requires only Ψ_0, Φ_0, and densities evolved through previous time propagation steps as functional inputs.

6.5 Initial-state dependence

We will now address an issue which we have so far largely avoided: the dependence on the initial states of the system. Both the Runge–Gross and the van Leeuwen proofs in Chapter 3 made it clear that the one-to-one correspondence of densities and potentials holds for a fixed initial state of the interacting or noninteracting system, Ψ_0 or Φ_0. The situation becomes dramatically simpler if the system starts from the ground state, since then the Hohenberg–Kohn theorem can be invoked and the initial-state dependence reduces to a dependence on the initial ground-state density. This assumption is made in most parts of this book for obvious reasons.

However, the existence proofs of TDDFT do not require that the system starts from its ground state at t_0. As we shall see, initial-state dependence and history dependence are very closely related to each other, and we will discover how this leads to new insights and rigorous constraints on the xc potential (Maitra, 2006*a*).

[6]This argument, known as the "propagation paradox," was used by Schirmer and Dreuw (2007) to raise doubts about the predictive value of TDDFT. The logical error of this argument—a circular cause-and-effect fallacy—consists in attempting to *construct* $v_s[n]$ during TDKS time propagation by using an inversion procedure which yields v_s from a *given* density. However, during a TDKS time propagation it is not the density which is given, but the external potential.

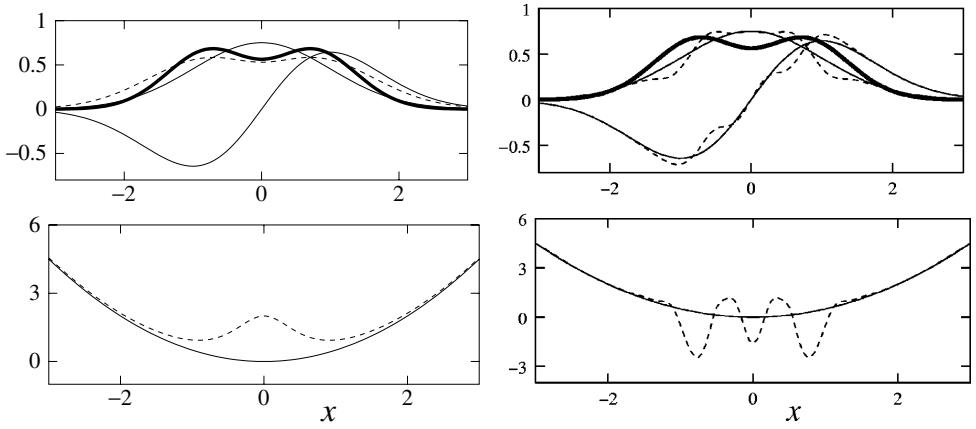

Fig. 6.5 Top panels: static density (6.55) (thick lines) and harmonic-oscillator states ξ_0 and ξ_1 (thin lines). Left: doubly occupied orbital (dashed line, top panel) associated with the modified harmonic potential (dashed line, bottom panel) which reproduces the density (6.55) as the ground-state density. [Reproduced with permission from APS from Maitra *et al.* (2002), ©2002.] Right: initial single-particle states $\widetilde{\xi}_0$ and $\widetilde{\xi}_1$ (dashed lines, top panel) and the associated initial single-particle potential (dashed line, bottom panel) which reproduces the density (6.55) as the stationary density during time propagation. [Reproduced with permission from APS from Maitra and Burke (2001), ©2001.]

6.5.1 An example

To get some feeling for the initial-state dependence of the potential, let us begin with a simple example (Maitra and Burke, 2001; Holas and Balawender, 2002; Maitra *et al.*, 2002). Let us consider the following one-dimensional static density function:

$$n(x,t) = \xi_0(x)^2 + \xi_1(x)^2 = \frac{1+2x^2}{\sqrt{\pi}}\, e^{-x^2}\,. \tag{6.55}$$

This function is constructed by taking the sum of the squares of the ground state $\xi_0(x)$ and the first excited state $\xi_1(x)$ of a simple harmonic oscillator with spring constant $k = 1$. It is illustrated by the thick lines in Fig. 6.5. The goal is to find a system of two noninteracting electrons in a spin singlet state which produces this density.

If we are restricted to static DFT, then the density function (6.55) must come from a ground state where both electrons reside in the same, doubly occupied orbital. Inversion of the static Kohn–Sham equation (see Appendix E) is straightforward and yields the effective potential $v_s[n]$, which is shown in the left panel of Fig. 6.5. It has the shape of a harmonic-oscillator potential with a small bump in the middle, and is the unique potential in static DFT which produces the density (6.55).

In TDDFT, the system is permitted to start with an initial many-body state that is not the ground state, as long as it produces the correct initial density and longitudinal current density. For instance, we can choose

$$\Phi_0(x_1,\sigma_1,x_2,\sigma_2) = 2^{-1/2}[\xi_0(x_1)\xi_1(x_2) + \xi_1(x_1)\xi_0(x_2)]\chi_-(\sigma_1,\sigma_2) \tag{6.56}$$

as the first excited singlet Kohn–Sham Slater determinant associated with the static harmonic-oscillator potential $\frac{1}{2}x^2$ [$\chi_-(\sigma_1,\sigma_2)$ denotes the antisymmetric spin state]. Since Φ_0 is a two-electron eigenstate, it produces the static density (6.55) at all times if the potential is kept constant at $\frac{1}{2}x^2$. This is illustrated in the left panel of Fig. 6.5.

But this is by no means the only way in which TDDFT can produce the density (6.55). Consider the alternative initial state

$$\widetilde{\Phi}_0(x_1,\sigma_1,x_2,\sigma_2) = 2^{-1/2}[\widetilde{\xi}_0(x_1)\widetilde{\xi}_1(x_2) + \widetilde{\xi}_1(x_1)\widetilde{\xi}_0(x_2)]\chi_-(\sigma_1,\sigma_2)\,, \tag{6.57}$$

where

$$\widetilde{\xi}_0(x) = \sqrt{1+f(x)\xi_1(x)^2}\,\xi_0(x)\,, \qquad \widetilde{\xi}_1(x) = \sqrt{1-f(x)\xi_0(x)^2}\,\xi_1(x)\,, \tag{6.58}$$

and $f(x) = c(256x^4 - 192x^2 + 12)\exp(-2x^2)$, where c is a numerical constant, which is chosen here as -0.1. It is easy to see that $\widetilde{\xi}_0$ and $\widetilde{\xi}_1$ are a pair of orthonormal functions and that $\widetilde{\Phi}_0$ reproduces the given density. However, in contrast to ξ_0 and ξ_1, the two functions $\widetilde{\xi}_0$ and $\widetilde{\xi}_1$ are not eigenstates of the same single-particle potential. Therefore, to keep the density (6.55) fixed, a time-dependent potential is needed. It can be constructed using the van Leeuwen procedure (see Section 3.3), and one finds the initial potential $v_s[n](x,t_0)$ shown in the right bottom panel of Fig. 6.5 (Maitra and Burke, 2001; Holas and Balawender, 2002).

This simple example shows that a stationary density can be produced by a system subject to a time-varying potential if the initial state is not a pure eigenstate. In the effective TDKS potential, this feature must be built into the initial-state dependence of the xc potential. Any approximate xc potential which ignores the initial-state dependence would predict the same potential in both cases.

More generally, a given time-dependent density can be produced by different time-dependent potentials and different initial states. The case of oscillating densities was discussed by Maitra and Burke (2002, 2007) in the context of the so-called Floquet theory, which is concerned with steady-state solutions of the time-dependent Schrödinger equation with time-periodic potentials (Shirley, 1965). Maitra and Burke gave explicit examples which demonstrate that such oscillating densities alone do not uniquely determine the potential. However, a Floquet formulation within TDDFT can be rigorously given if the initial Floquet state is specified,[7] in accordance with the Runge–Gross theorem. Earlier attempts at TDDFT formulations of Floquet phenomena (Deb and Ghosh, 1982; Telnov and Chu, 1997) did not consider this initial-state dependence and were thus incomplete.

6.5.2 Connection between history and initial-state dependence

According to the Runge–Gross theorem of Section 3.2 and our discussion of memory and causality in Section 6.4.1, the external potential in a time-dependent many-body system at time $t > t_0$, $v[n_{\{t_0,t\}},\Psi_0](\mathbf{r},t)$, is a unique functional of the initial many-body state Ψ_0 and the previous densities, where the notation $n_{\{t_0,t\}}$ represents all densities $n(\mathbf{r},t')$ with $t_0 < t' < t$.

[7] Notice that this does not involve any adiabatic switching process. All that is required is that the system is already in a Floquet state at the initial time.

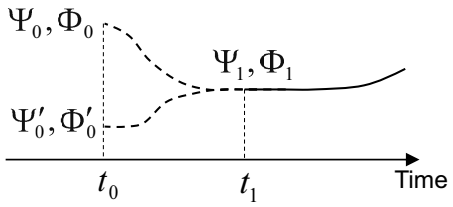

Fig. 6.6 Two different histories connecting to the same set of initial states Ψ_1 and Φ_1. Initial-state dependence can thus be transformed into history dependence.

Now let us pick some intermediate time $t_1 \in [t_0, t]$ at which the many-body wave function has evolved into $\Psi_1 = \hat{U}(t_1, t_0)\Psi_0$. Why not take Ψ_1 as a new initial state, and forget all that has happened before t_1? We can then again invoke the Runge–Gross theorem and state that the external potential $v[n_{\{t_1,t\}}, \Psi_1](\mathbf{r}, t)$ at time $t > t_1$ is a functional of Ψ_1 and the previous densities in the interval $t_1 < t' < t$. It is immediately obvious that

$$v[n_{\{t_0,t\}}, \Psi_0](\mathbf{r}, t) = v[n_{\{t_1,t\}}, \Psi_1](\mathbf{r}, t) \tag{6.59}$$

for all $t \geq t_1$.

Now let us apply the same reasoning to the noninteracting TDKS system, which leads us to

$$v_s[n_{\{t_0,t\}}, \Phi_0](\mathbf{r}, t) = v_s[n_{\{t_1,t\}}, \Phi_1](\mathbf{r}, t) \tag{6.60}$$

for all $t \geq t_1$, where $\Phi_1 = \hat{U}_s(t_1, t_0)\Phi_0$. Using the definition (6.49) of the xc potential, this immediately gives the exact condition

$$v_{\rm xc}[n_{\{t_0,t\}}, \Psi_0, \Phi_0](\mathbf{r}, t) = v_{\rm xc}[n_{\{t_1,t\}}, \Psi_1, \Phi_1](\mathbf{r}, t) \tag{6.61}$$

for all $t \geq t_1$. This means that we can absorb all the memory over the time interval $[t_0, t_1]$ into the initial states Ψ_1 and Φ_1: history dependence can be transformed into initial-state dependence. Equation (6.61) is an exact condition on the xc potential, and has to be satisfied by any approximate initial-state- and history-dependent functional. Of course, any adiabatic xc functional trivially satisfies this constraint.

Equation (6.61) immediately suggests that the reverse is also true and initial-state dependence can be transformed into history dependence. Things get even more interesting: as illustrated in Fig. 6.6, there are many histories that connect to a given set of initial states Ψ_1 and Φ_1, and they all give the same xc potential for times greater than t_1.

This opens up the possibility of getting rid of the initial-state dependence of the xc potential altogether: all we would have to do is find a pseudo-prehistory which starts from a ground state at some time $t_0 < t_1$ and ends up at the states Ψ_1 and Φ_1 at t_1. The initial-state dependence is then replaced by a history dependence starting from t_0. Does this mean that we can always get rid of initial-state dependence? The answer is no: there exist many-body states that cannot be reached by time evolution starting from a ground state (Maitra *et al.*, 2002). This is an example of a quantum control problem (see Section 16.3) where a given target state is not "ground-state evolvable."

6.6 Time-dependent variational principles

6.6.1 The Dirac–Frenkel stationary-action principle

In our review of ground-state DFT in Chapter 2, we saw the prominent role of the Rayleigh–Ritz variational principle: the many-body ground state of a system can be obtained as that state which minimizes the expectation value of the Hamiltonian. This minimum principle was a key element in the proof of the Hohenberg–Kohn existence theorem of DFT.

In the time-dependent case, no such minimum principle is available. However, there is a long tradition in quantum mechanics of deriving the time evolution of systems from other kinds of variational principles, called stationary-action principles. The most widely used one is the Dirac–Frenkel variational principle; other time-dependent variational principles have been discussed in the literature (Langhoff *et al.*, 1972; van Leeuwen, 2001).

We define the quantum mechanical action $\mathcal{A}$ of a many-body system as a functional of the many-body wave function $\Psi(t)$ between an initial time t_0 and a final time t_1:

$$\mathcal{A}[\Psi] = \int_{t_0}^{t_1} dt \left\langle \Psi(t) \left| i\frac{\partial}{\partial t} - \hat{H}(t) \right| \Psi(t) \right\rangle . \tag{6.62}$$

Let us now allow variations of the wave function $\Psi(t)$ that are arbitrary except for the requirement that they vanish at both ends of the time interval, $\delta\Psi(t_0) = \delta\Psi(t_1) = 0$. The true time evolution of the system is such that the action is stationary with respect to such variations:

$$\delta\mathcal{A}[\Psi] = 0 . \tag{6.63}$$

To prove this, we write the variation of the action as

$$\delta\mathcal{A}[\Psi] = \int_{t_0}^{t_1} dt \left\langle \delta\Psi(t) \left| i\frac{\partial}{\partial t} - \hat{H}(t) \right| \Psi(t) \right\rangle + \int_{t_0}^{t_1} dt \left\langle \Psi(t) \left| i\frac{\partial}{\partial t} - \hat{H}(t) \right| \delta\Psi(t) \right\rangle . \tag{6.64}$$

We now do an integration by parts in the second term:

$$\delta\mathcal{A}[\Psi] = \int_{t_0}^{t_1} dt \left\langle \delta\Psi(t) \left| i\frac{\partial}{\partial t} - \hat{H}(t) \right| \Psi(t) \right\rangle + \int_{t_0}^{t_1} dt \left\langle \left(-i\frac{\partial}{\partial t} - \hat{H}(t) \right) \Psi(t) \right| \delta\Psi(t) \right\rangle + i\langle \Psi(t)|\delta\Psi(t)\rangle \Big|_{t_0}^{t_1} . \tag{6.65}$$

The last term vanishes because of the boundary conditions on $\delta\Psi(t)$ at t_0 and t_1. To accomplish $\delta\mathcal{A}[\Psi] = 0$, the remaining two integrals must vanish as well, which immediately implies the time-dependent Schrödinger equation $[i\partial/\partial t - \hat{H}(t)]\Psi(t) = 0$.[8]

[8] To see this explicitly, notice that the variation of $\Psi(t)$ can be carried out independently for the real and the imaginary part. This implies that the real and imaginary parts of eqn (6.65) have to vanish separately, which can only be accomplished if the time-dependent Schrödinger equation holds.

6.6.2 The variational principle of TDDFT

The question of whether and how any of the established stationary-action principles carries over to TDDFT had remained an important problem for many years. Runge and Gross (1984) introduced a stationary-action principle for TDDFT closely related to the Dirac–Frenkel principle; unfortunately, this turned later out to be in conflict with causality, as we shall explain in Section 8.1.3. Van Leeuwen (1998, 2001) found an elegant way out of this causality dilemma by defining an action functional on a so-called Keldysh contour. This approach is related to nonequilibrium Green's function theory, and requires going into some technical details; we will do this in Section 13.2.

More recently, a rather straightforward alternative formulation of the TDDFT action principle was offered by Vignale (2008), which we shall now discuss. According to the fundamental existence theorems of Runge and Gross and of van Leeuwen (see Chapter 3), the wave function is a functional of the time-dependent density.[9] This means that the action becomes a density functional as well:

$$\mathcal{A}[n] = \int_{t_0}^{t_1} dt \left\langle \Psi[n](t) \left| i\frac{\partial}{\partial t} - \hat{H}(t) \right| \Psi[n](t) \right\rangle . \tag{6.66}$$

Next, we want to look at the variation of this functional, $\delta\mathcal{A}[n]$. The key question is, what boundary conditions to impose at t_0 and t_1? We are free to choose variations such that $\delta\Psi[n](t_0) = 0$, just as before. However, imposing $\delta\Psi[n](t_1) = 0$ would be too restrictive: it would mean that we allow only those variations of the density over the interval $t_0 < t < t_1$ which do not lead to a change in the wave function at t_1. In general, however, changing the density for times earlier than t_1 will have an influence on $\Psi[n](t_1)$ as a simple matter of cause and effect.

Using eqn (6.65) and the time-dependent Schrödinger equation, this leads to

$$\delta\mathcal{A}[n] = i\langle\Psi[n](t_1)|\delta\Psi[n](t_1)\rangle , \tag{6.67}$$

which should be contrasted with eqn (6.63). It thus turns out that there is no stationary-action principle (in the sense of a vanishing variation of the action) associated with the TDDFT action (6.66)! Let us now explore the consequences of this surprising result. We begin by writing the action (6.66) as

$$\mathcal{A}[n] = \mathcal{A}_0[n] - \int_{t_0}^{t_1} dt \int d^3r\, n(\mathbf{r},t) v(\mathbf{r},t) , \tag{6.68}$$

with the universal functional

$$\mathcal{A}_0[n] = \int_{t_0}^{t_1} dt \left\langle \Psi[n](t) \left| i\frac{\partial}{\partial t} - \hat{T} - \hat{W} \right| \Psi[n](t) \right\rangle , \tag{6.69}$$

where $\hat{T}$ and $\hat{W}$ are the kinetic-energy and electron–electron interaction operators defined in eqns (3.2) and (3.4). The variational principle (6.67) then tells us that

[9] Here and in the following, the dependence of $\Psi[n]$ on the fixed initial state Ψ_0 is implied but will not be explicitly indicated, since it does not play a significant role in the present context.

$$v(\mathbf{r},t) = \frac{\delta \mathcal{A}_0[n]}{\delta n(\mathbf{r},t)} - i \left\langle \Psi[n](t_1) \left| \frac{\delta \Psi[n](t_1)}{\delta n(\mathbf{r},t)} \right\rangle \right., \tag{6.70}$$

relating the external potential at time t to the functional derivative of the universal part of the action, plus a boundary term at time t_1. Since the potential and the action are both real quantities, the boundary term must be, too. The quantity $\langle \Psi(t_1) | \delta \Psi(t_1)/\delta n(\mathbf{r},t) \rangle$ is thus purely imaginary, which follows directly from the normalization of the wave function, i.e., the condition $\delta \langle \Psi | \Psi \rangle / \delta n = 0$.

More worrisome is the observation that the potential $v(\mathbf{r},t)$ at time t seems to depend on the upper limit t_1 of the time interval that we have used to define the action. If this were indeed the case then the potential would depend on the future—a blatant violation of causality—and our variational principle would be useless. Fortunately, this is not the case! The reason is a rather subtle one: it turns out that *both* terms on the right-hand side of eqn (6.70) violate causality individually, i.e., they depend on densities $n(\mathbf{r},t')$ with $t' > t$. However, these noncausal dependencies on the density cancel out exactly when the two terms are combined. The reader will be guided through a proof of this statement in Exercise 6.6. The dependence on t_1 thus drops out, and to indicate explicitly that causality is satisfied we can rewrite eqn (6.70) as

$$v(\mathbf{r},t) = \frac{\delta \mathcal{A}_0[n]\big|_{t_1=t_+}}{\delta n(\mathbf{r},t)} - i \left\langle \Psi[n](t_+) \left| \frac{\delta \Psi[n](t_+)}{\delta n(\mathbf{r},t)} \right\rangle \right., \tag{6.71}$$

where t_+ means a time infinitesimally later than t.

The same analysis can be repeated for a noninteracting TDKS system with the action functional

$$\mathcal{A}_s[n] = \mathcal{A}_{0s}[n] - \int_{t_0}^{t_1} dt \int d^3r \, n(\mathbf{r},t) v_s(\mathbf{r},t) \,, \tag{6.72}$$

where

$$\mathcal{A}_{0s}[n] = \int_{t_0}^{t_1} dt \left\langle \Phi[n](t) \left| i\frac{\partial}{\partial t} - \hat{T} \right| \Phi[n](t) \right\rangle \,. \tag{6.73}$$

The variational principle (6.67) leads to

$$v_s(\mathbf{r},t) = \frac{\delta \mathcal{A}_{0s}[n]}{\delta n(\mathbf{r},t)} - i \left\langle \Phi[n](t_1) \left| \frac{\delta \Phi[n](t_1)}{\delta n(\mathbf{r},t)} \right\rangle \right., \tag{6.74}$$

where, again, t_1 can be replaced by t_+.

Let us now relate the universal action functionals of the interacting and the noninteracting system:

$$\mathcal{A}_0[n] = \mathcal{A}_{0s}[n] - \mathcal{A}_{\rm H}[n] - \mathcal{A}_{\rm xc}[n] \,, \tag{6.75}$$

where the Hartree action functional is

$$\mathcal{A}_{\rm H}[n] = \frac{1}{2} \int_{t_0}^{t_1} dt \int d^3r \int d^3r' \, \frac{n(\mathbf{r},t) n(\mathbf{r}',t)}{|\mathbf{r}-\mathbf{r}'|} \tag{6.76}$$

and the xc action functional $\mathcal{A}_{\rm xc}[n]$ is defined by eqn (6.75). Combining eqns (6.70) and (6.74), we find the expected expression for the TDKS effective potential,

$$v_s(\mathbf{r},t) = v(\mathbf{r},t) + v_{\rm H}(\mathbf{r},t) + v_{\rm xc}(\mathbf{r},t)\,, \tag{6.77}$$

where the xc potential is given by

$$v_{\rm xc}(\mathbf{r},t) = \frac{\delta \mathcal{A}_{\rm xc}[n]}{\delta n(\mathbf{r},t)} + i\left\langle \Psi[n](t_1)\left|\frac{\delta\Psi[n](t_1)}{\delta n(\mathbf{r},t)}\right.\right\rangle - i\left\langle \Phi[n](t_1)\left|\frac{\delta\Phi[n](t_1)}{\delta n(\mathbf{r},t)}\right.\right\rangle. \tag{6.78}$$

As before, this expression is causal, and t_1 can be replaced by t_+. Notice that $v_{\rm xc}$ depends not only on the time-dependent density, but also on the initial states of the interacting and the noninteracting system, Ψ_0 and Φ_0.

The ground-state xc potential is defined as functional derivative of the xc energy functional, $v^0_{\rm xc}(\mathbf{r}) = \delta E_{\rm xc}[n_0]/\delta n_0(\mathbf{r})$. In the early days of TDDFT (Runge and Gross, 1984), it was assumed that the time-dependent xc potential could be expressed in a similar way, as a straightforward functional derivative of the xc action functional $\mathcal{A}_{\rm xc}[n]$. As we have seen, it is not as simple as that:[10] owing to causality requirements, additional boundary terms show up in eqn (6.78) for $v_{\rm xc}$. At first glance this seems to complicate matters considerably, standing in the way of any practical usefulness. Fortunately, it turns out that in many situations the boundary terms cancel out, making it relatively easy to work with the TDDFT action principle. One such situation occurs in the original proof of the generalized translational invariance of $v_{\rm xc}(\mathbf{r},t)$ (see Section 6.2.2), which utilized the corresponding invariance properties of the xc action functional (Vignale, 1995). As shown later (Vignale, 2008), the original proof (which in hindsight only worked because of a lucky compensation of errors) can be restored with little additional effort, paying proper attention to the boundary contributions. We shall encounter other examples of the usefulness of the xc action functional when we discuss the properties of the xc kernel of linear-response TDDFT in Section 8.2 and when we derive the TDOEP equation in Chapter 11.

We conclude this section by emphasizing that the TDKS equations, and the time-dependent xc potential, can be derived without recourse to an action-based variational principle, and that is in fact what we did in Section 4.1. The second observation is that the action is of no physical interest in and by itself; this is, of course, in complete contrast to the static case, where the value of the energy functional is of great importance. In the time-dependent case, the numerical value of the action is not related to any physical observable and is thus irrelevant (in fact, the total action functional $\mathcal{A}[n]$ equals zero when evaluated at the exact time-dependent density).

6.6.3 The adiabatic approximation

Let us now consider a special case, namely the action principle corresponding to the adiabatic approximation to the xc potential, which we discussed in Section 4.3. We define the adiabatic xc action functional in the following manner:

$$\mathcal{A}^{\rm A}_{\rm xc}[n] = \int_{t_0}^{t_1} dt\; E_{\rm xc}[n_0]\Big|_{n_0(\mathbf{r})\to n(\mathbf{r},t)}. \tag{6.79}$$

The adiabatic approximation to the xc potential, eqn (4.13), is then simply given by

[10] Except in the adiabatic approximation, as we shall discuss below.

$$v_{\rm xc}^{\rm A}(\mathbf{r},t) = \frac{\delta \mathcal{A}_{\rm xc}^{\rm A}[n]}{\delta n(\mathbf{r},t)} = \left.\frac{\delta E_{\rm xc}[n_0]}{\delta n_0(\mathbf{r})}\right|_{n_0(\mathbf{r})\to n(\mathbf{r},t)} = \left. v_{\rm xc}^0[n_0](\mathbf{r})\right|_{n_0(\mathbf{r})\to n(\mathbf{r},t)} , \tag{6.80}$$

i.e., there are no explicit boundary terms as in the exact expression in eqn (6.78). These terms are absent since the density dependence is instantaneous and causality is thus automatically (and trivially) satisfied. We will come back to this and related action principles when we discuss the TDOEP method in Chapter 11.

6.7 Discontinuity upon change of particle number

In Section 2.2.3 we discussed the properties of density functionals for varying particle number N, and we found that the static xc potential jumps by a constant, called $\Delta_{\rm xc}$, whenever the particle number passes through an integer [see eqn (2.65)]. Let us now see whether there is a counterpart of this behavior in the time-dependent case. This question was first systematically addressed by Mundt and Kümmel (2005), and we follow their arguments here.

6.7.1 Time-dependent ensembles and derivative discontinuity

The formal basis for discussing systems with varying particle numbers is given by the extension of TDDFT to time-dependent ensembles (Li and Tong, 1985; Li and Li, 1985), which we shall briefly review here, without going into any of the proofs.

The expectation value of any observable in a time-dependent ensemble can be written as

$$O(t) = {\rm tr}[\hat\rho(t)\hat O(t)] , \tag{6.81}$$

where

$$\hat\rho(t) = \sum_i p_i |\Psi_i(t)\rangle\langle\Psi_i(t)| \tag{6.82}$$

is the ensemble density operator. The time evolution of the density operator is given by the Liouville equation

$$i\frac{\partial\hat\rho}{\partial t} = [\hat H(t),\hat\rho] , \tag{6.83}$$

where $\hat H(t)$ is the time-dependent many-body Hamiltonian (3.1); eqn (6.83) is a generalization of the time-dependent Schrödinger equation (3.5), which describes the time evolution of pure states, to the case of ensembles.

Li and Tong (1985) proved that the density operator is a functional of the time-dependent density and of the initial ensemble,

$$\hat\rho(t) = \hat\rho[n,\hat\rho_0](t) . \tag{6.84}$$

The proof is similar to that of the Runge–Gross theorem, with the same assumptions about admissible external potentials (they must be Taylor-expandable about the initial time). This means that the expectation value of any observable becomes a functional of the time-dependent density and of the initial ensemble, $O[n,\hat\rho_0](t)$.

Likewise, it is straightforward to generalize the time-dependent Kohn–Sham formalism to the case of ensembles (Li and Li, 1985). The time-dependent ensemble Kohn–Sham equations are identical in form to the pure-state equations (4.7), with a time-dependent density

$$n(\mathbf{r},t) = \sum_{j=1}^{\infty} \gamma_j |\varphi_j(\mathbf{r},t)|^2 \,, \tag{6.85}$$

where the occupation numbers γ_j are fixed by the initial noninteracting ensemble, and add up to the given particle number $\sum_j \gamma_j = N$. In "ordinary" Kohn–Sham theory for nondegenerate ground states the occupation numbers are either zero or one (corresponding to occupied or unoccupied orbitals), whereas ensemble Kohn–Sham theory admits fractional occupation numbers. Systems with nonintegral total particle numbers are included in the formalism.

In the following, we shall restrict the discussion to systems which start in the ground state at the initial time t_0. In the case of the ground-state theory, we saw in Section 2.2.3 that the density operator corresponding to a particle number $N+w$ is given by (Perdew *et al.*, 1982; Perdew, 1985)

$$\hat{\rho}_0 = (1-w)|\Psi_0^N\rangle\langle\Psi_0^N| + w|\Psi_0^{N+1}\rangle\langle\Psi_0^{N+1}| \,. \tag{6.86}$$

In other words, the ensemble that minimizes the energy consists only of a mixture of states with N and $N+1$ particles. There are infinitely many other choices of the initial density operator $\hat{\rho}_0$ which correspond to a particle number $N+w$ (for instance, operators that mix states with $N-1$, N, $N+1$, and $N+2$ electrons). Each of these choices corresponds to an excited ensemble state and would be a valid initial state in the ensemble TDDFT formulation. However, only for the initial ground-state ensemble (6.86) is it possible to say anything about how the functionals change with particle number. Fortunately, this is not such a severe restriction as it seems: in Section 6.5.2, we showed that the initial-state dependence can often be replaced by a pseudo-prehistory, where the system starts from the ground state at an earlier time. From now on we shall assume that this is the case; the dependence on $\hat{\rho}_0$ then disappears, and $\hat{\rho}[n](t)$ becomes a functional of the time-dependent density only:

$$\hat{\rho}[n](t) = (1-w)|\Psi^N(t)\rangle\langle\Psi^N(t)| + w|\Psi^{N+1}(t)\rangle\langle\Psi^{N+1}(t)| \,. \tag{6.87}$$

Let us now see how this affects the time-dependent xc potential. We generalize eqn (6.78) to the case of nonintegral particle number $N+w$ and obtain

$$\begin{aligned} v_{\rm xc}^{N+w}(\mathbf{r},t) = {} & \frac{\delta}{\delta n(\mathbf{r},t)} \left[(1-w)\mathcal{A}_{\rm xc}^{N} + w\mathcal{A}_{\rm xc}^{N+1}\right] \\ & + i(1-w)\left\langle \Psi^N(t_1) \left| \frac{\delta\Psi^N(t_1)}{\delta n(\mathbf{r},t)} \right\rangle + iw \left\langle \Psi^{N+1}(t_1) \left| \frac{\delta\Psi^{N+1}(t_1)}{\delta n(\mathbf{r},t)} \right\rangle \right. \\ & - i(1-w)\left\langle \Phi^N(t_1) \left| \frac{\delta\Phi^N(t_1)}{\delta n(\mathbf{r},t)} \right\rangle - iw \left\langle \Phi^{N+1}(t_1) \left| \frac{\delta\Phi^{N+1}(t_1)}{\delta n(\mathbf{r},t)} \right\rangle \right. . \end{aligned} \tag{6.88}$$

At the initial time t_0, we know that there exists a discontinuity in the ground-state xc potential as the particle number passes through an integer N, given by eqn (2.65):

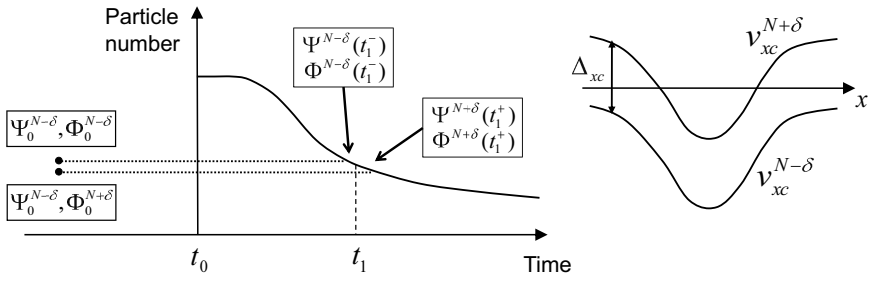

Fig. 6.7 Left: time-dependent particle number of a finite system undergoing an ionization process. The system passes through an integer number of particles N at time t_1. The interacting and noninteracting wave functions shortly before and after t_1 can be connected through pseudo-prehistories (dotted lines) to initial ground states with particle numbers $N-\delta$ and $N+\delta$. Right: schematic illustration of the discontinuity in the xc potential.

$$\begin{aligned}\Delta_{\rm xc}(t_0) &= \lim_{w\to 0}\left[v_{\rm xc}^{N+w}(\mathbf{r},t_0) - v_{\rm xc}^{N-w}(\mathbf{r},t_0)\right] \\ &= \left.\frac{\delta E_{\rm xc}[n]}{\delta n(\mathbf{r},t_0)}\right|_{N+} - \left.\frac{\delta E_{\rm xc}[n]}{\delta n(\mathbf{r},t_0)}\right|_{N-} . \end{aligned} \tag{6.89}$$

For finite times we obtain

$$\lim_{w\to 0}\left[v_{\rm xc}^{N+w}(\mathbf{r},t) - v_{\rm xc}^{N-w}(\mathbf{r},t)\right] = \left.\frac{\delta \mathcal{A}_{\rm xc}[n]}{\delta n(\mathbf{r},t)}\right|_{N+} - \left.\frac{\delta \mathcal{A}_{\rm xc}[n]}{\delta n(\mathbf{r},t)}\right|_{N-} , \tag{6.90}$$

since the boundary terms in eqn (6.88) drop out. It is tempting to identify the right-hand side of this equation with a time-dependent constant $\Delta_{\rm xc}(t)$, in analogy with the ground-state case. However, such an identification is difficult to justify in general: in the static case we took advantage of the Euler equation (2.19), which relates the functional derivative of the energy to the chemical potential. No such correspondence exists in the time-dependent case for the action functional. All we can say is that there is no reason to assume that the right-hand side of eqn (6.90) always vanishes.

For times $t > t_0$ but close to t_0, it can safely be assumed that the xc potential still exhibits a derivative discontinuity, since the time evolution of the system proceeds in a continuous manner (barring any pathologies) and cannot be expected to immediately erase the discontinuity. In the adiabatic limit of a slowly varying external potential the system stays close to the instantaneous ground state and there is a finite $\Delta_{\rm xc}$ at all times. Whether or not a $\Delta_{\rm xc}(t)$ exists in general remains an open question; in the following, we give some numerical evidence which strongly suggests that it does indeed.

6.7.2 Time-varying particle numbers

In practice, the discontinuity in the time-dependent xc potential plays an important role in TDDFT for strong-field processes that lead to ionization and/or dissociation of atomic and molecular systems. Figure 6.7 illustrates a typical scenario which holds, for instance, for an atom subject to a strong laser pulse. At the initial time t_0, the atom

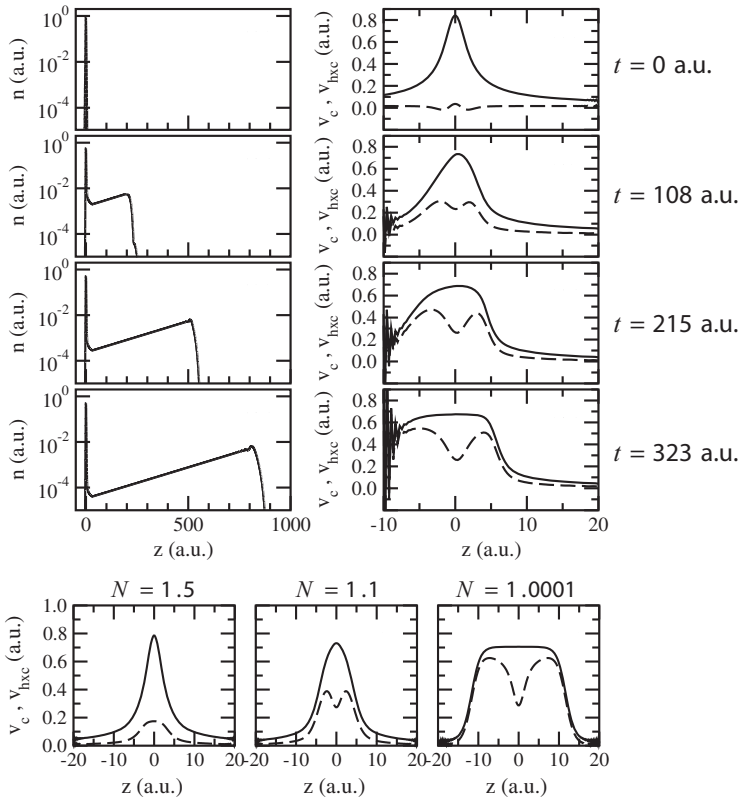

Fig. 6.8 Top: density $n(z,t)$ and potentials $v_{\rm Hxc}(z,t)$ (full lines) and $v_{\rm c}(z,t)$ (dashed lines) at various times for a one-dimensional helium atom in a static field switched on at $t = 0$. Bottom: static potentials $v_{\rm Hxc}(z)$ (full lines) and $v_{\rm c}(z)$ (dashed lines) for ground states with nonintegral electron numbers, as indicated. [Adapted with permission from APS from Lein and Kümmel (2005), ©2005.]

is in its ground state and has, obviously, an integer number of electrons. Under the influence of the laser the system starts to ionize, i.e., excitation processes take place which transfer electrons from bound to continuum states. The corresponding total loss of electrons, $N_{\rm esc}(t)$, can be calculated using the techniques of Section 5.1.2: in this case, the time propagation on a finite spatial grid is nonunitary owing to the presence of absorbing boundary conditions. However, even if we work with a very large grid so that the time propagation remains unitary, it is still possible (and reasonable) to define a central region around the system which effectively loses particles. From now on, our "system" is assumed to be defined via such a spatial region, or analyzing box, and we can therefore work with pure states rather than with time-dependent ensembles.

Let t_1 be the time at which the particle number of the system passes through the integer value N. We are specifically interested in the times t_1^- and t_1^+ immediately before and after t_1, characterized by interacting and noninteracting many-body states

$\Psi^{N+\delta}(t_1^-)$, $\Phi^{N+\delta}(t_1^-)$ and $\Psi^{N-\delta}(t_1^+)$, $\Phi^{N-\delta}(t_1^+)$. At t_1, the exact xc potential of the system jumps by a constant, $\Delta_{\rm xc}(t_1)$, as illustrated in the right-hand part of Fig. 6.7.

To see why this happens, and to make a connection with the arguments given in Section 6.7.1, we again invoke the assumption that there exist pseudo-prehistories,[11] *with fixed particle numbers*, that connect the states at times t_1^- and t_1^+ (which are infinitesimally close to each other) to ground states at some earlier time. In Fig. 6.7 we chose to let those ground states start prior to t_0, but this could have been at any time before t_1. The starting points of the two prehistories are infinitesimally close, and the trajectories remain parallel to each other. The initial discontinuity in the xc potential then carries all the way through to t_1. The discontinuity in the xc potential in TDDFT can therefore be viewed as an initial-state (or history) dependence along pseudo-prehistory trajectories with fixed infinitesimally different particle numbers.

Figure 6.8 shows a numerical example of how a discontinuity in the xc potential appears during the ionization of a one-dimensional model helium atom by a strong static field, switched on at time $t = 0$ (Lein and Kümmel, 2005). Here, the exact time-dependent xc potential was constructed from the exact density (see Appendix E), which in turn was obtained from the two-body Schrödinger equation.

As the particle number decreases from $N = 2$, a plateau begins to form in the Hartree-plus-correlation potential, which broadens and develops a sharp step as $N = 1$ is approached from above. The height of the step is found to be close to the difference between the ionization potentials of the neutral and the singly ionized atom. Notice that most of the step comes from the correlation potential, since here the electrons are of opposite spin and thus are not affected by the exchange interaction. Numerically, it is not possible to follow the dynamics for much longer, but it is clear that eventually the step will reach infinity. The potential is required to be zero at infinity and must therefore jump down by a constant (the step height) as N goes from $1 + \delta$ to $1 - \delta$.

Most of the currently used approximations to the xc potential fail to give a discontinuity as the system passes from $N + \delta$ to $N - \delta$ particles. Later, in Chapter 11, we will see that there exists a TDDFT method which does produce this effect, namely the TDOEP approach for producing time-dependent exact-exchange and self-interaction-corrected functionals. There, as well as in Chapters 15 and 16, we will explore the consequences of the discontinuity in the xc potential further and give more examples.

Exercise 6.1 Convince yourself that the coordinate-scaled many-body wave function $\Psi_{\gamma\beta}$ with $\gamma = 1/\lambda$ and $\beta = 1/\lambda^2$ satisfies the original time-dependent Schrödinger equation (3.5), with scaled coordinates $\mathbf{r}_i/\lambda$ and t/λ^2 but the full interaction strength.

Exercise 6.2 Show that the many-body wave function (6.24) satisfies the time-dependent Schrödinger equation (6.23) seen by an accelerated observer. Similarly, show that the Kohn–Sham wave function (6.29) satisfies eqn (6.28), seen by an accelerated observer.

Exercise 6.3 Consider the exchange part of the ALDA xc potential,

$$v_{\rm x}^{\rm ALDA}(\mathbf{r}, t) = -(3/\pi)^{1/3} n(\mathbf{r}, t)^{1/3} ,$$

[11] This argument evidently breaks down for states that are not ground-state quantum evolvable. This does not rule out the possibility that there nevertheless exists a discontinuity in the xc potential at time t_1.

and check that $v_{\rm x}^{\rm ALDA}(\mathbf{r},t)$ satisfies the condition of generalized translational invariance (6.37). Now, let's try our luck with the following nonadiabatic generalization of $v_{\rm x}^{\rm ALDA}(\mathbf{r},t)$:

$$\widetilde{v}_x[n](\mathbf{r},t) = -(3/\pi)^{1/3}\int_{-\infty}^{t} dt' h(t-t') n(\mathbf{r},t')^{1/3}\,,$$

where $h(t-t')$ is a "memory kernel" which has a maximum for $t=t'$ and goes to zero as $t-t'\to-\infty$. Furthermore, in order to guarantee that $\widetilde{v}_x[n](\mathbf{r},t)$ reduces to the LDA potential $v_x^{\rm LDA} = cn_0(\mathbf{r})^{1/3}$ in the adiabatic limit, we can impose the condition

$$\int_{-\infty}^{t} dt' h(t-t') = 1\,.$$

For example, $h(t-t') = \exp[-(t-t')]$ will do the job. So far so good—but does $\widetilde{v}_x[n](\mathbf{r},t)$ satisfy generalized translational invariance?

Exercise 6.4 Derive eqn (6.52) for the TDKS potential by inserting the model density (6.50) into eqn (6.51).

Exercise 6.5 Convince yourself that the functions $\widetilde{\xi}_1(x)$ and $\widetilde{\xi}_2(x)$ given in eqn (6.58) are not eigenstates of the same single-particle potential.

Exercise 6.6 Prove that $v(\mathbf{r},t)$, given by eqn (6.70), is independent of the upper time limit t_1. To do this, we need to show that

$$\frac{dv[n](\mathbf{r},t)}{dt_1} = \frac{d}{dt_1}\frac{\delta\mathcal{A}_0[n]}{\delta n(\mathbf{r},t)} - i\frac{d}{dt_1}\left\langle \Psi[n](t_1)\left|\frac{\delta\Psi[n](t_1)}{\delta n(\mathbf{r},t)}\right.\right\rangle = 0\,, \qquad t_1 > t.$$

Let's first deal with the second term on the right-hand side. Carry out the differentiation with respect to t_1, using the time-dependent Schrödinger equation at t_1 and a partial integration, and show that

$$-i\frac{d}{dt_1}\left\langle \Psi[n](t_1)\left|\frac{\delta\Psi[n](t_1)}{\delta n(\mathbf{r},t)}\right.\right\rangle = -\int d^3r' n(\mathbf{r}',t_1)\,\frac{\delta v[n](\mathbf{r}',t_1)}{\delta n(\mathbf{r},t)}\,.$$

Next, convince yourself, using the time-dependent Schrödinger equation, that $\mathcal{A}_0[n]$ can also be represented as

$$\mathcal{A}_0[n] = \int_{t_0}^{t_1} dt \int d^3r\; n(\mathbf{r},t) v[n](\mathbf{r},t)\,.$$

From this, it is straightforward to evaluate $(d/dt_1)\delta\mathcal{A}_0/\delta n(\mathbf{r},t)$ and then to go on and show that $dv[n](\mathbf{r},t)/dt_1 = 0$.

Exercise 6.7 Show that a rigid translation of the density,

$$n(\mathbf{r},t) \longrightarrow n'(\mathbf{r},t) = n(\mathbf{r}+\mathbf{x},t)\,,$$

induces the following change in the xc action functional to first order in $n'-n$:

$$\delta\mathcal{A}_{\rm xc}[n] = -i\langle\Psi[n](t_1)|\delta\Psi[n](t_1)\rangle + i\langle\Phi[n](t_1)|\delta\Phi[n](t_1)\rangle\,, \tag{6.91}$$

where $\delta\Psi[n](t_1) = \Psi[n'](t_1) - \Psi[n](t_1)$ and similarly for $\delta\Phi[n](t_1)$. Go on from there to prove the zero-force theorem for the xc potential, eqn (6.9).